UNIVERSITA' DEGLI STUDI DI PADOVA

DIPARTIMENTO DI SCIENZE ECONOMICHE ED AZIENDALI "MARCO FANNO"

DIPARTIMENTO DI MATEMATICA "TULLIO LEVI CIVITA"

CORSO DI LAUREA MAGISTRALE IN ECONOMICS AND FINANCE

TESI DI LAUREA

"INTEREST RATE DERIVATIVES PRICING: FROM THE SINGLE TO THE MULTIPLE CURVE FRAMEWORK. CALIBRATION OF THE HULL-WHITE MODEL USING CAP VOLATILITIES"

RELATORE:

CH.MO PROF. CLAUDIO FONTANA

LAUREANDO/A: TOMMASO PIAZZA

MATRICOLA N. 1189860

ANNO ACCADEMICO 2019 – 2020

Il candidato dichiara che il presente lavoro è originale e non è già stato sottoposto, in tutto o in parte, per il conseguimento di un titolo accademico in altre Università italiane o straniere.
Il candidato dichiara altresì che tutti i materiali utilizzati durante la preparazione dell'elaborato sono stati indicati nel testo e nella sezione "Riferimenti bibliografici" e che le eventuali citazioni testuali sono individuabili attraverso l'esplicito richiamo alla pubblicazione originale.

The candidate declares that the present work is original and has not already been submitted, totally or in part, for the purposes of attaining an academic degree in other Italian or foreign universities. The candidate also declares that all the materials used during the preparation of the thesis have been explicitly indicated in the text and in the section "Bibliographical references" and that any textual citations can be identified through an explicit reference to the original publication.

Firma dello studente

Interest rate derivatives pricing: from the single to the multiple curve framework. Calibration of the Hull-White model using cap volatilities.

Tommaso Piazza

November 16, 2020

Acknowledgments

Ringrazio la mia famiglia per essere stata in questi anni un sostegno costante, un appoggio vitale senza il quale non avrei avuto la forza necessaria per arrivare a questo importante traguardo.
Ringrazio il Prof. Claudio Fontana per l'attenzione e il supporto che mi ha sempre fornito durante questo lavoro di ricerca, dandomi la possibilità di approfondire un campo estremamente affascinante e ricco di stimoli.
Ringrazio tutti gli amici, i compagni e i professori con cui ho avuto l'opportunità di condividere la strada percorsa durante il biennio magistrale, ringrazio tutti quanti hanno contribuito a impreziosire questo percorso.
Ringrazio Be Consulting e i colleghi che mi hanno affiancato in questi ultimi mesi, dandomi la possibilità di entrare a far parte di un ambiente lavorativo affascinante e dinamico.

Contents

Introduction

Broadly speaking, interest rate derivatives are financial instruments enabling companies and financial institutions to effectively manage their cash and funding needs. Indeed, interest rate derivatives are normally purchased because they offer *insurance* against adverse changes of interest rates, i.e. they are acquired for hedging purpose. However, there exist also two other reasons leading agents to enter interest rate derivative contracts: speculation and arbitrage. Speculators use derivatives as *bets* on future market movements, while arbitrageurs use derivatives to exploit riskless opportunities in financial markets.
The goal of this thesis is to discuss interest rate derivatives pricing, its evolution after the financial crisis of 2007 and, finally, the implementation of a calibration algorithm for the term structure of the interest rate.

In the first part of this dissertation we discuss the paradigm shift unleashed by the financial crisis in interest rate modelling: before the crisis, practitioners used to adopt a pricing framework based on a single yield curve, which was used both for determining future payments and for discounting them. However, the financial markets undergone a deep evolution after the crisis. Indeed, counterparty and liquidity risk - which were not considered until the financial disruption - suddenly become essential to determine the future value of a contract. The new pricing framework took the name of multiple curve framework, since it is characterised by the presence of a single discount curve - usually bootstrapped by OIS bonds if the derivative contract is collateralized - and by multiple yield curves to determine future payments - one yield curve for each different IBOR tenor structure. These issues are presented and discussed in Chapter 1.
In Chapter 2 we illustrate the different steps a practitioner should undertake when pricing derivatives and we then focus on the most critical passages. The first step to price an interest rate derivative is to build an appropriate set of yield and discount curves; this can be done applying the bootstrapping and interpolation methods we indicate in Section 2.1. Another important step regards the term structure modelling of interest rates. We present the analysis of short rate models provided by Grbac and Runggaldier (2015), which provide a framework with multiple factors which can be used to describe the term structure equation of several short rate models. Finally, Monte Carlo simulation for derivatives' prices is introduced.

In Chapter 3 we present the proof of the Vasicek and of the Hull-White models for the short rate. We then describe the payoffs of interest rate options using the Hull-White model and we use this formulation to describe the price of cap and floor options by considering them as portfolios of, respectively, put and call options[1]. The theoretical formulations provided in Chapter 3 are then *translated* in MATLAB code in Chapter 4: indeed, we use market quotes of cap options' volatilities and prices, entering them in the calibration scheme for the Hull-White model described in Chapter 3.

Finally, we remark that the Hull-White calibration algorithm discussed and implemented respectively in Chapter 3 and Chapter 4 is not anymore considered by practitioners when dealing with interest rate derivatives pricing, because they are not able to effectively describe the volatility. Conversely, nowadays practitioners prefer to adopt term structure models which allow to account for more complex volatility terms. Therefore, the reader should consider the analysis developed in Chapter 3 and Chapter 4 more as an exercise than a practical tool to be used in daily fixed-income trading desk's operations. Furthermore, we refer to the introduction of Part 2 for some important assumptions on the distribution of interest rates. These assumptions are necessary to calibrate the Hull-White model according to the framework provided in Chapter 3.

[1]The formulation of cap option as a portfolio of put options is presented in Section 3.3.1.

Part I

The multiple curve framework: a general introduction

Chapter 1

Basic concepts

The purpose of this chapter is to provide the reader with the essential tools to understand the theoretical developments and the practical applications that are, respectively, deepened and implemented in the following chapters.
This chapter is structured into two main sections. In the first section we present some basic concepts of interest rate theory, introducing the key assumptions and elements upon which interest rate models have been built and studied in the last decades; furthermore, we provide a general overview of term structure modelling in the single curve framework, from short rate models to Libor market models. In the second section, we briefly describe how the financial crisis begun in the second half of 2007 radically changed long-standing habits; furthermore, we relate these behavioural shifts to the evolution of the one curve framework, which was adopted before the financial crisis by market agents when pricing OTC plain vanilla and exotic interest rate derivatives. The findings we introduce in the last section are necessary to understand why the one curve world and the multiple curve world must be studied with two distinct approach. The multiple curve framework is then developed in the second chapter of this thesis.
There exist a broad literature discussing term structure modelling in the single curve world. The most important contributions we have considered when developing the first and the second section are - for the term structure modelling - Björk (2009) and Brigo and Mercurio (2006) and - for the shift from the single to the multiple curve framework - Grbac and Runggaldier (2015) and Bianchetti and Carlicchi (2013).

1.1 Interest rate theory: basic concepts

In this section we explain how to model zero coupon bond price processes $P(t,T)$ with $T > 0$ under the no arbitrage hypothesis. The first step is to define the short rate process

as the solution of a SDE under the objective probability measure $\mathbb{P}$

$$dr(t) = \mu(t, r(t))dt + \sigma(t, r(t))dW^{\mathbb{P}}(t) \tag{1.1}$$

and to define the price process of a money market account, $B(t)$, as

$$dB(t) = r(t)B(t)dt \tag{1.2}$$

We observe that the short rate $r(t)$ is given a priori and, consequently, the money market account $B(t)$ is the only exogenously known (risk-free) asset.
We assume that the financial market is composed of a number M of zero coupon bonds, in addition to the risk-free asset $B(t)$. However, these assumptions imply that a market conceived in this way lacks of completeness because there are no exogenously given assets other than the risk-free asset. Therefore, it is not possible to completely determine the price of the other M bonds depending only on the short rate process $r(t)$ and on the condition of no arbitrage. This negative answer is quite straightforward: since we consider bonds as interest rate derivatives, we need a sufficient number of exogenously given underlying assets in order to carry out arbitrage pricing. Indeed, the completeness condition is satisfied if and only if the number n of exogenously given assets - not considering in this group the risk-free account $B(t)$ - equals the number m of random sources.
According to Björk (2009), we can solve this problem taking as given the price of a bond with maturity j and pricing the bonds with maturities $i < j$ and $i = 0, 1, ..., j-1$ in terms of the short rate process $r(t)$ and of the price of the j-bond.
Therefore, the author assumes that the price of a bond j for every maturity j is a function F of three real variables $t, r(t)$ and T

$$P(t, T) = F(t, r(t); T) \tag{1.3}$$

where $F(T, r; T) = 1$ for all $r(t)$.
We select a portfolio V composed by two bonds with maturities S and T and weights given by (u_S, u_T). The portfolio is described by the process

$$dV = V\left\{u_T \frac{dF^T}{F^T} + u_S \frac{dF^S}{F^S}\right\} \tag{1.4}$$

where the price processes of the two i-bonds, with $i = S, T$, are determined by the Itô formula

$$dF^i = F^i \alpha_i dt + F^i \sigma_i dW^{\mathbb{P}}$$

where

$$\alpha_i = \frac{F^i_t + \mu F^i_r + \frac{1}{2}\sigma^2 F^i_{rr}}{F^i},$$
$$\sigma_i = \frac{\sigma F^i_r}{F^i}.$$

The resulting portfolio is risk-free because its process is determined by the drift term only. Furthermore, given that the self-financing and the no arbitrage conditions are satisfied, we obtain that the portfolio's return must be equal to the to the short rate $r(t)$. Hence, we obtain that the process of the portfolio can be also represented as

$$dV = V\left\{\frac{\alpha_S\sigma_T - \alpha_T\sigma_S}{\sigma_T - \sigma_S}\right\}dt = Vr(t)dt \tag{1.5}$$

where the second equivalence of equation (1.5) implies that

$$\frac{\alpha_S(t) - r(t)}{\sigma_S(t)} = \frac{\alpha_T(t) - r(t)}{\sigma_T(t)} = \lambda(t). \tag{1.6}$$

The implication of equation (1.6) represents one of the key assumptions upon which term structure modelling is built: all the zero coupon bonds $P(t,T)$ which are freely traded in a no-arbitrage market have the same risk premium, $\lambda(t)$, also called market price of risk.

The elements defined until this point are useful to finally introduce the term structure equation, a partial differential equation (PDE) satisfied by the process $F(t)$

$$\begin{cases} F_t^T + \{\mu - \lambda\sigma\}F_r^T + \frac{1}{2}\sigma^2 F_{rr}^T - rF^T = 0, \\ F^T(T,r) = 1 \end{cases} \tag{1.7}$$

Unfortunately, the term structure equation (1.7) cannot be solved until the parameters λ, μ and σ are exogenously taken.
A stochastic representation of equations (1.7) can be obtained through the application of Itô formula to the process

$$exp\left\{-\int_0^s r(u)du\right\}F^T(s, r(s)),$$

and assuming that F^T satisfies the term structure equation.
Finally, using the methodology we have employed in Appendix A, we are able to obtain the Feynman-Kac transformation of F^T.
Therefore, we are able to define the following representation of the general term structure equation for the price $\Pi(t,\Phi)$, where $\Phi(r(T))$ is a general claim at time T,

$$\begin{cases} F_t + \{\mu - \lambda\sigma\}F_r + \frac{1}{2}\sigma^2 F_{rr} - rF = 0, \\ F(T,r) = \Phi(r). \end{cases} \tag{1.8}$$

where $F(t,r;T)$ is represented as

$$F(t,r;T) = E^{\mathbb{Q}}\left[exp\left\{-\int_t^T r(s)ds\right\} \times \Phi(r(T))\middle|\mathcal{F}(t)\right], \tag{1.9}$$

where $\mathcal{F}(t)$ is a sigma-algebra and the expectation is taken under the λ-depending martingale measure $\mathbb{Q}$, considering for the r-dynamics under the risk neutral measure $\mathbb{Q}$

$$\begin{cases} dr(s) = \{\mu - \lambda\sigma\}ds + \sigma dW^{\mathbb{Q}}(s), \\ r(t) = r. \end{cases} \tag{1.10}$$

Before moving on to a broad description of the most important models for the short rate, we should first introduce the Girsanov's theorem. Indeed, we need a Girsanov transformation to move from an interest rate process under the objective probability measure $\mathbb{P}$ to a corresponding process under the risk neutral probability measure $\mathbb{Q}$. The Girsanov transformation is important because it affects only the drift term of a process, but not its diffusion term. This property allows us to estimate the diffusion term under the objective probability measure $\mathbb{P}$, and then estimating the other paramenters using the estimated diffusion parameter in the process under the risk neutral probability measure $\mathbb{Q}$.
Therefore, according to the definition provided by Björk (2009), a Girsanov transformation of a standard Brownian motion under the objective probability measure $\mathbb{P}$ into a process with a Brownian motion under the risk neutral measure $\mathbb{Q}$ is

$$dW^{\mathbb{P}} = \phi(t)dt + dW^{\mathbb{Q}}(t), \tag{1.11}$$

where the Brownian motion $W^{\mathbb{P}}$ is defined in the probability space $(\Omega,\ \mathcal{F},\ \mathbb{P})$ and $\phi(t)$ is a vector process. The transformation is operated through a process G

$$\begin{cases} dG(t) = \phi(t)G(t)dW^{\mathbb{P}}(t), \\ G(0) = 1 \end{cases}$$

whose expected value under the objective measure $\mathbb{P}$ is assumed to be

$$E^{\mathbb{P}}\big[G(T)\big] = 1,$$

and the risk neutral probability measure on the sigma-algebra $\mathcal{F}(T)$ is defined as

$$G(T) = \frac{d\mathbb{Q}}{d\mathbb{P}}.$$

1.1.1 Models for the short rate

We present some of the standard models that are used to describe the short rate under the risk neutral measure $\mathbb{Q}$. These models are characterized by a parameter vector α,

affecting both the drift and the diffusion terms

$$dr(t) = \mu(t, r(t); \alpha)dt + \sigma(t, r(t); \alpha)dW^{\mathbb{Q}}(t). \tag{1.12}$$

The assessment of the parameter vector α in the general case (1.12) can be attained through the procedure we have briefly outlined after having applied the Girsanov's theorem to the interest rate process in the $\mathbb{P}$ measure. Hence, the first step we need to take is to define the drift term, but - unfortunately - we are not able to retrieve the drift term's parameters directly from the observation of $r(t)$ under the real measure $\mathbb{P}$. Therefore, we should first select a specific model involving a given number of parameters. Then, we should compare the theoretical term structure solving the term structure equation (1.7), $P(t, T; \alpha)$, with the empirical term structure that we have built after having collected market data, $P^*(t, T; \alpha)$. Finally, we should recursively input the parameter vector α in equation (1.12) until the theoretical term structure matches the empirical term structure. Therefore, we obtain an *estimated* parameter α^*.
We put the estimated value of α, α^*, into μ and σ, using the risk neutral probability measure $\mathbb{Q}$.
This procedure enables us to calculate the price, $\Pi(t, \Phi)$, of an interest rate derivative enabling owner to exercise a claim $\Phi(r(T))$ at time T. The price process of the interest rate derivative is the solution of the term structure equation (1.8).
The procedure we have just described in general terms is called the *calibration* of an interest rate model using market data and, as we show theoretically in Chapter 3 and empirically in Chapter 4, it represents the core element around which this final dissertation is built. Indeed, we present in the following chapters the results of the calibration of the Hull-White model, a short rate model, using the market data of cap volatilities.

Many of the models that we discuss later can easily be treated with an analytical and a computational perspective if they have an affine term structure. A model possesses an affine term structure if the term structure is

$$P(t, T) = F(t, r(t); T) \tag{1.13}$$

where

$$F(t, r; T) = \exp\left[A(t, T) - B(t, T)r\right] \tag{1.14}$$

where $A(t, T)$ and $B(t, T)$ are deterministic functions. Furthermore, the model can be defined effortlessly if the parameters of the drift term and of the diffusion term are also affine and time dependent

$$\mu(t, r) = \alpha(t)r + \beta(t)$$
$$\sigma(t, r) = \sqrt{\gamma(t)r + \delta(t)}$$

Thus, the model has an affine term structure whose deterministic functions $A(t, T)$ and

$B(t,T)$ - according to Björk (2009) - solve the systems of equations

$$\begin{cases} \frac{\partial B(t,T)}{\partial t} + \alpha(t)B(t,T) - \frac{1}{2}\gamma(t)B^2(t,T) = -1 \\ B(T,T) = 0 \end{cases} \tag{1.15}$$

and

$$\begin{cases} \frac{\partial A(t,T)}{\partial t} = \beta(t)B(t,T) - \frac{1}{2}\gamma(t)B^2(t,T) \\ A(T,T) = 0. \end{cases} \tag{1.16}$$

Analytical tractability for affine term structure models is used to better understand the Vasicek and the Hull-White version of the Vasicek model which we analyze in detail in Chapter 3.

An in-depth discussion of the different classes is out of the scope of this thesis; indeed, there already exist a huge literature - among the most popular textbooks on interest rate modelling there are Brigo and Mercurio (2006), Björk (2009) and, for modelling in the multiple curve framework, Caspers and Kienitz (2017). Therefore, we briefly sketch only the most popular short rate models, as they were listed in the textbook of Brigo and Mercurio (2006).

1. Vasicek
$$dr(t) = k[\theta - r(t)]dt + \sigma dW^{\mathbb{Q}}(t) \tag{1.17}$$

2. Cox-Ingersoll-Ross
$$dr(t) = k[\theta - r(t)]dt + \sigma\sqrt{r(t)}dW^{\mathbb{Q}}(t) \tag{1.18}$$

3. Dothan
$$dr(t) = ar(t)dt + \sigma r(t)dW^{\mathbb{Q}}(t) \tag{1.19}$$

4. Exponential Vasicek
$$dr(t) = r(t)[\eta - a\ln r(t)]dt + \sigma r(t)dW^{\mathbb{Q}}(t) \tag{1.20}$$

5. Hull-WHite
$$dr(t) = k[\theta(t) - r(t)]dt + \sigma dW^{\mathbb{Q}}(t) \tag{1.21}$$

6. Black-Karasinski
$$dr(t) = r(t)[\eta(t) - a\ln r(t)]dt + \sigma r(t)dW^{\mathbb{Q}}(t) \tag{1.22}$$

7. CIR++

$$\begin{cases} dr(t) = k[\theta - x(t)]dt + \sigma\sqrt{x(t)}dW^{\mathbb{Q}}(t) \\ r(t) = \phi(t) + x(t) \end{cases} \tag{1.23}$$

8. Shifted exponential Vasicek

$$\begin{cases} dr(t) = x(t)[\eta - a\ln x(t)]dt + \sigma x(t)dW^{\mathbb{Q}}(t) \\ r(t) = \phi(t) + x(t) \end{cases} \tag{1.24}$$

Short rate models were the first interest rate models to be developed and they are still extremely useful for practitioners for risk management and pricing. Indeed, the processes we have just listed are necessary to describe the stochastic discount factor which is used to compute the present value of the expected payoff $\Phi(r(T))$

$$P(t,T) = E^{\mathbb{Q}}\left[exp\left\{-\int_t^T r(s)ds\right\} \times \Phi(r(T))\middle|\mathcal{F}(t)\right].$$

The different models are driven by different factors, shaping in different ways both the drift and the stochastic terms. In order to be used in practice, interest rate models should have the important feature of being flexible and numerically tractable; this particular characteristic is held by interest rate models with an affine term structure, and, observing the list we have sketched above, all the short rate models except for the Dothan model have an affine term structure.
Short rate models can be distinguished - according to the classification operated by Caspers and Kienitz (2017) - into Gaussian models (e.g. Vasicek model, Ho-Lee model and Hull-White model), square root models (e.g. Cox-Ingersoll-Ross model) and multiple factors models (e.g. G2++ m. and Hull-White 2 factors model).

Another important class of interest rate models is the one of instantaneous forward rate models. These models were developed on the Heath-Jarrow-Morton (HJM) framework. The HJM framework can be formulated using the following SDE

$$\begin{cases} df(t,T) = \mu(t,T)dt + \sigma(t,T)dW^{\mathbb{Q}}(t) \\ f(0,T) = f^{mkt}(0,T) \end{cases} \tag{1.25}$$

where $f^{mkt}(0,T)$ is the instantaneous forward rate which is observed in the market at time 0. The parameters can be calculated applying a calibration algorithm symilar to the one we have previously described when discussing short rate models. Therefore, it can be proved[1] that, by the no-arbitrage principle, the drift parameter can be also represented as

$$\mu(t,T) = \sigma(t,T)\left(\int_t^T \sigma(t,u)du\right).$$

[1]See Brigo and Mercurio (2006).

Finally, the HJM model can be represented as

$$\begin{cases} df(t,T) = \sigma(t,T)\left(\int_t^T \sigma(t,u)du \right) dt + \sigma(t,T)dW^{\mathbb{Q}}(t) \\ f(0,T) = f^{mkt}(0,T) \end{cases} \tag{1.26}$$

and following Section 5.1 in Brigo and Mercurio (2006) the zero coupon bond price process can be calculated applying the Itô formula to the equation of the instantaneous forward rate; furthermore, the authors derive the instantaneous short rate from the fact that it is equal to the instantaneous forward rate. The implication of the HJM framework is very important for interest rate theory: indeed, specifying the drift term using the volatility structure enables us to determine the whole yield curve by simply specifying the initial condition and the volatility σ. According to Caspers and Kienitz (2017), the most considerable disadvantage of the HJM model is that a general volatility function could lead to a model which is not anymore Markovian and, consequently, which could not be solved anymore with a PDE.

Another important class of interest rate models is the one represented by market models. As the name suggests, market models differ from short rate and instantaneous forward rate models because they are used to model interest rates which are directly observed in the market. Depending on the type of rate observed, we distinguish between Libor market models and Swap market models. We refer to Brigo and Mercurio (2006) and to Caspers and Kienitz (2017) to a complete analysis of Libor and Swap market models.

1.1.2 Overview of linear interest rate instruments

In this section we briefly introduce the most significant plain vanilla interest rate instruments. We discuss the instrument's payoff and pricing formulas using as main reference the pricing framework provided in Ametrano and Bianchetti (2013) and Bianchetti and Morini (2013). We use vector notation for Swaps and Overnight Indexed Swaps (OIS).

Deposits

Deposits (Depos) are zero coupon unsecured contracts and they are usually OTC traded. The payoff of a Depo is

$$D(T_i, T_i) = N[1 + R^{depo}(t, T_i)\tau_i], \tag{1.27}$$

where R^{depo} is the interest rate paid over the deposit, τ_i indicates the time partition occurring in the time interval $[t, T_i]$, N is the notional amount of the deposit account, and

T_i is the maturity of the deposit. The discounted value of a depo account at time t is

$$D(t,T_i) = NP(t,T_i)\big[1 + R^{depo}(t,T_i)\tau_i\big] \tag{1.28}$$

where $P(t,T_i)$ is the zero coupon bond used for discounting.

Forward Rate Agreement

Forward Rate Agreements (FRAs) have two different legs starting at time t. The floating leg pays the spot IBOR rate $L(T_{i-1},T_i)$[2] fixed at time $t = T_{i-1-\Delta}$[3] over the period $[T_{i-1},T_i]$. The fixed leg pays the fixed rate K over the period $[T_{i-1},T_i]$.
The price of the FRA at time t is

$$\begin{aligned} FRA(t,T_i,K) &= NP(t,T_i)\Big\{E_t^{\mathbb{Q}^{T_i}}\Big[L(T_{i-1},T_i) - K\Big]\Big\}\tau_i \\ &= NP(t,T_i)\Big[F(t,T_{i-1},T_i) - K\Big]\tau_i \end{aligned} \tag{1.29}$$

where the expected value is computed under the T_i-forward measure $\mathbb{Q}^{T_i}$ with numeraire $P(t,T_i)$. The relationship between the market IBOR rate and the bond implied forward rate is described in (1.33).
The FRA rate is defined as the fixed rate K making null the price of the FRA, therefore

$$R^{FRA}(t,T_i) = F(t,T_{i-1},T_i). \tag{1.30}$$

The FRAs are priced in the market according to the following principle: payments occurring at time T_i are anticipated (and discounted) at time T_{i-1}. Before introducing the FRA market price, we should apply a small variation in the notation. Indeed, we note the curves used to discount the payoffs in a different way to the forward curves used to assess the future value of the payoffs. The discount curve is then noted with a subscript d. The reason for this different notation regards the coexistence of curves used only for discounting and of curves used to assess the forward payments. Notwithstanding we discuss this argument in Chapter 2, we need to use this notation to make this formulation consistent with the developments we provide later. Ametrano and Bianchetti (2013) derived the price of a market FRA

$$\begin{aligned} FRA^{mkt}(t,T_i,K) &= NP_d(t,T_{i-1}) \\ &\times \left\{1 - \frac{1+K\tau_i}{1+F_d(t,T_{i-1},T_i)\tau_{d,i}} E_t^{\mathbb{Q}^{T_i}}\left[\frac{1+L_d(T_{i-1},T_i)\tau_{d,i}}{1+L(T_{i-1},T_i)\tau_i}\right]\right\}, \end{aligned} \tag{1.31}$$

[2] In this thesis we refer to the spot IBOR rate as $L(T_{i-1},T_i)$ and to the forward IBOR rate as $L(t,T_{i-1},T_i)$.

[3] For simplicity we assume that the time when the FRA starts coincides with the time when the IBOR rate is fixed.

where $\tau_{d,i}$ represents the time partition occurring in the discount curve and τ_i the time partition in the other yield curves. The FRA rate of the market-priced FRA is

$$R^{FRA,mkt}(t,T_i) = \frac{1}{\tau_i}\left\{ \frac{1 + F_d(t,T_{i-1},T_i)\tau_{d,i}}{E_t^{\mathbb{Q}^{T_i}}\left[\frac{1+L_d(T_{i-1},T_i)\tau_{d,i}}{1+L(T_{i-1},T_i)\tau_i}\right]} - 1 \right\}. \tag{1.32}$$

We observe that the market price of a FRA depends on the models for the spot and forward rates which are used as the reference rates for the discount curve

$$\begin{aligned} L_d(T_{i-1},T_i) &= \frac{1}{\tau_{d,i}}\left[\frac{1}{P_d(T_{i-1},T_i)} - 1\right], \\ F_d(t,T_{i-1},T_i) &= \frac{1}{\tau_{d,i}}\left[\frac{P_d(t,T_{i-1})}{P_d(t,T_i)} - 1\right]. \end{aligned} \tag{1.33}$$

Before the crisis, the forward IBOR rate was assumed to be equal to the forward rate defined using zero coupon bonds. However, this equivalence is not anymore satisfied: as we discuss in Section 1.2 and in Section 2.2.2, the financial crisis operated as a breaking mechanism, making the forward IBOR rate riskier than the forward rate.

Futures

Futures are interest rates derivatives whose payoff is comparable to the FRA one: the difference between these two products is that futures contracts are exchange-traded derivatives, while FRAs are OTC contracts. The Futures' payoff at time T_{i-1}, the interest fixing date, is

$$\Pi(T_{i-1},T_i) = N\Big[1 - L(T_{i-1},T_i)\Big], \tag{1.34}$$

and futures present value at time t is given by

$$\begin{aligned} Futures(t,T_i) &= E_t^{\mathbb{Q}}\Big[\Pi(T_{i-1},T_i)\Big] \\ &= N\Big\{1 - E_t^{\mathbb{Q}}\Big[L(T_{i-1},T_i)\Big]\Big\} \\ &= N\Big[1 - R^{Futures}(t,T_i)\Big], \end{aligned} \tag{1.35}$$

where $R^{Futures}(t,T_i)$ is the futures' rate, $\mathbb{Q}$ is the risk neutral probability measure associated with the bank account numeraire and the settlement date of futures payments is T_{i-1}.

However, the forward rate $L(t,T_{i-1},T_i)$ is not a martingale under the measure $\mathbb{Q}$, requiring a model for the dynamics of the forward rate with a convexity adjustment term[4].

[4]The forward rate $L(t,T_{i-1},T_i)$ was a martingale under $\mathbb{Q}$ in the single curve framework which was commonly adopted before the financial crisis. Nowadays, this relationship is not true anymore. We discuss this issue in the Chapter 2.

The convexity adjustment generally accounts for the volatility of the forward rate and the correlations between spot rates and forward rates. Therefore, the Futures' rate takes the form

$$R^{Futures}(t,T_i) = E_t^{\mathbb{Q}}\Big[L(T_{i-1},T_i)\Big] = E_t^{\mathbb{Q}^{T_i}}\Big[L(T_{i-1},T_i)\Big] + C^{Futures}(t,T_{i-1}) \tag{1.36}$$

where $\mathbb{Q}^{T_i}$ is the T_i-forward probability measure associated to the numeraire $P(t,T_i)$ and $C^{Futures}$ is the convexity adjustment term.
Since futures contracts are traded on public exchanges, they need to be regulated through the day-by-day marking to market of their market movements. Therefore, daily losses and profits on futures contracts need to be considered through the computation of a margin account, which - according to Ametrano and Bianchetti (2013) - takes the form

$$\Delta(t,t-1,T_i) = \frac{N'}{n}[Futures(t,T_i) - Futures(t-1,T_i)],$$

where n is the tenor of the contract and N' is the number of a traded unit with size of 1 million USD.
The standard structure of the contract, the daily margination and the low transaction costs make futures contracts very liquid interest rate derivatives.

Swap

Swaps contracts are OTC-traded interest rate derivatives consisting of two different legs. The floating leg depends on the IBOR rate $L(T_{i-1},T_i)$ and the fixed leg depends on a rate K. The two counterparties of the contract agree to exchange the net cash flows according to a predetermined time schedule $\mathbf{T} = t,T_1,...,T_n$. The interest rate swap could be considered as a collection of FRA contracts on different time intervals. Hence, the price of an interest rate swap (IRS) is - using vector notation - equal to

$$\mathbf{IRS}(t,\mathbf{T},K) = N[R^{IRS}(t,\mathbf{T}) - K]A(t,\mathbf{T}), \tag{1.37}$$

where N is the notional amount and the annuity $A(t,\mathbf{T})$ is

$$A(t,\mathbf{T}) = \sum_{i=1}^{n} P_d(t,T_i)\tau_i \tag{1.38}$$

and the swap rate $R^{IRS}(t)$ is defined as

$$R^{IRS}(t,\mathbf{T}) = \frac{\sum_{i=1}^{n} P_d(t,T_i)F(t,T_{i-1},T_i)\tau_i}{A(t,\mathbf{T})}, \tag{1.39}$$

where the numerator indicates the present value of the floating leg. The relation between the IRS rate and the swap annuity is such that the price of a portfolio of ZCBs could be represented as

$$R^{IRS}(t,\mathbf{T}) \times A(t,\mathbf{T}) \cong P(t,T_0) - P(t,T_n). \tag{1.40}$$

OIS

Overnight Indexed Swaps (OIS) are a particular version of IRS where the floating leg depends on overnight interest rates. The floating leg pays a compounded rate, $R^{overnight}(T_i,\mathbf{T})$, compounded from the overnight rates payed over the intervals (T_{i-1},T_i)[5]. We should note that the compounded rate $R^{overnight}(T_i,\mathbf{T})$ is different from the single overnight rate $R^{overnight}(T_{i,j-1},T_{i,j})$ payed over the period $[T_{i,j-1},T_{i,j}]$. Finally, the compounded overnight rate is

$$R^{overnight}(T_i,\mathbf{T}) = \frac{1}{\tau_i}\left\{\prod_{j=1}^{n_i}\left[1 + R^{overnight}(T_{i,j-1},T_{i,j})\tau_j\right] - 1\right\} \tag{1.41}$$

where τ_j is the overnight time partition and τ_i is the yearly time partition. Therefore, the present value of the OIS contract is

$$OIS(t,\mathbf{T},R^{overnight},K) = N\left[R^{OIS}(t,\mathbf{T}) - K\right]A(t,\mathbf{T}) \tag{1.42}$$

where

$$R^{OIS}(t,\mathbf{T}) = \frac{\sum_{i=1}^{n} P(t,T_i)R^{overnight}(t,\mathbf{T})\tau_i}{A(t,\mathbf{T})} \tag{1.43}$$

Assuming an hedging strategy with perfect collateral, we can formulate the OIS overnight rate $R^{OIS}(t,\mathbf{T})$ is equal to

$$\begin{aligned} A(t,\mathbf{T})R^{OIS}(t,\mathbf{T}) &= P(t,T_0) - P(t,T_n) \\ R^{OIS}(t,\mathbf{T}) &= \frac{P(t,T_0) - P(t,T_n)}{A(t,\mathbf{T})} \end{aligned} \tag{1.44}$$

where $P(t,T)$ are ZCBs used as collateral.

Basis swap

Basis swaps are interest rate derivatives where two counterparties exchange the net cash flows resulting from two floating legs. The two floating legs depends on two floating IBOR rates with two different tenors x and y. The reason for consider two different tenors is related to the multiple curve framework and we adopt this notation to make these formulas

[5] $\mathbf{T}$ indicates the time schedule for the compounded rate $R^{overnight}(T_i,\mathbf{T})$.

consistent with the bootstrapping formulas in Section 2.1.1.
Basis swaps are defined in two ways, depending on the structure of the contract. We indicate the payment schedules of the two IRSs, with respective tenors x and y, as $\mathbf{T_x}$ and $\mathbf{T_y}$.
The first method we can use to build a basis swap consists of a swap with two floating legs plus an interest rate spread Δ. Therefore, we can define the present value of this portfolio as

$$\begin{aligned}\mathbf{BSS}(t, \mathbf{T_x}, \mathbf{T_y}, \Delta) &= \mathbf{IRS}(t, \mathbf{T_x}) - \mathbf{IRS}(t, \mathbf{T_y}, \Delta) \\ &= N \left[\sum_{i=1}^{n_x} P_x(t, T_i) F_x(t, T_{i-1}, T_i) \tau_{x,i} - \right. \\ &\left. - \sum_{j=1}^{n_y} P_y(t, T_j) \left[F_y(t, T_{j-1}, T_j) + \Delta(t; \mathbf{T_x}, \mathbf{T_y}) \right] \tau_{y,j} \right] \\ &= \mathbf{IRS}(t, \mathbf{T_x}) - \mathbf{IRS}(t, \mathbf{T_y}) - N\Delta(t, \mathbf{T_x}, \mathbf{T_y}) A_y(t, \mathbf{T_y}),\end{aligned} \tag{1.45}$$

where τ represents the time partition and the annuity is

$$A_y(t, \mathbf{T_y}) = \sum_{j=1}^{n_y} P_y(t, T_j) \tau_{y,j} \tag{1.46}$$

and, imposing the portfolio's present value equal to zero, we obtain the basis swap spread

$$\Delta(t, \mathbf{T_x}, \mathbf{T_y}) = \frac{\mathbf{IRS}(t, \mathbf{T_x}) - \mathbf{IRS}(t, \mathbf{T_y})}{N A_y(t, \mathbf{T_y})}. \tag{1.47}$$

In the second method, we build a portfolio using two floating vs fixed swaps. The two swaps have different tenors and they have the same fixed leg K[6]. We define the two swaps borrowing from equation (1.37)

$$\begin{aligned}\mathbf{IRS_x}(t, \mathbf{T_x}, \mathbf{T}, K) &= N[R_x^{IRS}(t, \mathbf{T_x}, \mathbf{T}) - K] A(t, \mathbf{T}) = 0 \\ \mathbf{IRS_y}(t, \mathbf{T_y}, \mathbf{T}, K) &= N[R_y^{IRS}(t, \mathbf{T_y}, \mathbf{T}) - K] A(t, \mathbf{T}) = 0\end{aligned} \tag{1.48}$$

and the interest rate spread is defined as

$$\begin{aligned}\Delta(t, \mathbf{T_x}, \mathbf{T_y}, \mathbf{T}) &= R_x^{IRS}(t, \mathbf{T_x}, \mathbf{T}) - R_y^{IRS}(t, \mathbf{T_y}, \mathbf{T}) \\ &= \frac{\sum_{i=1}^{n_x} P_x(t, T_i) F_x(t, T_{i-1}, T_i) \tau_{x,i} - \sum_{j=1}^{n_y} P_y(t, T_j) F_y(t, T_{j-1}, T_j) \tau_{y,j}}{A(t, \mathbf{T})} \\ &= \frac{\mathbf{IRS}(t, \mathbf{T_x}) - \mathbf{IRS}(t, \mathbf{T_y})}{N A(t, \mathbf{T})}.\end{aligned} \tag{1.49}$$

As observed by Ametrano and Bianchetti (2013) the two methods of building a basis swap return two different results and the difference between the two results is measured by the

[6]We generally refer to the payment schedule of the fixed legs as $\mathbf{T}$.

spread

$$\Delta(t, \mathbf{T_x}, \mathbf{T_y}) = \frac{A_y(t, \mathbf{T_y})}{A(t, \mathbf{T})} \Delta(t, \mathbf{T_x}, \mathbf{T_y}, \mathbf{T}). \tag{1.50}$$

The basis swap spread is non-negative when the floating rate of the first swap is greater than the floating rate of the second swap.

1.1.3 Overview of most used interest rates

The spot IBOR rate $L(T_{i-1}, T_i)$ we have defined in the previous sections is the underlying interest rate of the vast majority of interest rate derivatives. There are many typologies of IBOR interest rates in the interbank money markets, depending on the currency area they are located in. IBOR rates differ for fixing and publication methods, tenor and panel of the contributing banks. In this section we briefly describe the most important interest rates used in the interbank market, such as the London Interbank Offered Rate (LIBOR), the Euro Interbank Offered Rate (EURIBOR) and the Euro Overnight Index Average (EONIA). The descriptions of each single interest rate refer to the publicly available informations which have been publishen on the official website of the designated contributor agent; all the informations are updated as of June 2020.

LIBOR

The London Interbank Offered Rate (LIBOR) was published for the first time in 1986 by the British Banker's Association, the LIBOR is under the admnistrative responsibility of the Intercontinental Exchange (ICE) and it is actually calculated by the data provider Thomson Reuters. The LIBOR is the primary benchmark rate set by the International Swaps and Derivatives Association (ISDA) for the OTC transactions. However, ISDA is reforming its reference parameters and LIBOR will not be published anymore after the end of 2021.
The LIBOR is fixed depending on the declarations of a group of selected banks, which - every business day of the London business calendar - submit to Thomson Reuters the interest rate they could borrow funds at in a reasonable inter-bank market size just prior to 11 a.m. GMT for some maturities in different currencies. Thomson Reuters computes the rate fixings at 11:45 a.m. GMT - after waiting the banks had adjusted their initial submissions. For each maturity, the calculation agent computes the average of the interest rates lying in the second and third quartiles of the polled data.
LIBOR rates are calculated for seven tenors (overnight, one week, one month, two months, three months, six months, one year) with respect to five different currencies (CHF, EUR, GBP, JPY, USD), then resulting in 35 single rates for every London business day.
There are 8, 12 or 16 selected banks for each currency and they are deputed by an

independent committee. The contributors panel is built with the aim of giving the closest representation of the trading activity related to a single currency in the London money market. The set of the contributors is reviewed semiannually depending on the dimension of the trading activity, the reputation and the trading expertise of the selected financial institutions. Table 1.1 shows the LIBOR panel composition as of June 2020.

Panel composition - LIBOR					
	USD	GBP	EUR	CHF	JPY
Bank of America NA	X				
Barclays Bank plc	X	X	X	X	X
BNP Paribas SA		X			
Citibank NA	X	X	X	X	
Cooperatieve Rabobank U.A.	X	X	X		
Crédit Agricole CIB	X	X			
Credit Suisse AG	X		X	X	
Deutsche Bank AG	X	X	X	X	X
HSBC Bank plc	X	X	X	X	X
JPMorgan Chase Bank NA	X	X	X	X	X
Lloyds Bank plc	X	X	X	X	X
Mizuho Bank Ltd		X	X		X
MUFG Bank Ltd	X	X	X	X	X
National Westminster Bank plc	X	X	X	X	X
Royal Bank of Canada	X	X	X		
Santander UK plc		X	X		
Société Générale		X	X	X	X
Sumitomo Mitsui BC Ltd	X				X
The Norinchukin Bank	X				X
UBS AG	X	X	X	X	X

Table 1.1: Contributing banks for each single LIBOR currency. Source: Intercontinental Exchange.

EURIBOR

EURIBOR was published for the first time in 1998, it is actually under the administrative responsibility of the European Money Market Institute (EMMI) and the Global Rate Set System Ltd (GRSS) is its calculation agent. It is the rate at which financial institutions located in EU and EFTA countries could borrow funds in the unsecured money market. EURIBOR is compliant with the Benchmarks Regulation (BMR) and, after the adjustment process to the new regulatory framework, has been confirmed as the reference rate for existing contracts and for contracts starting by January 2020 .
EURIBOR is published on every TARGET2[7] calendar day at 11 a.m. CET for five dif-

[7]TARGET2 is the payment infrastructure owned and managed by the Eurosystem. It is the platform for processing and executing payments denominated in EUR between the EU countries central banks and the commercial banks whose branches and subsidiaries are located in the European Union.

ferent tenors (one week, one month, three months, six months, one year). EURIBOR is computed as the average of the submissions received by a panel of selected contributing banks, after discarding the top and the bottom 15% of the polled interest rates.
The panel of banks submitting EURIBOR rates is made of 18 entities, which are displayed in Table 1.2. The banks are selected to guarantee an adequate representation of the euro money market and they are required to cope with the requirements and the obligations set by EMMI in the EURIBOR Governance Framework.

As anticipated before, EURIBOR is the object of a recently started reform plan of the

Panel composition - EURIBOR			
Belgium	Belfius	**Luxembourg**	Caisse d'Epargne de l'Etat
France	BNP-Paribas	**Netherlands**	ING Bank
	HSBC France	**Portugal**	Caixa Geral De Depositos
	Natixis	**Spain**	Banco Bilbao Vizcaya Argentaria
	Crédit Agricole		Banco Santander
	Société Générale		CECABANK
Germany	Deutsche Bank		CaixaBank SA
	DZ Bank	**UK**	Barclays
Italy	Intesa Sanpaolo		
	Unicredit		

Table 1.2: Contributing banks for country. Source: European Money Markets Institute.

EMMI authority. The final goal of the process is to enhance benchmark standards, in order to preserve the market from manipulation opportunities, to improve the transparency of the submitted rates and to augment the market's capability to be more robust and resilient during stress periods.

Other IBOR rates

There are many other IBOR rates, referring to currency areas characterised by smaller and less developed money markets. We just list the other IBOR rates, without deepening their features: AUD BBSW (Australian Bank Bill Rate, published by the Australian Financial Markets Association), BUBOR (Budapest Interbank Offered Rate, published by the Hungarian Forex Company), CAD CDOR (Canadian Dealer Offered Rate, published by the Montreal Exchange), DKK CIBOR (Copenaghen Interbank Offered Rate, published by the Danish Bankers Association), JIBAR (Johannesburg Interbank Average Rate, published by the Johannesburg Stock Exchange) and JPY TIBOR (Tokyo Interbank Offered Rate, published by the Japanese Bankers Association).

EONIA

The Euro Overnight Index Average (EONIA) is the weighted average of the interest rates paid over unsecured overnight interbank lending transactions executed by banks located in EU and EFTA countries. EONIA was published for the first time in January 1999; on October 2019, the EMMI decides that the EONIA will be computed - until 3 January 2022 - applying a fixed spread of 8.5 basis points over the Euro Short Term Rate (€STR). €STR is the new unsecured overnight benchmark rate substituting EONIA. The European Central Bank calculates the EONIA rate on behalf of the EMMI and it publishes EONIA at 9.15 a.m. CET on each TARGET2 calendar business day.

€STR

€STR represents the wholesale unsecured overnight interbank borrowing cost of euro area banks. It was published for the first time on 2 October 2019, following the recommendations of a private working group and a public consultation which lead EMMI to release a new benchmark framework.
€STR is computed as a volume weighted trimmed average of the volume-weighted distribution of interest rates lying between the second and third quartiles of the distribution. The observations are extracted from the wholesale market deposits reported by the credit institutions according to the standards set by the Money Market Statistical Regulation. €STR is published by the European Central Bank at 8:00 a.m. CET on each TARGET2 calendar business day.
Among the most important result of the overnight interest rates reform, there is the indication of the private sector group which is working on behalf of the EMMI authority: indeed, market participants in operations involving overnight rates in the Euro Money Market are invited to smoothly substitute EONIA with €STR as the benchmark interest rate for all contracts and products.

FED Fund Rate

The Federal Fund Rate is the interest rate paid on USD overnight unsecured borrowing transactions of reserve balances at the Federal Reserve Bank of New York between depository institutions (banks and credit unions). FED Fund Rate is under the administrative responsibility of the Federal Reserve Bank of New York since its first publication in 1954. It is computed as a volume weighted average and it is published every business day at 9:00 a.m. EST.

SOFR

The Secured Overnight Financing Rate (SOFR) is the interest rate paid on overnight borrowing transactions of USD cash with the collateralization of USD Treasury bonds. It is under the administrative responsibility of the Federal Reserve Bank of New York and it was published for the first time in April 2018. It is calculated as a volume weighted trimmed average and it is published every business day at 8:30 a.m. EST.

SONIA

The Sterling Overnight Index Average (SONIA) is the interest rate paid on GBP overnight unsecured borrowing bilateral or brokered transactions of wholesale funds. It is under the administrative responsibility of the Bank of England; it was published for the first time in March 1997 and it was reformed in April 2018. It is computed as a volume-weighted trimmed average depending on the second and third quartiles of the volume weighted distribution of interest rates of the daily data of GBP money market. It is published every business day at 9:00 a.m. GMT.

SARON

The Swiss Average Rate Overnight (SARON) is the interest rate paid on overnight repo transactions in the CHF money market. It was published for the first time in 2009 and it was reformed in 2017 according to the new standards set by the International Organization of Securities Commissions (IOSCO). It is calculated as a volume weighted average of the interest rates paid on repos concluded during the current trading day: indeed, it is published every ten minutes.

TONAR

The Tokyo Overnight Average Rate (TONAR, also called MUTAN) is the interest rate paid on JPY overnight unsecured borrowing transactions in the JPY money market. It is under the administrative responsibility of the Bank of Japan and it was published for the first time in 1996. It is calculated as the volume weighted average of the interest rates submitted by a set of selected brokers of the JPY money market. TONAR is published every business day at 10 a.m. JST.

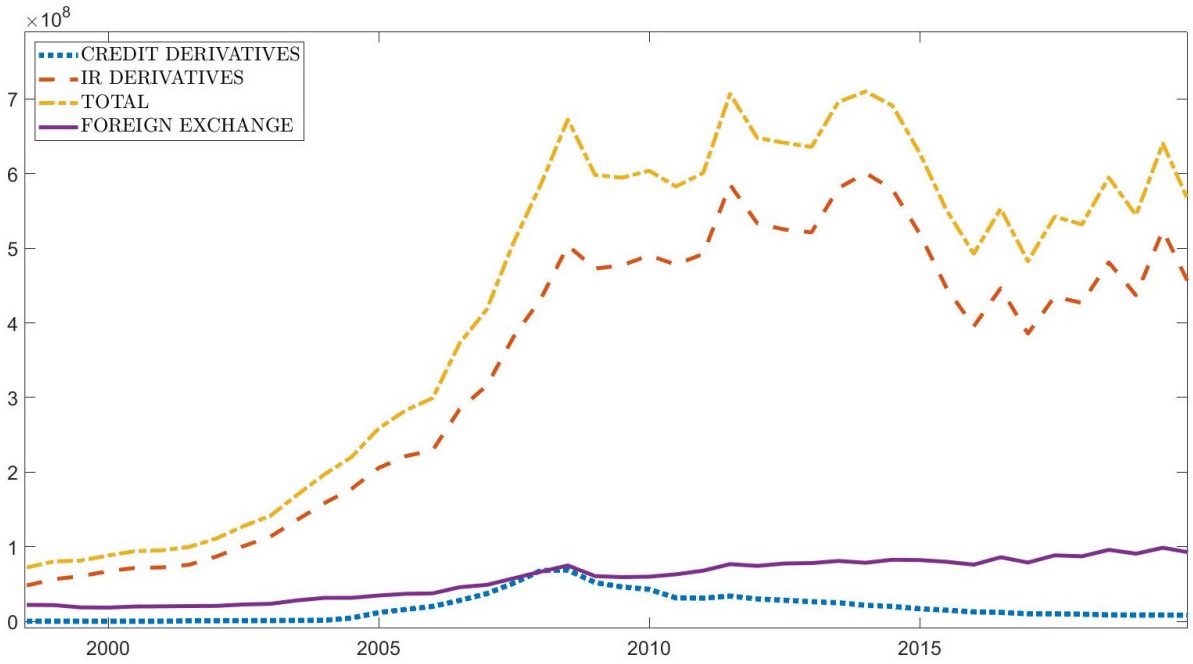

Figure 1.1: OTC derivatives notional amount outstanding by derivative class. Semi-annual observations over the period 1998-2019. Source: Bank for International Settlements.

1.2 The market after the credit crunch: a new pricing framework

In the last twenty years, the volume of outstanding derivatives which are traded over-the-counter (from now on we refer to them as OTC derivatives) has been constantly stepping up. As we can see from the Figure 1.1, the OTC derivatives notional amount was equal to 72 trillions of US dollars on January 1998 and it increased up to 558.5 trillions of US dollars on December 2019 - it was approximately 6.5 times the world GDP in 2018.
OTC interest rate derivatives are the largest share of OTC derivatives, accounting for 448.97 trillions of US dollars: interest rate derivatives' share is nearly 80% and FX and credit derivatives - the other two biggest class of derivatives - weigh respectively 16.50% and 1.45%. The dimension of the OTC derivatives market seems impressively big if compared with the world GDP. However, focusing only on the notional value of derivative contracts could be misleading. Indeed, we should consider a second measure in order to have closest view of the *real* size of the OTC derivatives market: the gross market value, which is defined as the replacement cost of a contract at its market value. The gross market value of the global OTC derivatives market was equal to 11.59 trillions of US dollars in the second half of 2019.
The Tables 1.3 and 1.4 show, respectively, the notional amounts outstanding and the gross market values of the three main classes of interest rate derivatives - forward rate agreements (FRAs), swaps and options - depending on the currencies they are denominated in, during the second half of 2019. We observe that interest rate derivatives are

most frequently denominated in the following currencies: EUR denominated interest rate derivatives' gross market value accounts for 4.09 trillions USD, USD interest rate derivatives' gross value is 1.65 trillions USD and GBP interest rate derivatives' gross value is 1.19 trillions USD. Observing the type of derivative contract, we notice that swap contracts are the most popular type of interest rate derivatives: indeed, swaps' gross market value amounts for nearly 90% of the gross value of all OTC interest rate derivatives.
The financial instruments in Tables 1.3 and 1.4 are the elementary tools of the interest rate risk management strategies that are adopted by major financial institutions all over the world, not only in the currency area they refer to.

Notional amounts outstanding - second semester 2019						
	TOT	USD	EUR	JPY	GBP	CHF
Total interest rate contracts	448965	159804	117173	37843	44146	3669
FRAs	67431	34984	19763	20	6954	630
Swaps	341292	103019	83863	36151	35368	3012
Total options	39916	21801	13547	1673	1824	26

Table 1.3: The notional amount of OTC interest rate derivatives depending on the currencies the contracts are denominated in. The amounts are expressed in billions of US dollars and they refer to the second half of 2019. Source: Bank for International Settlements.

The interest rate derivatives' market radically changed after the financial crisis in 2007, permanently modifying the conception of uncertainty and the risk aversion of the agents operating in financial markets. Grbac and Runggaldier (2015) consider the historical IBOR-OIS swap spread as a measure for the additional risk paid on swap contracts after the financial crisis. The IBOR-OIS swap spread best describes the reason behind the collapse of the financial sector: EURIBOR dynamics in the period from January 2007 to December 2012 reflects the increase of credit and liquidity risk within the European interbank unsecured market, leading the EURIBOR-EONIA swap spread to peak during 2009 and during the sovereign debt crisis in 2012. As Veronesi (2016), we take the spread between EURIBOR rates and EONIA as a proxy of the disruption suffered by financial markets. In Figure 1.2 we reproduce the spreads between four different maturities EURIBOR rates (1M, 3M, 6M, 12M) and the EONIA rate in the time interval from January

Gross market values - second semester 2019						
	TOT	USD	EUR	JPY	GBP	CHF
Total interest rate contracts	8352	1657	4093	471	1194	58
FRAs	204	47	96	0	24	2
Swaps	7463	1395	3625	445	1120	52
Total options	685	215	372	25	50	3

Table 1.4: The gross market value of OTC interest rate derivatives depending on thecurrencies the contracts are denominated in. The amounts are expressed in billions ofUS dollars and they refer to the second half of 2019. Source: Bank for International Settlements.

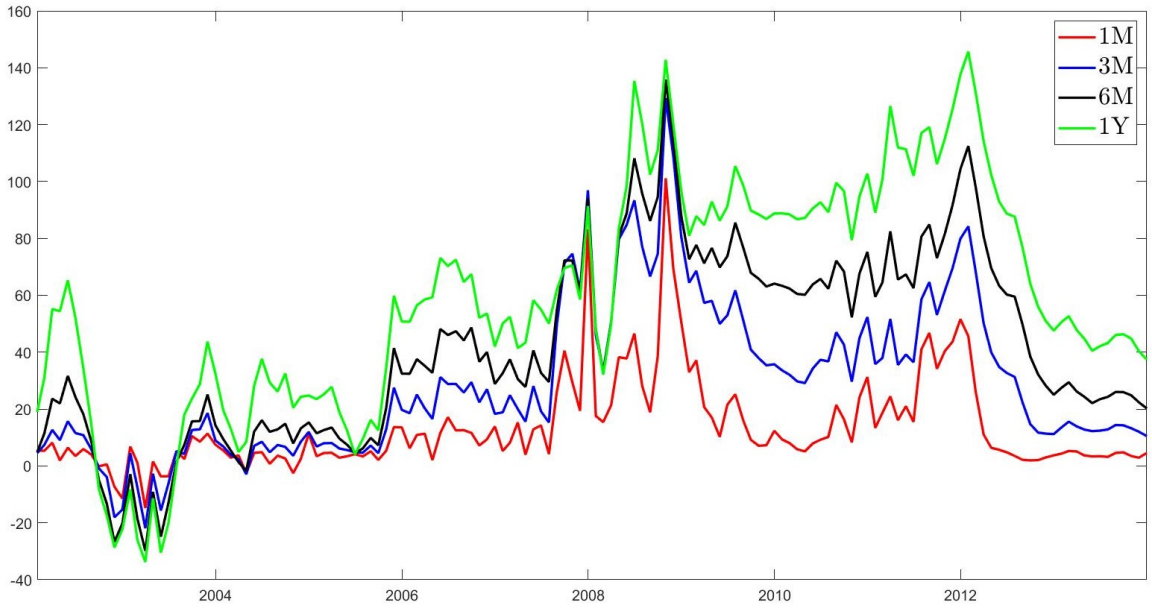

Figure 1.2: Monthly historical observations for EURIBOR1M-EONIA spread, EURIBOR3M-EONIA spread, EURIBOR6M-EONIA spread, EURIBOR1Y-EONIA spread in the period Jan2003-Dec2013. Spread values are measured in basis points on the left side. Sources: Thomson Reuters' Eikon; ECB.

2003 to December 2013. We observe that the spread was negligible before the financial crisis, since the credit and liquidity risk premia paid in the interbank market were insignificant; after August 2007, the spread dramatically increased and it started decreasing only after central banks adopted monetary policies to counteract the financial distress.
The divergence between the EURIBOR rates and EONIA can also be appreciated in Figure 1.3, where we have plotted the monthly historical observations of the rates in the time interval from January 1994 to July 2020. Furthermore, we note that the interest rates' curves whose tenor is greater are perceived as riskier.

The greater risk attributed to interest rates with a long-term maturity can be decomposed into three risk sub-elements. Indeed, when two counterparties enter into an interest rate swap whose floating leg is tied to EURIBOR rate with a given tenor, the two entities could face:

1. Borrowing and liquidity risk: counterparty 1 needs to borrow funds to pay counterparty 2, but it is prevented from borrowing because of a liquidity crunch;
2. Counterparty 1's default risk: counterparty 1 fails and does not settle the required payment;
3. Counterparty 2's default risk: counterparty 2 fails and does not settle the required payment.

As indicated by Grbac and Runggaldier (2015), a study of Filipovic and Trolle (2013)

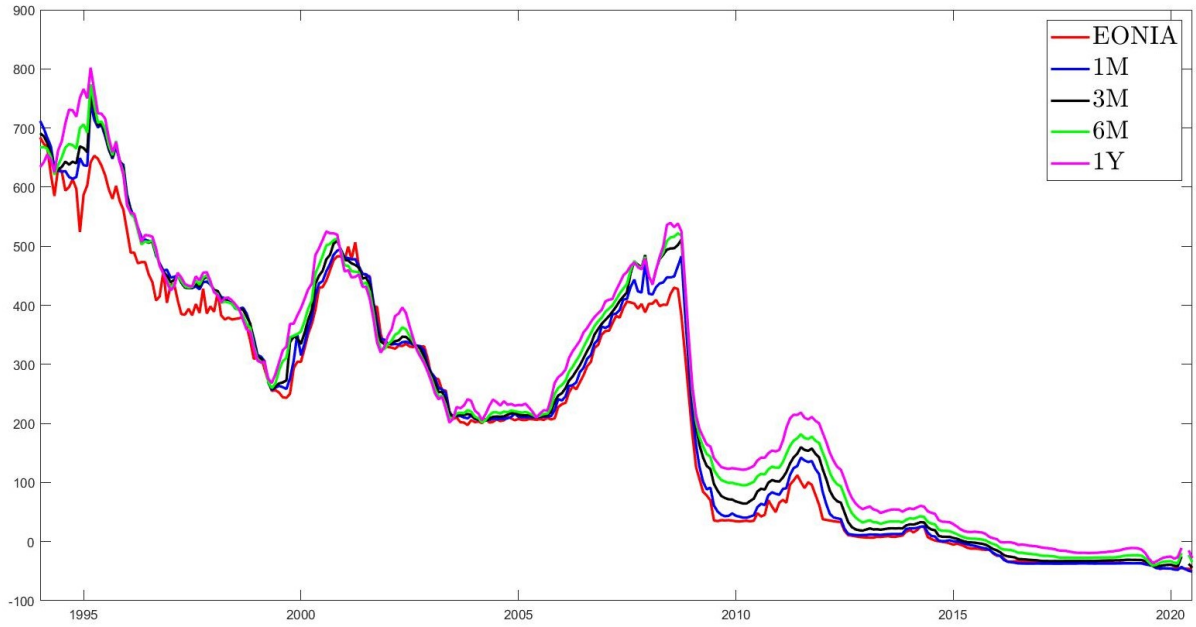

Figure 1.3: Monthly historical observations for EONIA, EURIBOR1M, EURIBOR3M, EURIBOR6M, EURIBOR1Y in the period Jan1994-Jul2020. Interest rates are measured in basis points on the left side. Sources: Thomson Reuters' Eikon; ECB.

assess that the default risk component was the main driver of the overall interbank risk during the period from August 2007 to January 2011.

The interbank risk was considered to be negligible before the financial crisis and, consequently, it didn't entered the interest rate derivatives pricing framework which was used by financial markets practitioners until 2007. However, after the credit crunch suffered by financial markets in 2007, these elements could not be neglected anymore: liquidity and default risks implied by IBOR rates were too significant to make IBOR rates dynamics close to the one of OIS rates[8] and they must be necessarily considered when pricing interest rate derivatives whose payments are tied to IBOR rates.

We should moreover consider that, as we have observed in Figure 1.2 and Figure 1.3, additional interbank riskiness affects in a different way IBOR interest rates depending on their tenor. The displacement of the IBOR curves after the financial crisis is described in Bianchetti (2011) and it can be depicted as the representation in Figure 1.4: on the left side of the figure we have the IBOR curve before the credit crunch; on the right side of the curve we have a market segmentation into different rate curves with different tenors, the highest segmented curve correspond to the curve bearing the highest perceived risk. The segment on the top right represents the IBOR12M curve, the segment below represents the IBOR6M curve and so on until we reach the segment on the bottom right, which represents the OIS rate curve.

Therefore, the credit and liquidity crunch unleashed by the financial crisis of 2007 can be considered - according to Bianchetti (2011) - as a "simmetry breaking mechanism" lead-

[8] As we pointed out in Subsection 1.1.3, EONIA is considered the benchmark risk-free rate from market participants.

ing to a world where a single short rate process is not sufficient anymore to model and describe the term structure of interest rate curves with different tenors; indeed, interest rate derivatives whose underlying interest rates have different tenors must be considered as characterised by dissimilar interest rate dynamics when assessing their future value.
We try to better explain the shift in the pricing framework after the financial crisis introducing the pricing of a basis swap. Before the credit crunch, all floating legs were priced using a single IBOR curve and, therefore, they had the same future value; the future cash flows were then discounted using the same IBOR curve. After the credit crunch, the floating legs may not be replicated anymore with a single yield curve but they were determined using different IBOR curves for each different payment's tenor; then, the future cash flows were discounted using an IBOR curve, in case of unsecured transactions, or an OIS curve, in case of secured transactions.
The relationship between forward IBOR rates $L(t, T_{i-1}, T_i)$ and bond implied forward rates $F(t, T_{i-1}, T_i)$ before the financial crisis was equal to

$$L(t, T_{i-1}, T_i) = \frac{1}{\tau_i} E^{\mathbb{Q}^{T_i}} \left[\frac{1}{P(T_{i-1}, T_i)} - 1 \middle| \mathcal{F}(t) \right] = \frac{1}{\tau_{d,i}} \left[\frac{P_d(t, T_{i-1})}{P_d(t, T_i)} - 1 \right] = F(t, T_{i-1}, T_i). \tag{1.51}$$

Indeed, the forward IBOR rate was calculated as the conditional expected value of the spot IBOR rate under the T_i-forward probability measure $\mathbb{Q}^{T_i}$. However, after the market segmentation unleashed by the financial crisis, the relationship in equation (1.51) was not satisfied anymore

$$L(T_{i-1}, T_i) = \frac{1}{\tau_i} \left[\frac{1}{P(T_{i-1}, T_i)} - 1 \right]. \tag{1.52}$$

A new representation of the spot and forward IBOR rates is provided in Section 2.2.2.
The combination of OIS discounting and the presence of different risky rates for different yield curves dislodged interest rate modelling from a single curve framework to a multiple curve one. The multiple curve framework is discussed in detail in Chapter 2.

1.2.1 Unsecured and secured transactions

In this section we broadly describe the characteristics of unsecured and secured financial transactions, pointing how the financial crisis impacted on the collateral choices of financial operators.
Starting from the foundations, we refer to a collateral as the cash amount or the set of assets which a borrower pledges to a lender when entering into a secured loan. Therefore, we can define a secured financial transaction as an agreement where the lender receives the collateral if the borrower fails to repay the debt she owes or, if the borrower meets her obligations, the collateral - and, eventually, the interest accumulated on it - is returned by the lender to the borrower. Vice versa, an unsecured transaction doesn't provide any protection for the lender because no collateral is required to any of the two counterparties

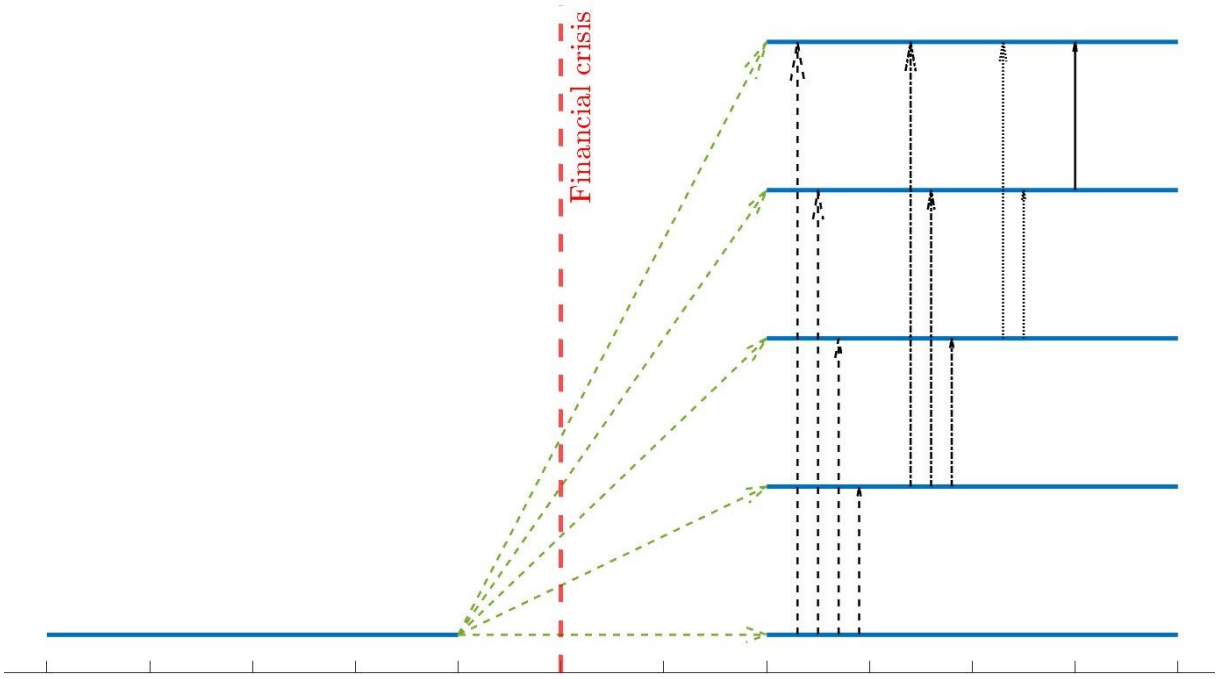

Figure 1.4: Graphic reprentation of the curve displacement after the financial crisis. The left side of the figure represents the single IBOR yield curve which was used to derive all the i-tenor yield curves before the finacial crisis. The right side of the figure represents the market segmentation occurred after the financial crisis: the i-tenor yield curve is derived by instruments with different underlying i-tenor interest rate dynamics. Source: Bianchetti (2011).

when entering the transaction.

After the financial crisis, it becomes clear that counterparty credit risk was an important element to consider. Indeed, we observe a contraction of unsecured transactions in Figure 1.5: while the share in total average turnover of unsecured inter-bank transactions in the Euro Money Market was approximately equal to one fifth before 2007, it started decreasing until it reached 4.45% in 2013. On the opposite side, secured market consolidated as the largest share of the Euro Money Market immediately after the crisis. As indicated by the Financial Stability Review released by the ECB on December 2010, the secured market transactions cleared by central counterparties increased from a 41% share of total turnover in 2009 to a 45% in 2010; the reason underlying this shift is twofold: together with the necessity of lowering counterparty credit risk, the increase was related to a greater number of European financial institutions joining the repo platforms developed by central counterparties.

When entering into a secured financial transaction the two counterparties have to commit an agreed amount to a collateral account. The collateral, which remains a property of the collateral giver, is object of two different analysis. The first one is related to the periodical mark-to-market activity of the value of the financial contract and it concerns the integration of the value of the collateral by the counterparty whose position has lost in value. The second analysis entering the contract is related to the computation and the

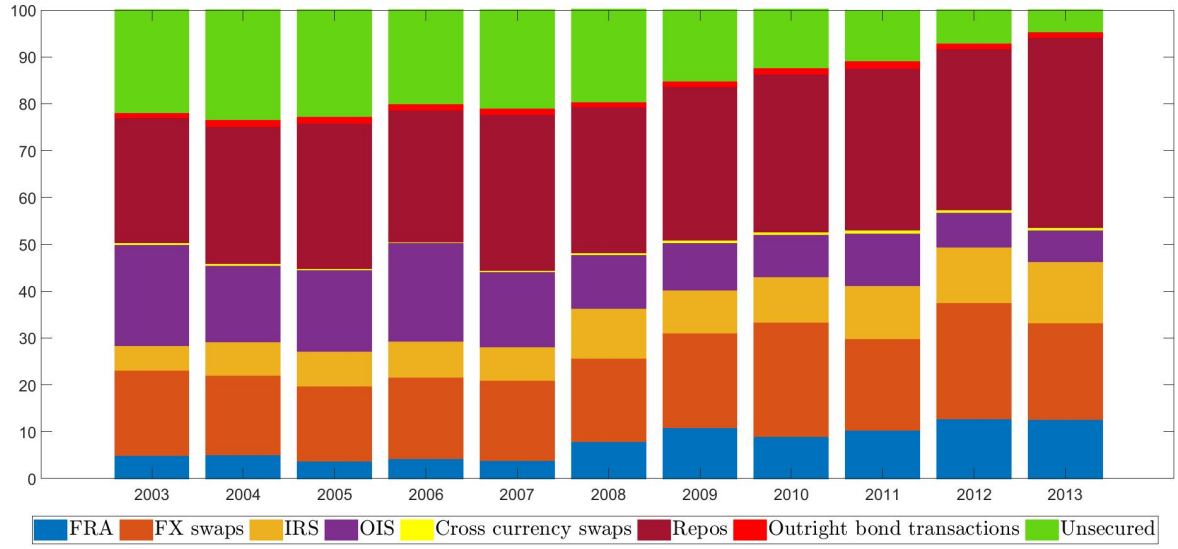

Figure 1.5: Shares in total average daily turnover of inter-bank transactions executed in the Euro Money Market during the time period from January 2003 to December 2013. The share of unsecured market transaction generally refers to all market segments and instruments. Source: Money Market Survey, ECB data.

payment of the interests accredited to a single counterparty on her collateral account. The mechanisms ruling the continuous assessment of the market value of the contract and of the compounded interests on the collateral account are defined depending the transaction is bilateral or between multiple counterparties.
There exist two main *contract* structure in order to regulate an OTC secured transaction:

1. The most used contracts for two counterparties entering an OTC bilateral transaction are the ISDA master agreement and the Credit Support Annex (CSA). Master agreements are proposed and defined by the International Swaps and Derivatives Association (ISDA), they provide the general terms applying to a certain type of transactions; ISDA master agreements have three attached documents - the Schedule, the Confirmation letter and, the most important, the CSA. The CSA establishes the collateral characteristics and the margination rules; it can be considered as the *core* document of the contract. In Europe, the market practice is represented by the UK CSA with the transferral of the property of the collateral to the creditor from the debitor. In USA, the market practice is represented by the US CSA with no transferral of the property of the collareral.

2. The alternative used by multiple counterparties when entering a secured contract is the central clearing of the contract. Central clearing is operated by central counterparties (CCPs) or clearing houses (CHs), which usually specialize in particular market segments and market instruments, e.g. the most important CCPs for the clearing of IRS and credit default swaps are the ones operated by Intercontinental Exchange (ICE) in USA and UK. The role of a CCP is to centralise the OTC trans-

actions and to reduce the counterparty risk borrowed by each single agent entering the contract. Risk reduction is obtained by the CCP imposing participation constraints, providing a guarantee fund and asking for the posting of collateral into the CCP's account - an initial margin is posted at the beginning and a variation margin is posted by the counterparty whenever the value of the daily marked-to-market position of any counterparty decreases. Furthermore, the CCP nets all the payments between the counterparties, minimizing the liquidity needs - and the liquidity risk - of counterparties involved in multiple payments.

As we have observed in Figure 1.5, the secured transactions represents the lion share in the inter-bank money market. The predominance of secured transactions is mainly justified by three reasons: the individual preferences of market agents towards transactions with limited counterparty risk, the market practice of entering into contracts regulated by CSA agreements or by central clearing and, finally, the regulatory framework that was built by national and international regulators after the financial crisis.
European Market Infrastructure Regulation (EMIR) represents one of the most considerable effort put bu the European regulator with the aim to reduce the systemic risk and to improve the financial stability of European financial markets. The regulation imposes mandatory risk management practices and disclosure requirements to financial counterparties, which have to adapt their operations to a set of common rules regarding OTC derivatives, CCPs and trade repositories.
In order to provide an example, we now consider the EMIR collatereal requirements on the derivatives' transactions of the investment funds located in the Euro area. According to the observations reported in the Financial Stability Review of May 2020, the notional amount of the cumulated derivative exposures of investment funds was close to 13 EUR trillion with interest rate derivatives, equity derivatives, and foreign exchange derivatives accounting for almost 90% of the overall notional value; Figure 1.6 explains the composition of derivative portfolios for each class of mandate pursued by an investment fund. The regulation introduced daily settlement of initial/variation margins for a large amount of derivative portfolios. The effect, which can be observed in Figure 1.7, was an increase of the collateralisation of derivative portfolios in the last year, in order to comply with the deadlines set by the EMIR with the posting of initial and variation margin - also for non central-cleared transactions.

The shift from unsecured to secured financial transactions after the financial crisis led financial counterparties to another shift in their operations: from IBOR discounting curve to OIS discounting curve. Indeed, as observed by Hull and White (2013), almost every financial institutions entering into a collateralized transaction, notwithstanding it is regulated by central clearing or by a bilateral ISDA master agreement, adopts OIS rates as a proxy of the risk-free interest rates in order to evaluate their portfolios; vice versa, IBOR rates are used by financial institutions when discounting the future value of their

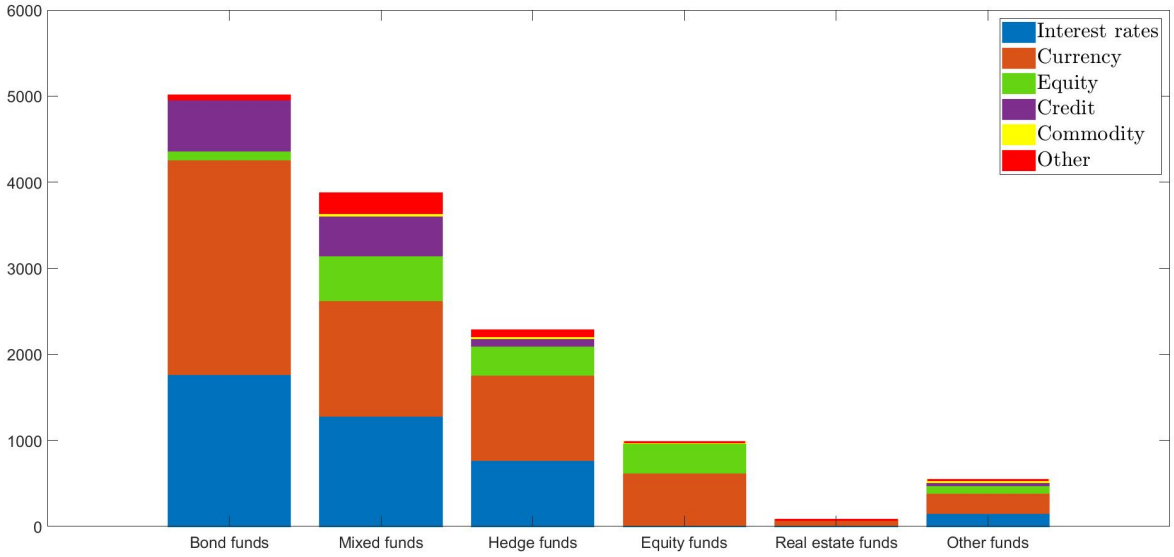

Figure 1.6: Derivative portfolios by fund strategy. Derivatives are measured in EUR billions and they represent the size observed as of March 2020. Source: EMIR reporting data, European Central Bank (2020).

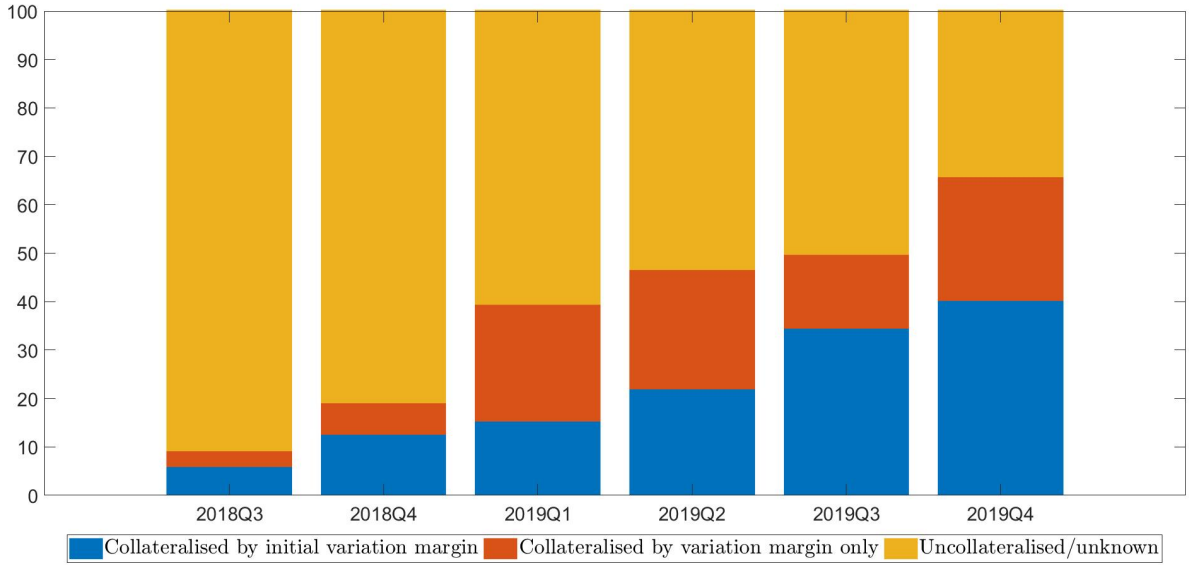

Figure 1.7: Collateralisation of derivative portfolios of euro area investment funds. Data are shown as percentages of the notional amount estimated at the end of the respective quarter. Source: EMIR reporting data, European Central Bank (2020).

uncollateralized portfolios.
These conclusions are implied by the assumption of no arbitrage. Indeed, the future cash flows deriving from a collateralized transaction should be discounted using the same interest rate of the funding rate which, in this case, is equal to the collateral rate. Being the collateral posted as a cash amount or as a portfolio of very liquid and safe assets, e.g. treasury bonds, the interest rate applied to the collateral is the risk-free one. On the opposite side - by the same no arbitrage assumption, the future cash flows of uncollateralized contracts are discounted using the funding rate on the money market.
The differences between OIS and IBOR discounting are analyzed in Bianchetti and Carlicchi (2013), which observe the differences of the premia paid over caps and floors when discounted using the EONIA-based discount curve and the EURIBOR-based discount curve: the premia computed using the EURIBOR curve imply an higher risk premia than the premia obtained through EONIA discounting; the same relationship is obtained by the authors when observing that the EONIA implied volatilities are systemically lower than the EURIBOR implied volatilities.

Summing up, in this chapter we observed the sources accompanying pricing frameworks in financial markets from a single curve world to a multiple curve world: the presence of risky interest rates leading to multiple yield curves used to evaluate future cash flows and - depending on the collateralization of the contract - the presence of different discounting curves.

Chapter 2

Pricing derivatives with the multiple curve framework

Interest rate derivatives pricing in the multiple curve framework is adopted by practitioners when market quotes are not available because of the complexity of the derivative's structure they need to price. These kind of interest rate derivatives are commonly called *exotic* derivatives and their payoffs depend on multiple segments of the term structure - e.g. Bermudan swaptions depend on as many swap rates as there are exercise dates; on the opposite side, less complex or *vanilla* interest rate derivatives depend only on one or two rates in the term structure - e.g. cap and floor options are commonly priced as portfolios of caplets and floorlets, and each single payment depends only on a single rate. The procedure a quantitative analyst should follow in order to price an exotic interest rate derivative can be generalized in the following steps:

1. Bootstrapping a single discount curve, multiple yield curves and multiple volatility cubes[1] using linear financial instruments and vanilla options;

2. Assume a specific model to evaluate an interest rate process - for example, selecting the Hull-White model to describe the short rate;

3. Select a vanilla interest rate derivative which can be priced assuming no arbitrage and whose prices are quoted by data providers - for example, cap and floor options can be priced using the Black formula and treating them as portfolios of caplets and floorlets;

[1] Volatility cubes are matrices whose *dimensions* are given by date, tenor and volatility. The volatility cube is usually interpolated from volatilities quotes through a bootstrapping algorithm. For example, caps/floors volatility cubes are normally quoted by data providers and they are usually represented as a matrix - like the one we provided in Table 4.1, representing a simplified version whose dimensions are given only by the expiry and the strike value.

4. Calibrate - using an appropriate calibration algorithm - the chosen model using the quotes of the financial instruments we have selected in the previous step;

5. Price exotic interest rate derivatives using the calibrated model and a Monte Carlo simulation;

6. Build an hedging strategy deriving the Greeks and using a set of linear financial instruments as hedging instruments.

This chapter can be considered as the general framework in which the analysis and the study we develop in Chapter 3 and Chapter 4 can be contextualized. Our goal is not to build a comprehensive pricing tool for exotic options, implementing all the different steps we listed above. Conversely, we limit ourselves to the implementation of a calibration algorithm in Chapter 4, estimating the parameters of the Hull-White model using the quoted volatilities of cap options. Therefore, we discuss in the first section of this chapter the principal bootstrapping procedures of the discount curve and of the yield curves. The key steps of term structure modelling - points from 2. to 4. - are presented in the second section, discussing the multiple curve extension of short rate models and focusing on the Hull-White version of the Vasicek short rate model. In the third and last section we shortly discuss Monte Carlo simulation for short rate models.

2.1 Yield curves construction

2.1.1 Bootstrapping formulas

According to Grbac and Runggaldier (2015) and Henrard (2014) there exist two distinct methods of constructing multiple yield curves starting from market quotes: the first method is the *exact fit*, where yield curves are retrieved applying bootstrapping and interpolation to a set of linear financial instruments; the second method is the *best fit*, where the yield curves are assumed to have a precise form, e.g. Nelson-Siegel formula or Svensson formula, whose parameters are later calibrated from market data. As the section's title makes clear, we discuss only the first method.
Before diving in the bootstrapping formulas, the selection of financial instruments must be done according to two principles: homogeneity and funding, which make bootstrapping consistent with the IBOR curves' segmentation involved by the multiple curve framework. These general principles can be found both in Ametrano and Bianchetti (2013) and in Henrard (2014). The homogeneity rule requires that the linear financial instruments used to bootstrap the yield curves must have the same rate tenor of the interest rate derivatives which are priced using the bootstrapped yield curves; the same applies for the linear

financial instruments used to hedge interest rate derivatives. The funding rule requires that the discounting curve must be derived by an interest rate which is consistent with the interest rate payed over the funding account; this relationship satisfies the principle of no-arbitrage.

The recursive procedure underlying the bootstrapping of financial instruments radically changed with respect to the one based on the single curve framework we have described in Chapter 1. The presence of multiple yield curves and of a single discount curve leads to the development of a new approach when dealing with vanilla financial instruments; this approach is best described by Ametrano and Bianchetti (2013), representing, together with Andersen and Piterbarg (2010), the principal reference we have considered for this section.

The multiple curve framework requires the adoption of several yield curves y^m_{tn}, depending on the m-fundamental variable of the term structure and on the different tenor tn of the interest rate. In our analysis we consider the fundamental variables $m = P_{tn}(t,T), FRA(t,T_i,K)$. We then contemplate yield curves derived by zero coupon bonds $P_{tn}(t,T)$ paying an interest rate with tenor tn and yield curves derived by FRA rates $R^{FRA,mkt}_{tn}(t,T+tn)$, which are derived by zero coupon bonds with tenor tn[2]. The most common tenors are $tn = \{overnight, 1M, 3M, 6M, 12M\}$.

Ametrano and Bianchetti (2013) define the yield curves for $t < T$

$$y^{FRA}_{tn}(t) := \{T \to F_{tn}(t,T,T+tn)\}, \tag{2.1}$$

$$y^{P}_{tn}(t) := \{T_i \to P_{tn}(t,T)\}, \tag{2.2}$$

Bootstrapping requires we carefully handle all the specific instruments used to build a particular section of the term structure. The complexity of bootstrapping instruments selection arises from the observation that similar market instruments could present very different prices depending on their underlying. Moreover, they could present a different market liquidity, making their quotes less informative.

These features, together with the respect of the homogeneity and the funding principles, require that we carefully select which instruments we should include when bootstrapping points of the curve at a given maturity. Furthermore, we should consider that many instruments overlap in many section of the term structure: these overlaps could affect the quality of the bootstrapped curve, since the vector of dates of the term structure - the bootstrapping pillars of the term structure - coincides with the time schedule of the selected instruments.

When approaching yield curve bootstrapping, a practitioner should consider that the resulting bootstrapped curve is characterised by several features. Indeed, the main characteristics of a yield curve are:

[2]Remember from equation (1.30) that $R^{FRA,mkt}_{tn}(t,T+tn) = F(t,T,T+tn)$.

1. the ZCB's rate conventions - the day count convention in European financial markets equals the year fraction of the rate process to $\frac{actual}{365}$;

2. the FRA rate conventions - the day count convention in European financial markets equals the year fraction of the rate process to $\frac{actual}{360}$;

3. the reference date t of the the yield curve, such that $P(t,t) = 1$. The reference date in European markets is equal to the spot date, which is fixed two business days after today;

4. time pillars, determining which points of the yield curve are obtained through bootstrapping and which other are obtained through interpolation;

5. the currency;

6. the business calendar - TARGET2 calendar is adopted in European financial markets;

7. type of interpolation, see Subsection 2.1.2;

8. the choice between endogenous or exogenous discount curves.

One of the most subtle issues among those we have just listed regards the difference between endogenous and exogenous bootstrapping. Endogenous bootstrapping is coherent with the assumptions of the single curve framework and it consists in discounting a general yield curve y^m_{tn} using the yield curve of zero coupon bonds, y^P_{tn}; on the opposite, exogenous bootstrapping is consistent with the funding principle of the multiple curve framework and it requires that the discount factors are taken from an a priori given yield curve y^P_d, which is consistent with the yield curve of the collateral. This issue is discussed both in Ametrano and Bianchetti (2013) and in Henrard (2014). They both conclude that - using Henrard (2014) words - endogenous bootstrapping is the "wrong number used in the wrong formula to obtain the correct result". Indeed, notwithstanding endogenous bootstrapping is not consistent with the new pricing framework and it leads to important deviations of the prices and hedging strategies of interest rate derivatives, it is still a good option to get the right market prices of bootstrapped linear financial instruments, e.g. FRA and IRS. Endogenous bootstrapping is discussed later in this chapter, when presenting the *pseudo* bonds used for discounting in Section 2.2.
Finally, yield curves are built using different type of bootstrapping instruments, which are selected after considering for probable overlaps in some sections of the term structure and trying to exclude the majority of overlapping financial instruments. Furthermore, practitioners should consider instruments which are as liquid as possible, because their quotations are more reliable. The construction of a yield curve over the time interval from today to a long term maturity, e.g. 30 years, is also considered when selecting bootstrapping instruments.

In the following paragraphs, the bootstrapping formulas related to the most popular bootstrapping instruments are presented.

Deposits

In Chapter 1 we defined the present value of an OTC traded Deposit as equation (1.28). Exchange traded deposits are normally selected to build the short-term section of the yield curves y^m_{tn}. Indeed, the first pillar of the FRA curve (2.1) is directly obtained from the market rate $R^{depo}_{tn}(t, T_i) = L(t, T_i)$, which refer to a set of i-deposits with maturity T_i and tenor $tn = T_i - t$. The reader should note that, with respect to equation (1.28), we added the subscript tn to the deposit and to the depo rate, in order to account for the different tenors of the considered interest rates. Indeed, a deposit paying IBOR rate with a long tenor bears a greater amount of risk than deposit paying an IBOR rate with a shorter tenor.
The pillars at time $t < T_i$ of the discount curve (2.2) are extracted from

$$P_{tn}(t, T_i) = \frac{1}{1 + R^{depo}_{tn}(t, T_i)\tau_i} \tag{2.3}$$

where the variable τ_i indicates the time partition.

FRA

Market FRAs are used to bootstrap the short-term section of the yield curves y^m_{tn}. The pillars of the curve y^{FRA}_{tn} for $t < T_i$ are directly obtained using the market FRA rates $R^{FRA,mkt}_{tn}(t, T_i)$. The pillars of the discount curve y^P_{tn} for $t < T_i$ are obtained applying a bootstrapping algorithm based on

$$P_{tn}(t, T_i) = \frac{P_{tn}(t, T_{i-1})}{1 + R^{FRA,mkt}_{tn}(t, T_i)\tau_i}. \tag{2.4}$$

The limit of the market FRA rate for T_{i-1} going to t is equal to the interest rate of the exchange traded deposit

$$\lim_{T_{i-1} \to t} R^{FRA,mkt}_{tn}(t, T_i) = R^{depo}_{tn}(t, T_i). \tag{2.5}$$

Futures

Market future, $Futures(t, T_i)$, can be used to build the pillars of the FRA curve y^{FRA}_{tn} for $t < T_i$. The pillars of the FRA curve are directly obtained modifying equation (1.36) and

they are equal to

$$F_{tn}(t, T_{i-1}, T_i) = R_{tn}^{Futures}(t, T_i) - C_{tn}^{Futures}(t, T_i^e) \tag{2.6}$$

where T_i^e is the expiry date of the contract and $C^{Futures}$ is the convexity adjustment term. The expiry date T_i^e is defined such that the settlement lag is equal to the time interval between the fixing date and the expiry date.
On the other side, the pillars of the discount curve y_{tn}^P for $t < T_i$ are obtained applying a recursive algorithm based on

$$P_{tn}(t, T_i) = \frac{P_{tn}(t, T_{i-1})}{1 + [R_{tn}^{Futures}(t, T_i) - C_{tn}^{Futures}(t, T_i^e)]\tau_i} \tag{2.7}$$

where τ_i represents the year fraction occurring between the expiry date T_i^e and T_i.

IRS

IRS contracts are used to bootstrap the long-term section of the yield curves. The fixed leg of the IRS is paid annually and it follows the payment schedule $\mathbf{S} = \{s, ..., S_j\}$, while the floating leg follows the calendar of the underlying IBOR rate and, therefore, its payment schedule is $\mathbf{T} = \{t, ..., T_i\}$. We refer to the notation introduced in Section 2.1.1. The pillars of the discount curve y_{tn}^P and the pillars of the FRA curve y_{tn}^{FRA} when $T_i = S_j$ are respectively obtained applying the bootstrapping algorithms

$$F_{tn}(t, T_{i-1}, T_i) = \frac{R_{tn}^{IRS}(t, T_i)A_d(t, T_i) - \sum_{\alpha=1}^{i-1} P_d(t, T_\alpha)F_{tn}(t, T_{\alpha-1}, T_\alpha)\tau_i}{P_d(t, T_i)\tau_i} \tag{2.8}$$

$$P_{tn}(t, T_i) = \frac{P_d(t, T_i)P_{tn}(t, T_{i-1})}{R_{tn}^{IRS}(t, T_i)A_d(t, T_i) - \sum_{\alpha=1}^{i-1} P_d(t, T_\alpha)F_{tn}(t, T_{\alpha-1}, T_\alpha)\tau_i + P_d(t, T_i)} \tag{2.9}$$

where

$$A_d(t, T_i) = \sum_{\alpha=1}^{i} P_d(t, T_\alpha)\tau_i = A_d(t, T_{i-1}) + P_d(t, T_i)\tau_i. \tag{2.10}$$

If the fixed schedule $\mathbf{S}$ and the floating schedule $\mathbf{T}$ are equal, the above equations reduce to

$$F_{tn}(t, T_{i-1}, T_i) = \frac{R_{tn}^{IRS}(t, T_i)A_d(t, T_i) - R_{tn}^{IRS}(t, T_{i-1})A_d(t, T_{i-1})}{P_d(t, T_i)\tau_i} \tag{2.11}$$

$$P_{tn}(t, T_i) = \frac{P_d(t, T_i)P_{tn}(t, T_{i-1})}{R_{tn}^{IRS}(t, T_i)A_d(t, T_i) - R_{tn}^{IRS}(t, T_{i-1})A_d(t, T_{i-1}) + P_d(t, T_i)}. \tag{2.12}$$

OIS

As already mentioned at the end of Chapter 1, OIS contracts are used to bootstrap the discount curve. Indeed, the collateral rate used for collateralised financial instruments is the overnight rate underlying OIS contracts and, according to the *funding* principle we have previously outlined, this rate must be consistent with the one used for discounting. The FRA curve, whose tenor, tn, is overnight and whose time fraction τ is equal to 1 day, is obtained as

$$F_c(t, T_{i-1}, T_i) = \frac{1}{\tau_i}\left\{\frac{P_c(t, T_{i-1})\left[1 + R_{tn}^{OIS}(t, T_i)\tau_i\right]}{\left[R_{tn}^{OIS}(t, T_{i-1}) - R_{tn}^{OIS}(t, T_i)\right]A_c(t, T_{i-1}) + P_c(t, T_{i-1})} - 1\right\}, \quad (2.13)$$

and the discount curve is obtained as

$$P_c(t, T_i) = \frac{\left[R_{tn}^{OIS}(t, T_{i-1}) - R_{tn}^{OIS}(t, T_i)\right]A_c(t, T_i) + P_c(t, T_{i-1})}{1 + R_{tn}^{OIS}(t, T_i)\tau_i}, \quad (2.14)$$

where the subscript c refers to the fact that the rate of the collateral is used as the rate of the discounting curve and the annuity term $A_c(t, T_i)$ is defined in equation (1.38). Ametrano and Bianchetti (2013) provide also the single curve version of equations (2.13) and (2.14), which can then be represented as

$$F_c(t, T_{i-1}, T_i) = \frac{1}{\tau_i}\left\{\frac{P_c(t, T_{i-1})\left[1 + R_{tn}^{OIS}(t, T_{i-1})\tau_i\right]}{1 - R_{tn}^{OIS}(t, T_i)A_c(t, T_{i-1})} - 1\right\}, \quad (2.15)$$

$$P_c(t, T_i) = \frac{1 - R_{tn}^{OIS}(t, T_i)A_c(t, T_i)}{1 + R_{tn}^{OIS}(t, T_i)\tau_i}. \quad (2.16)$$

Basis swaps

Basis swaps are used to bootstrap the long-term section of the yield curves. Basis swaps are used in the multiple curve framework to retrieve IRS on multiple underlying IBOR tenor (e.g. 1M, 3M, 12M), starting from a different IBOR tenor (e.g. 6M).
Therefore, we can extrapolate the IRS rate on a given tenor, tn, from a basis swap receiving IBOR with tenor tn and paying IBOR 6M

$$R_{tn}^{IRS}(t, \mathbf{T}, \mathbf{S}) = R_{6M}^{IRS}(t, \mathbf{T}, \mathbf{S}) + \Delta(t, \mathbf{T_{tn}}, \mathbf{T_{6M}}, \mathbf{S}) \quad (2.17)$$

where the quoted basis spread $\Delta(t, \mathbf{T_{tn}}, \mathbf{T_{6M}}, \mathbf{S})$ for an interest rate basis swap with the two aforementioned swaps as underlying satisfies the following equation

$$\Delta(t, \mathbf{T_{tn}}, \mathbf{T_{6M}}, \mathbf{S}) = -\Delta(t, \mathbf{T_{6M}}, \mathbf{T_{tn}}, \mathbf{S}). \quad (2.18)$$

2.1.2 Interpolation

The financial instruments we have listed in the previous section are used to build the pillars of a discrete yield curve. However, if we want to build a continuous curve for a period longer than two years[3], we need more informations to fill the empty areas between the nodes we have retrieved with the bootstrapping procedures illustrated before. The technique of *completing* the *missing* values of the yield curve is called interpolation. In this section we provide a review of the most considered local and global interpolation methods, underlining their strengths and their critical issues.
Interpolation must be handled with care because, depending on the technique we decide to apply, a wrongly-interpolated curve could lead to slightly different economic interpretations or it could lead to sub-optimal hedging strategies after having computed imprecise risk factors (i.e. sensitivities) over some portions of the interpolated curve. This subsection refers extensively to the analysis developed in Chapter 5 of Kienitz (2014).

Constant interpolation

Constant interpolation is the most simple method. The constant interpolation can be obtained equalling the *missing* values to the closest node on the left or, alternatively, to the closest node on the right. However, we observe from Figure 2.1 that the resulting curve is not continuous and, therefore, we can say that constant interpolation doesn't represent a reasonable approach.

Linear interpolation

Linear interpolation is a simple method too. The yield curve at time t, y_t, is obtained applying the straightforward formula

$$y_t = \frac{t - t_{i-1}}{t_i - t_{i-1}} x_i + \frac{t_i - t}{t_i - t_{i-1}} x_{i-1}$$

where x_i and x_{i-1} are the values of the nodes for $t_{i-1} \leq t \leq t_i$. We observe from Figure 2.1 that the yield curve is continuous but not globally differentiable. A broad review of the most common linear interpolators can be found in Hagan and West (2006), which focus their analysis on linear and cubic spline methods.

[3]Henrard (2014) states that for period longer than two years there is quite often only one yearly observation for a specific yield curve and, consequently, there are as many *missing* values as the number of business days.

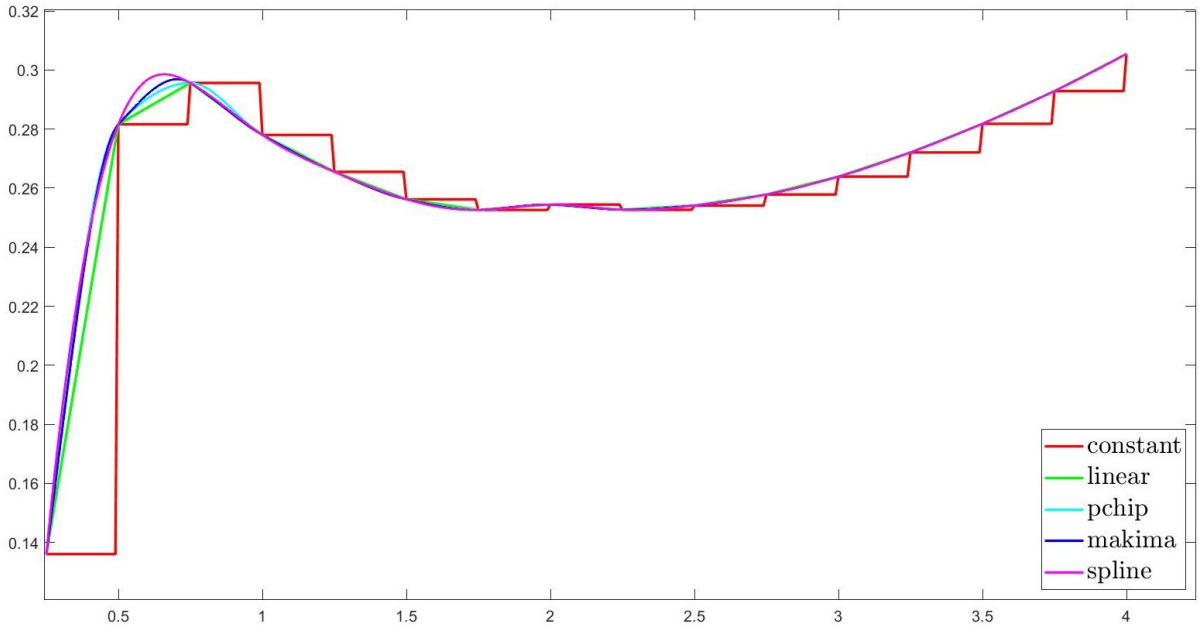

Figure 2.1: Different interpolation methods applied to an hypothetical yield curve. We apply the interpolation methods of the Matlab function *interp1* to an hypothetical yield curve. The *pchip* method refers to shape-preserving piecewise cubic interpolation. The *makima* method refers to a modified Akima cubic Hermite interpolation and it is modified to avoid outliers. The *spline* method refers to a spline interpolation using not-a-knot end conditions.

Cubic spline interpolation

The spline interpolation returns us a continuous and differentiable yield curve. It is obtained applying the function

$$y_t = a_i(t - t_i)^3 + b_i(t - t_i)^2 + c_i(t - t_i) + d_i. \tag{2.19}$$

The equation has $4(n-1)$ unknown parameters, where n is the number of interpolated time pillars. The equation has also the following constraints: $n-1$ left interval bounds, $n-1$ right interval bounds, $n-2$ constraints given by the differentiability assumption and additional constraints on the partial derivatives of the curve with respect to time. Therefore, when we choose the values of the partial derivatives of the curve we are also choosing the slope of the interpolated curve. We now provide a series of methods - as they are listed in Kienitz (2014) - fixing additional n constraints to fully assess the functional dependence.

1. Together with $n-2$ differentiability constraints, we postulate equal to zero the second partial derivatives of the curve with respect to time when time is equal to t_1 and t_n. This interpolation method is called natural cubic spline;

2. Together with $n-2$ differentiability constraints, we apply linear interpolation to the

nodes between t_0 and t_1 and we apply constant interpolation to the nodes between t_{n-1} and t_n;

3. Together with $n-2$ differentiability constraints, we apply quadratic interpolation to the nodes between t_0 and t_1 and we apply linear interpolation to the nodes between t_{n-1} and t_n. This is the McCulloch-Kochin spline interpolator;

4. Together with $n-2$ differentiability constraints, we choose the parameters c_1 and c_N, which represent respectively the slope of the quadratic function passing through the first three points and the slope of the function passing through last three nodes. This is the deBoor spline interpolator;

The different cubic spline interpolation methods could distinctly affect the quality and the behavior of the interpolated curve. Indeed, the simple splines we have introduced in this subsection show sometimes oscillatory behavior, other times they do not lead to a monotonic behavior, or, since we use nodes from different intervals, these methods could lead extreme convexity and lack of locality. Locality is an important property to consider when evaluating different interpolation methods: a curve is interpolated with a *local* method if the effect of a change of its underlying rate is observed only in a time interval which is as close as possible to the time of the interest rate's shift; indeed, an interpolation method is *local* if it "takes into account the data in that region, and not the data some distance away" (Hagan and West (2006)). Lack of locality could negatively affect the assessment of the risk factors over the interpolated curve.
Another considerable issue is related to the fact that the bootstrapping procedures require the interpolation of unknown values inside the bootstrapping mechanism itself: indeed, when dealing with different financial instruments with different time schedules, it is quite unusual - if not impossible - that the bootstrapped rates up to a given time exactly match the schedule of the inputs which are necessary to compute the rates from then on. Ametrano and Bianchetti (2013) address three main vulnerabilities of applying non-local interpolation techniques inside the bootstrapping algorithm. The first issue is that the shape of the early sections of the yield curve continuously change while adding other nodes to the bootstrapped yield curve. The second problem is related to imprecise deltas, whose effect overcomes the node upon which the hedging ratio is calculated. Finally, they observe a lower computational performance of the bootstrapping algorithm and, consequently, a smaller efficiency of the computed hedging ratios.
In the next subsections we introduce some alternatives which have been proposed to overcome those critical issues.

Hermite splines

Hermite splines try to solve the locality problem setting the parameters of equation (2.19) as

$$
\begin{aligned}
a_{i-1} &= \frac{-2\frac{x_i - x_{i-1}}{t_i - t_{i-1}} - s_i - s_{i-1}}{(t_i - t_{i-1})^2}, \\
b_{i-1} &= \frac{3\frac{x_i - x_{i-1}}{t_i - t_{i-1}} - s_i - 2s_{i-1}}{t_i - t_{i-1}}, \\
c_{i-1} &= s_{i-1} \quad \text{and} \quad d_{i-1} = x_{i-1},
\end{aligned}
$$

where the parameter s_i can be freely chosen by the analyst.

Bessel splines

Bessel splines are obtained imposing the following shape to the parameter s_i

$$
s_{i-1} = \frac{(t_i - t_{i-1})\frac{x_i - x_{i-1}}{t_i - t_{i-1}} + (t_i - t_{i-1})\frac{x_{i-1} - x_{i-2}}{t_{i-1} - t_{i-2}}}{t_i - t_{i-1}}
$$

We refer to Kienitz (2014) for further improvements of Bessel splines by considering different formulations of the parameter s_i. Bessel splines make interpolation as local as possible.

Harmonic splines

Harmonic splines are obtained imposing the following formulation to the parameter s_i

$$
\frac{1}{s_{i-1}} = \frac{\Big[t_{i-1} - t_{i-2} + 2(t_i - t_{i-1})\Big](t_{i-1} - t_{i-2})}{3(t_i - t_{i-2})(x_{i-1} - x_{i-2})} + \frac{\Big[2(t_{i-1} - t_i) + t_i - t_{i-1}\Big](t_i - t_{i-1})}{3(t_i - t_{i-2})(x_i - x_{i-1})}
$$

Harmonic splines consistently limit the problem of non-locality of interpolation.

Kruger splines

The interpolated curve resulting from Kruger splines is monotonic. The lack of monotonicity is solved imposing the following constraints to the partial derivative of the curve at each time t_i

$$
\frac{\partial y(t_i)}{\partial t} = \begin{cases} 0 & \text{if slope changes after } t_i \\ 2\left(\frac{t_{i+1} - t_i}{x_{i+1} - x_i} - \frac{t_i - t_{i-1}}{x_i - x_{i+1}}\right)^{-1} & \text{otherwise} \end{cases}
$$

and the partial derivatives of the curve at time t_1 and at time t_n are set to be respectively equal to

$$\frac{\partial y(t_1)}{\partial t} = \frac{3(x_2 - x_1)}{2(t_2 - t_1)} - \frac{y(t_2)}{2} \text{and} \quad \frac{\partial y(t_n)}{\partial t} = \frac{3(x_n - x_{n-1})}{2(t_n - t_{n-1})} - \frac{y(t_n)}{2}.$$

Tension splines

Tension splines are useful to limit non-locality problems of interpolated curves. Tension splines are determined by additional n constraints on the second partial derivative of the curve

$$\frac{\partial^2 y(t)}{\partial t^2} = \frac{t_{i+1} - t}{t_{i+1} - t_i}\left(\frac{\partial^2 y(t_i)}{\partial t^2} - \sigma^2 y(t_i)\right) + \frac{t - t_i}{t_{i+1} - t_i}\left(\frac{\partial^2 y(t_{i+1})}{\partial t^2} - \sigma^2 y(t_{i+1})\right) + \sigma^2 y(t)$$

where σ is the *tension* parameter which is used to localize the tension spline. A broad review about tension splines can be found in Andersen (2007), but, according to Henrard (2014), the interpolation framework proposed by the author should be handled with care, since it is not suitable for the multiple curve framework.

Effects of interpolation on hedging strategies

When dealing with options modelling in Chapter 4, we don't consider hedging strategies. However, we believe it is useful to introduce the effects that different interpolation techniques could have on hedging; and we address this issue by referring to the results reported by Henrard (2014). Before going on, we should remember that, when computing hedging ratios, only the interest rate's level and the chosen interpolator method affect the sensitivities: indeed, the market price of a single financial instruments used to determine a single node of the interpolated curve does not affect the prices of the other instruments in the calibrating basket.
Henrard (2014) computes the hedging ratios for a forward swap starting in 18 months and with a maturity of 7 years and 6 months. The hedging strategies are obtained as a ratio between the delta of the forward swap at each node and the delta of the financial instruent used to calibrate that node. The author reports huge differences between the deltas computed in different interpolation schemes, accounting for differences between different sensitivities for a single node up to 30%. The divergences between deltas under different interpolation schemes lead to contrasting hedging strategies. Considering a forward swap with a notional amount of 100 million USD, the linear interpolation requires hedging spot instruments with a notional amount of 200 million, the cubic spline technique requires 530 million and the double quadratic technique requires 330 million.

2.2 Short rate models in the multiple curve framework

Term structure modelling is one of the most important step of the pricing mechanism described at the beginning of this chapter. In this section, we discuss only short rate models for the term structure in the multiple curve framework. We focus on exponentially affine factor models, avoiding to consider for exponentially quadratic models. We discuss only this specific class of term structure models because it is preparatory to the construction of the calibration algorithm for the Hull-White model we describe in the second part of this dissertation.
One of the most complete analysis of short rate models in the multiple curve framework is the one provided in Chapter 2 of Grbac and Runggaldier (2015), which emphasize the study of Vasicek and Hull-White models.
The exponentially affine models discussed by Grbac and Runggaldier (2015) show correlation between the short rate and the spread payed over different tenors. The three elements to be considered to understand the framework developed by the two authors are the short rate $r(t)$, the spread $s_{tn}(t)$ for each tenor tn and the difference $\Delta(t)$ between two consecutive spreads, e.g. $\Delta(t) = s_2(t) - s_1(t)$ for $tn = 1, 2$. In order to simplify the presentation, Grbac and Runggaldier (2015) consider just two tenors.

The framework developed by Grbac and Runggaldier (2015) is built on the assumption that the short rate $r(t)$, the spread $s_{tn}(t)$ and the spread difference $\Delta(t)$ are driven by different factors $\psi_i(t)$ with $i = 1, 2, 3, 4$. The processes of the factors under the risk neutral probability measure $\mathbb{Q}$ can be specified as

$$d\psi_i(t) = \big(a_i - b_i\psi_i(t)\big)dt + \sigma_i\sqrt{c_i\psi_i(t) + d_i}dW_i^{\mathbb{Q}}(t). \tag{2.20}$$

Each i-factor is independent of the others because its Brownian motion $W_i^{\mathbb{Q}}(t)$ is independent of the other random motions. The first factor drives the short rate, the rate spread and the difference between spreads; the authors consider for the correlations between the short rate and the spreads and between the short rate and the spread difference adding a multiplicative factor ρ to the dynamics of the three objects. Furthermore, the other three factors are considered to be specific of each process they appear in. We can describe the three processes as

$$\begin{aligned} r(t) &= \psi_1(t) + \psi_2(t) \\ s(t) &= \rho_s\psi_1(t) + \psi_3(t) \\ \Delta(t) &= \rho_\Delta\psi_1(t) + \psi_4(t) \end{aligned} \tag{2.21}$$

where the first factor is described by equation (2.20) with $c_1 = 0$ and $d_1 = 1$

$$d\psi_1(t) = \big(a_1 - b_1\psi_1(t)\big)dt + \sigma_1 dW_1^{\mathbb{Q}}(t) \tag{2.22}$$

while the other factors are described by equation (2.20).

There are several ways to improve the capacity of the processes to fit the original term structure. Indeed, parameters a_i can be modified to be time varying parameters rather than constant parameters. This choice ascribes additional complexity to the analytical and computational treatments. Another strategy to improve the term structure fit is the construction of a different formulation for $r(t)$

$$r(t) = \psi_1(t) + \psi_2(t) + \phi(t)$$

where $\phi(t)$ represents a time deterministic shift. Using time varying a_i parameters in the equation representing a mean-reverting process, (2.22), yields the Hull-White model.

2.2.1 The affine model class: Vasicek and CIR models

According to Grbac and Runggaldier (2015), the process $\psi(t)$ can be modelled using a Vasicek representation assuming that the parameters in equation (2.20) take the form $c_i = 0$ and $d_i = 1$.

$$d\psi(t) = \big(a - b\psi(t)\big)dt + \sigma dW^{\mathbb{Q}}(t). \tag{2.23}$$

The authors studied the term structure equation starting from a transformation of the factor $\psi(t)$ and considering two additional parameters γ and K. The transformation of $\psi(t)$ can be represented as a conditional expectation on the sigma-algebra $\mathcal{F}(t)$

$$E\bigg\{ \exp\bigg[-\int_t^T \gamma\psi(s)ds - K\psi(T)\bigg]\bigg|\mathcal{F}(t)\bigg\} = \exp\big[A(t,T) - B(t,T)\psi(t)\big]. \tag{2.24}$$

The terms $A(t,T)$ and $B(t,T)$ satisfy the system

$$\begin{cases} \frac{\partial B(t,T)}{\partial t} - bB(t,T) + \gamma = 0 \\ \frac{\partial A(t,T)}{\partial t} = aB(t,T) - \frac{\sigma^2}{2}B^2(t,T) \end{cases} \tag{2.25}$$

where $A(T,T) = 0$ and $B(T,T) = K$ and the solutions solving the system are

$$\begin{aligned} B(t,T) &= K\exp\big(-b(T-t)\big) - \frac{\gamma}{b}\bigg[\exp\big(-b(T-t)\big) - 1\bigg] \\ A(t,T) &= -a\int_t^T B(s,T)ds + \frac{\sigma^2}{2}\int_t^T B^2(s,T)ds \\ &= -a\bigg[\frac{1-\exp\big(-b(T-t)\big)}{b}\bigg(K - \frac{\gamma}{b}\bigg) + \frac{\gamma}{b}(T-t)\bigg] \\ &+ \frac{\sigma^2}{2}\bigg[\frac{1-\exp\big(-2b(T-t)\big)}{2b}\bigg(K^2 + \frac{\gamma^2}{b^2} - 2K\frac{\gamma}{b}\bigg) \\ &+ \frac{\gamma^2}{b^2}(T-t) - 2\bigg(1 - \frac{\gamma}{b}K\bigg)\frac{1-\exp\big(-b(T-t)\big)}{b}\bigg]. \end{aligned} \tag{2.26}$$

A proof of the Vasicek model can be found in Chapter 3 where we present the single factor version of the model.

The Cox-Ingersoll-Ross version of the Vasicek model is obtained substituting for $c_i = 1$ and $d_i = 0$ in factors' equations (2.21) and, omitting the i-subscript to generalize, we obtain that

$$d\psi(t) = \big(a - b\psi(t)\big)dt + \sigma\sqrt{\psi(t)}dW^{\mathbb{Q}}(t). \tag{2.27}$$

Furthermore, the values of $A(t,T)$ and $B(t,T)$ in the expected value of equation (2.24) conditional on the sigma-algebra $\mathcal{F}(t)$ become

$$\begin{cases} \frac{\partial B(t,T)}{\partial t} - bB(t,T) - \frac{\sigma^2}{2}B^2(t,T) + \gamma = 0 \\ \frac{\partial A(t,T)}{\partial t} = aB(t,T) \end{cases} \tag{2.28}$$

with $B(T,T) = K$ and $A(T,T) = 0$ and the solution solving the system are provided by Grbac and Runggaldier (2015)

$$\begin{aligned} B(t,T) &= \frac{K\Big(h + b + \exp\big(h(T-t)\big)(h-b)\Big) + 2\gamma\Big(\exp\big(h(T-t)\big) - 1\Big)}{K\sigma^2\Big(\exp\big(h(T-t)\big) - 1\Big) + h - b + \exp\big(h(T-t)\big)(h+b)} \\ A(t,T) &= \frac{2a}{\sigma^2}\log\left(\frac{2h\exp\big(\frac{(T-t)(h+b)}{2}\big)}{K\sigma^2\big(\exp\big(h(T-t)\big) - 1\big) + h - b + \exp\big(h(T-t)\big)(h+b)}\right) \end{aligned} \tag{2.29}$$

where $h = \sqrt{b^2 + 2\gamma\sigma^2}$. Finally, the authors found that the price of an OIS bond can be represented - for $\gamma = 1$ and $K = 0$ - as

$$\begin{aligned} P(t,T) &= E^{\mathbb{Q}}\left\{\exp\left[-\int_t^T \Big(\psi_1(u) + \psi_2(u)\Big)du\right]\middle|\mathcal{F}(t)\right\} \\ &= \exp\Big[A_1(t,T) + A_2(t,T) - B_1(t,T)\psi_1(t) - B_2(t,T)\psi_2(t)\Big]. \end{aligned}$$

Example: a three factors framework

Grbac and Runggaldier (2015) provided also a framework with three factors. The processes of the factors under the risk neutral probability $\mathbb{Q}$ are

$$\begin{aligned} d\psi_1(t) &= (a_1 - b_1\psi_1(t))dt + \sigma_1 dW_1^{\mathbb{Q}}(t) \\ d\psi_i(t) &= (a_i - b_i\psi_i(t))dt + \sigma_i\sqrt{c_i\psi_i(t) + d_i}dW_i^{\mathbb{Q}}(t), \quad i = 2,3. \end{aligned} \tag{2.30}$$

Furthermore, the processes of the factors under the T-forward measure $\mathbb{Q}^T$ are

$$\begin{aligned}
d\psi_1(t) &= \Big(a_1 - \big(\sigma_1\big)^2 B_1(t,T) - b_1\psi_1(t)\Big)dt + \sigma_1 dW_1^{\mathbb{Q}^T}(t) \\
d\psi_2(t) &= \Big(a_2 - d_2\sigma_2^2 B_2(t,T) - \psi_2(t)\big(b_2 + c_2\sigma_2^2 B_2(t,T)\big)\Big)dt + \sigma_2\sqrt{c_2\psi_2(t) + d_2}\,dW_2^{\mathbb{Q}^T}(t) \\
d\psi_3(t) &= \big(a_3 - b_3\psi_3(t)\big)dt + \sigma_3\sqrt{c_3\psi_3(t) + d_3}\,dW_3^{\mathbb{Q}^T}(t)
\end{aligned} \tag{2.31}$$

where the $W_i^{\mathbb{Q}^T}$ Brownian motions with $i = 1, 2, 3$ are mutually independent and the functions $B_1(t,T)$ and $B_2(t,T)$ are given by

$$\begin{aligned}
B_1(t,T) &= -\frac{1}{b}\big[\exp\big(-b(T-t)\big) - 1\big] \\
B_2(t,T) &= \frac{2\big[\exp\big(h(T-t)\big) - 1\big]}{h - b + (h+b)\exp\big(h(T-t)\big)}
\end{aligned}$$

with $h := \sqrt{b^2 + 2\sigma^2}$. The proof is provided in Section 2.1.2 of Grbac and Runggaldier (2015).

The probability distribution of the process of the first factor under the T-forward measure $\mathbb{Q}^T$ is Normal with mean μ_{ψ_1} and variance σ_{ψ_1} which are respectively given by

$$\begin{aligned}
\mu_{\psi_1} &= \exp(-b_1 t)\Big(\psi_1(0) + \Big(\frac{a_1}{b_1} - \frac{\sigma_1^2}{b_1^2}\Big)\Big(\exp(b_1 t - 1)\Big) + \frac{\sigma_1^2}{2b_1^2}\exp(-b_1 T)\Big(\exp(2b_1 t) - 1\Big)\Big) \\
\sigma_{\psi_1} &= \frac{\sigma_1^2}{2b_1}\Big(\exp(2b_1 t) - 1\Big)\exp(-2b_1 t).
\end{aligned}$$

Conversely, the distribution of the processes of the other two factors follow different distributions depending on the values of the parameter c_i and d_i for $i = 2, 3$ in equation (2.30). Indeed, for $c_i = 1$ and $d_i = 0$ the processes follow a Noncentral chi-squared distribution under the T-forward measure $\mathbb{Q}^T$ with k degrees of freedom and the a parameter λ. Conversely, for $c_i = 0$ and $d_i = 1$ the processes have a Normal distribution.

2.2.2 Formulation of the IBOR rate after the crisis

As introduced in Chapter 1, after the credit crunch unleashed by the financial crisis of 2007 the IBOR rates $L(T,S)$ for $S > T$ were determined also by counterparty and liquidity risk, such that the spread between IBOR and OIS rates became not negligible anymore

$$L(T,S) \neq F(T,T,S) = \frac{1}{S-T}\Big(\frac{1}{P(T,S)} - 1\Big). \tag{2.32}$$

The approach developed by Henrard (2014) is to use "pseudo-discount factors" derived by pseudo bond $P^*(t,T)$ which are not traded in public markets and are supposed to be affected by the same risks determining the IBOR rates. Therefore, the IBOR rate can be

represented as

$$L(T,S) = \frac{1}{S-T}\Big(\frac{1}{P^*(T,S)} - 1\Big). \tag{2.33}$$

The expected value of the pseudo bond price $P^*(t,T)$ conditional on the sigma-algebra $\mathcal{F}(t)$ under the risk neutral probability measure $\mathbb{Q}$ is given by the short rate process $r(t)$ and by a spread process $s(t)$ incorporating the risks borne by interbank transactions

$$P^*(t,T) = E^{\mathbb{Q}}\bigg[\exp\bigg(-\int_t^T \big(r_u + s_u\big)du\bigg)\bigg|\mathcal{F}(t)\bigg]. \tag{2.34}$$

Grbac and Runggaldier (2015) used a variation of the model presented in (2.21) to obtain a representation of $P^*(t,T)$ and of prices of interest rate derivatives. They assume that the short rate and the spread are respectively described by

$$\begin{aligned} r(t) &= \psi_1(t) + \psi_2(t) \\ s(t) &= \rho\psi_1(t) + \psi_3(t) \end{aligned} \tag{2.35}$$

where the coefficient ρ measures the intensity of the correlation between factor $\psi_1(t)$ and factor $\psi_2(t)$. Furthermore, the authors assume that the processes of factor $\psi_1(t)$ has the same form of (2.22) and factors $\psi_2(t)$ and $\psi_3(t)$ have the same form of (2.20) with $c_i = 0$. Therefore, the three factors follow mean-reverting Vasicek-like dynamics under the risk neutral probability $\mathbb{Q}$

$$\begin{aligned} d\psi_1(t) &= \big(a_1 - b_1\psi_1(t)\big)dt + \sigma_1 dW_1^{\mathbb{Q}}(t) \\ d\psi_2(t) &= \big(a_2 - b_2\psi_2(t)\big)dt + \sigma_2 dW_2^{\mathbb{Q}}(t) \\ d\psi_3(t) &= \big(a_3 - b_3\psi_3(t)\big)dt + \sigma_3 dW_3^{\mathbb{Q}}(t) \end{aligned} \tag{2.36}$$

Grbac and Runggaldier (2015) obtain that the price of a zero coupon bond on the OIS rate can be described as

$$P(t,T) = \exp\Big(A(t,T) - B_1(t,T)\psi_1(t) - B_2(t,T)\psi_2(t)\Big) \tag{2.37}$$

while the pseudo bond can be described as

$$\begin{aligned} P^*(t,T) &= \exp\Big(A^*(t,T) - B_1(t,T)\psi_1(t) - B_2(t,T)\psi_2(t) - B_3^*(t,T)\psi_3(t) - \rho B_1(t,T)\psi_1(t)\Big) \\ &= P(t,T)\exp\Big(A^*(t,T) - A(t,T) - \rho B_1(t,T)\psi_1(t) - B_3^*(t,T)\psi_3(t)\Big) \end{aligned} \tag{2.38}$$

where the terms $A(t,T)$, $A^*(t,T)$ and $B_i(t,T)$ for $i = 1,2,3$ are given by (2.26). The above formulation allows for the definition of the price of the pseudo bond $P^*(t,T)$ in terms of the OIS zero coupon bond $P(t,T)$, providing the theoretical foundations to develop an adjustment factor which accounts for the prices' shift after the financial crisis.

Finally, the authors provide the representation of the forward IBOR rate

$$L(t,T,S) = \frac{1}{S-T}\left[\frac{\exp\Big(A(t,S) - A^*(t,S) + \rho B_1(t,S)\psi_1(t) + B_3(t,S)\psi_3(t)\Big)}{P(t,S)} - 1\right]$$

The short rate models described in this section are used by practitioners to assume that the investigated stochastic variable, i.e. the short rate, can be described by one given model. The assessment of the parameters of the model is done applying the appropriate calibration algorithm to a basket of calibration instruments whose prices and volatilities are quoted in the market. The calibrated parameters are then used to price more complex interest rate derivatives using Monte Carlo simulation to *estimate* future payments of the exotic derivative. In the following section we briefly discuss the functioning of Monte Carlo simulation.

2.3 Monte Carlo simulation for short rate models

Monte Carlo simulations and their practical application have been extensively discussed: indeed, Section 3.9.4 and Section 3.11.2 of Brigo and Mercurio (2006) provide several solutions to approach the Monte Carlo simulation of the prices of swaptions and Bermudan swaptions, while Chapter 7 and Chapter 8 of Kienitz and Wetterau (2012) and Appendix A of Caspers and Kienitz (2017) provide a more general framework. Moreover, we refer to Tebaldi and Veronesi (2016) for the numerical representation of the Vasicek and CIR models: the models are first represented as discretizations of the corresponding continuous processes and they are used to effectively sample the short rates. Tebaldi and Veronesi (2016) also provide a Monte Carlo simulation for the evaluation of callable bonds and, more generally, of American options.

Monte Carlo simulation is based on the evolution governing the stochastic processes we are interested in. The key idea underlying the Monte Carlo simulation is that we can repeat several times a random experiment in order to evaluate risky events, e.g. future payments. Indeed, the future payoffs of a financial instrument are assumed to be governed by a path or a scheme, returning the simulated payoffs. The *estimated* payoffs are then discounted and averaged to obtain the price of the interest rate derivative. Usually, practitioners simulate payoffs under different Monte Carlo scenarios, leading them to as many simulated prices as the number of different scenarios. The distribution of the prices is then statistically evaluated, returning the mean price in the pre-selected confidence interval.

We assume that the payoff of an interest rate derivative at time T is a function $V(T, r(T))$ depending on time and on the short rate $r(t)$. The present value of the payoff under the

risk neutral measure $\mathbb{Q}$ is equal to

$$V(t) = E^{\mathbb{Q}}\Big[- \int_t^T r(u)du \times V(T, r(T))\Big|\mathcal{F}(t)\Big],$$

requiring thus the Monte Carlo simulation of the short rates in the time interval $[t, T]$. Under the T-forward measure $\mathbb{Q}^T$ the expected value becomes

$$V(t) = P(t,T)E^{\mathbb{Q}^T}\Big[V(T, r(T))|\mathcal{F}(t)\Big],$$

requiring the simulation of the short rate at time T and the analytical formulation of the zero coupon bond price $P(t, T)$. The logical structure of Monte Carlo simulation of the derivative price under the T-forward measure can be summarized as:

1. Choose an appropriate T-forward measure such that $t < T_n = T$, where T_n is the last date of the specified time grid for simulation $\mathcal{T} := \{T_1, ..., T_n\}$ with $t < T_1$;

2. Create a recursive sequence of statements, normally called *loop* in computing language, for each j Monte Carlo scenario with $j = 1, ..., m$

   (a) use the selected short rate model under the T-forward measure $\mathbb{Q}^T$ to create a sample of the underlying short rates with tenor tn $\{r^j_{tn}(T_1), ..., r^j_{tn}(T_n)\}$ and a sample of the short rates used for discounting $\{r^j_d(T_1), ..., r^j_d(T_n)\}$;

   (b) simulate the pillars of the yield curve for each different date $\{T_1, ..., T_n\}$;

   (c) first compute the prices of zero coupon bonds

   $$\{P^j_{tn}(t, T_1), P^j_{tn}(t, T_1 + tn), ..., P^j_{tn}(t, T_n), P^j_{tn}(t, T_n + tn)\}$$

   and then compute the equivalent forward rates for $i = 1, ..., n$

   $$F^j_{tn}(t, T_i, T_i + tn) = \frac{1}{\tau}\left[\left(\frac{P^j_{tn}(t, T_i + tn)}{P^j_{tn}(t, T_i)}\right) - 1\right];$$

   (d) compute the prices of the zero coupon bonds used as discount factors

   $$\{P^j_d(t, T_1), ..., P^j_d(t, T_n)\};$$

   (e) compute the future cash flows of the derivative $\{V^j(T_1), ..., V^j(T_n)\}$;

3. Compute the final price as the average of the sum of the payoffs under each different j-scenario

$$V(t) = P_d(t, T)\left[\frac{1}{m}\sum_{j=1}^{m}\sum_{i=1}^{n}\frac{V^j(T_i)}{P^j_d(T_i, T)}\right].$$

2.4 Three-factor model: a simulation

The goal of this Section is to exploit the multiple curve models developed by Grbac and Runggaldier (2015) to build a simulation framework that enables us to analyse the future evolution of interest rates. The framework is based on the decomposition of interest rates in the risk-free component and in the spread component. Indeed, the simulation is used to describe the relationship between risky rates with different tenors and the risk-free rate, which it has been already discussed in this Chapter and in Chapter 1. As we already know, the interest rate curves are characterised by different spreads depending on their underlying tenors: the interest rates whose tenors are longer are higher than interest rates with shorter tenors. The spreads between the OIS rate and IBOR rates depend on equations (2.32) and (2.33). The graphical representation of tenor related spreads affecting interest rate curves is provided in Figure 1.4.
The algorithm in Appendix D simulates the interest rate curves depending on the parameters we have selected to model the stochastic processes of the factors characterizing the risk-free and the spread components. Therefore, the simulation algorithm can be used to represent the segmentation of the interest rate curves by considering the effect that different values of the parameters of the factor models have on the interest rates.
We assume that the interest rates are described by the same three-factor Vasicek model presented in Subsection 2.2.2. Indeed, we assume that the OIS rate - the risk-free rate $r(t)$ of the model - is modelled by two Vasicek-like factors, ψ_1 and ψ_2. Conversely, the risky rates - $r(t) + s(t)$ - are described by the same two factors of the risk-free rate and by an additional factor. Since the model in Subsection 2.2.2 considers only for two tenors, the third factor is used to describe the magnitude of the spread related to the longest tenor. Therefore, we assume that there exist as many stochastic factors ψ_3^{tn} as the number of considered tenors. The tenors we consider in our analysis are $tn = 1M,\ 3M,\ 6M,\ 12M$. Furthermore, we also consider factor correlation between the risk-free rate and the spread. Finally, the decomposition of the risky rates in two components - the risk-free rate and the spread - can be represented as

$$\begin{aligned} r(t) &= \psi_1(t) + \psi_2(t) \\ s^{tn}(t) &= \rho\psi_1(t) + \psi_3^{tn}(t), \end{aligned} \tag{2.39}$$

where ρ is the correlation and the factors of the model are described by the equations

$$\begin{aligned} d\psi_1(t) &= \big(a_1 - b_1\psi_1(t)\big)dt + \sigma_1 dW_1^{\mathbb{Q}}(t) \\ d\psi_2(t) &= \big(a_2 - b_2\psi_2(t)\big)dt + \sigma_2 dW_2^{\mathbb{Q}}(t) \\ d\psi_3^{tn}(t) &= \big(a_3^{tn} - b_3\psi_3^{tn}(t)\big)dt + \sigma_3 dW_3^{\mathbb{Q},tn}(t) \end{aligned} \tag{2.40}$$

where the index tn refers to the different LIBOR tenors $tn = 1M,\ 3M,\ 6M,\ 12M$ and where the Brownian motions are mutually independent. We are thus able to evaluate

how the mean reversion level a_i, the reversion speed b_i and the volatility σ_i influence the interest rate curves.
A short explanation of the functioning of the algorithm is therefore provided and the evidence of the simulation of USD LIBOR rates with different tenors - 1M, 3M, 6M and 12M - and of the USD OIS interest rate is provided at the end of the Section.

Simulation technique

The simulation algorithm in Appendix D is built using MATLAB and it is composed of a *main.m* function and of an object, $hwfactor.m$. The object uses a priori values of the model parameters and observed interest rate curves as inputs to simulate risk-free interest rates and risky interest rates. The output of the simulation algorithm is a set of 100 matrices with dimensions 61×45. Each matrix represents a simulation trial k for k=1,...,100. Every k-matrix contains as many interest rate curves as the number of dates of the time schedule of the *input* interest rate curves: indeed, the starting date of the simulated i-curve of the k-matrix is the date t_i for i=1,...,45 of the time schedule of the *input* curve. The i-curve is simulated from the date t_i up to 5 years (the simulation interval is composed of 60 months), where the dates of the simulation interval are generally indicated as $t_i^{j,k}$ where j=1,...,60. The simulated curves are obtained by a zero coupon bond starting at time t_i and with maturity $t_i^{j,k}$.
The algorithm works according to the following steps:

1. Input: market observed risky rate curve (i.e. LIBOR6M), market observed proxy of risk-free rate curve (i.e. OIS rate)[4], a priori values of the parameters in the equations (2.40), number of trials of the simulation (i.e. 100 trials), length of the simulation interval (i.e. 5 years), yearly partition of the simulation interval (i.e. $\frac{1}{12}$);

2. The parameters are used to build the Vasicek models of the three factors using the *hwv* MATLAB function;

3. The factors are simulated using the *simBySolution* property of the *hwv* function. We first consider the time schedule of the market rate curves we have defined at step 1, where each date is referred as t_i with $i = 1, ..., 45$. The factors of the model are then simulated up to 5 years (60 months) - the selected simulation interval - starting from the initial date t_1. We therefore obtain simulated values for each date t_1^j for j=1,...,60. The simulation is then repeated 100 times, resulting in 60×100 simulated values for each $t_1^{j,k}$ date for $k = 1, ..., 100$. Finally, the factors are recursively simulated up to 5 years taking every single date t_i as initial date, resulting in 60×45×100 simulated values for each $t_i^{j,k}$ date.

[4]The time schedule of the risk-free rate curve and the time schedule of the risky rate curve must be the same, i.e. t_i for $i = 1, ..., 45$.

Eventually, the simulated paths of the three factors are collected in as many matrices as the number of trials, 100. The number of rows of each matrix is equal to the number of dates of the simulation interval, 60, and the number of columns is equal to the number of dates t_i of the time schedule of the market rate curves;

4. The price of a risk-free bond and the price of a risky bond are computed using respectively equation (2.37) and equation (2.38), the simulated factors at step 3 and the a priori values of the parameters. The prices are collected in as many matrices as the number of trials, where the matrices have the same dimensions of the factors' matrices;

5. The simulated risk-free rates and the simulated risky rates are retrieved by the prices at step 4 and they are allocated in a scheme of matrices similar to the one used for the prices, with the only exception that there is an additional row used to contain the interest rates observed in the market. The resulting 100 matrices have dimensions 61×45.
   Eventually, the LIBOR rates in the matrices can be generally represented as $L(t_i, t_i^{j,k})$ for i=1,...,61 and k=1,...,100.

We apply the simulation algorithm to observed market rates as of 19 June 2020: USD OIS rate, LIBOR1M rate, LIBOR3M rate, LIBOR6M rate and LIBOR12M rate. The data are retrieved by the data provider Thomson Reuters' Eikon. The length of the time schedule of the interest rate curves is 30 years and the initial point of the time schedule is 3M (i.e. 3 months after the 19 June 2020).
The choice of the fictitious parameters to model the stochastic factors considers for the fact that the Vasicek model allows the factors to be negative with a not null probability. Therefore, we must select the parameters of the factors' models in order to have a very high probability of obtaining positive spreads between the risky rates and the risk-free rate. The parameter guaranteeing this condition is satisfied is obviously the mean reversion level, together with reasonable values of the reversion speed and of the volatility. Finally, the parameters are selected in order to describe different levels of risk: the factors modelling the risk-free rate have lower mean reversion levels than the additional factors modelling the interest rate spreads. The values of the parameters we consider in our simulation are similar to the ones selected by Grasselli and Miglietta (2016), which use values of 0.01 and 0.005 for the volatility and a factor correlation of 0.5.
We use the parameters $a_1 = 0.002 \times 0.1$, $b_1 = 0.1$, $\sigma_1 = 0.003$, $a_2 = 0.004 \times 0.08$, $b_2 = 0.08$, $\sigma_2 = 0.003$, $a_3^{LIBOR1M} = 0.004 \times 0.08$, $a_3^{LIBOR3M} = 0.008 \times 0.08$, $a_3^{LIBOR6M} = 0.011 \times 0.08$, $a_3^{LIBOR12M} = 0.016 \times 0.08$, $b_3 = 0.08$,$\sigma_3 = 0.005$. The correlation parameter, ρ, is fix to 0.4. Finally, we choose 100 trials and a simulation period of 5 years with monthly partition. The average values of the simulated interest rates for the next 5 years starting from time 19 $June$ $2020 + 3M$ (i.e. the initial date of the time schedule of the market curves) is represented in Figure 2.2. To put it another way, the mean is obtained by

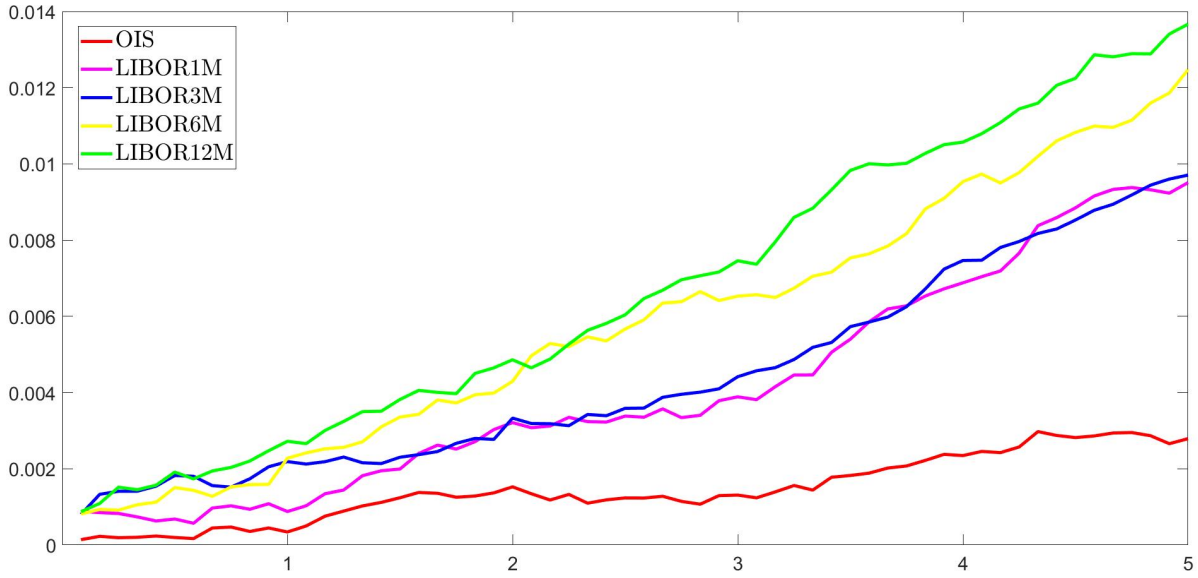

Figure 2.2: Simulated interest rates in the interval from 3 months to 5 years after 19 June 2020.

averaging the elements of the first columns of the 100 matrices with dimension 61×45 which we have obtained as output of the simulation algorithm: the result is a 61×1 vector containing the average simulated values up to 5 years. We observe that the selected parameters are coherent with the hypothesis that the spreads between each risky rates and the risk-free rate are strictly positive and that the spreads are increasing with the length of the underlying tenor of the interest rate. We observe that this relationship is not satisfied anymore if we increase the volatility of the factors: $\sigma_1 = 0.011$, $\sigma_2 = 0.01$, $\sigma_3 = 0.015$. In Figure 2.3 the increased volatility makes the interest rate curves less steady, since the shifts of the interest rates are sharper than the shifts in Figure 2.2. The high volatility determines negative LIBOR1M-OIS and LIBOR3M-OIS spreads and it makes the LIBOR6M riskier than the LIBOR12M rate.

Finally, we consider the scenario where the reversion speed is lower than in the base scenario in Figure 2.2: $b_1 = 0.02$, $b_2 = 0.02$, $b_3 = 0.03$. We observe in Figure 2.4 that the lower reversion speed makes the interest rate curves converge to smaller values after five years (LIBOR12M is 0.008, while it was close to 0.014 in the base scenario). Furthermore, the LIBOR1M-OIS spread, the LIBOR3M-OIS spread and the LIBOR6M-OIS spread are null or negative for the first three years.

Conversely, if we consider for very small volatilities and higher values of the reversion speed, we obtain steady interest rate curves, strictly positive spreads and we reduce the probability of overlaps between the risky curves.

Figures 2.2, 2.3 and 2.4 represent the interest rates which are simulated in the time interval going from 3 months after 19 June 2020 up to 5 years later. However, the algorithm simulates the interest rates in the following 5 years from each date of the schedule of the market observed curves: for example, we can simulate interest rate from 6 months after 19 June 2020 up to 5 years. Plotting together the simulated curves starting for each date

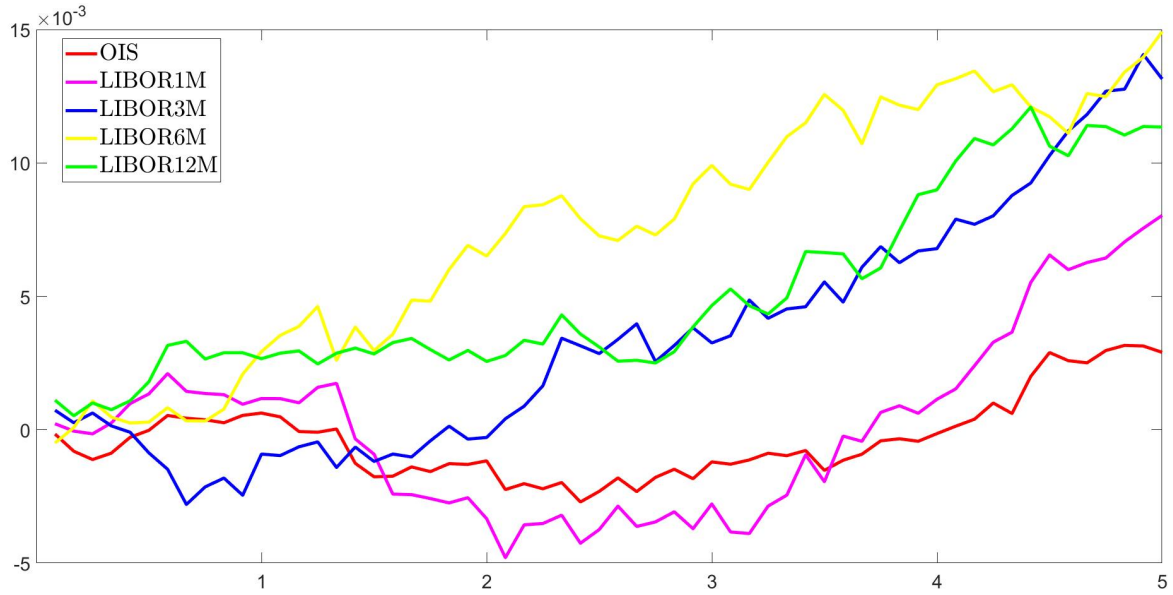

Figure 2.3: Simulated interest rates in the interval from 3 months to 5 years after 19 June 2020. The stochastic factors have higher volatilities than the factors determining the risk-free rate and the spreads in Figure 2.2.

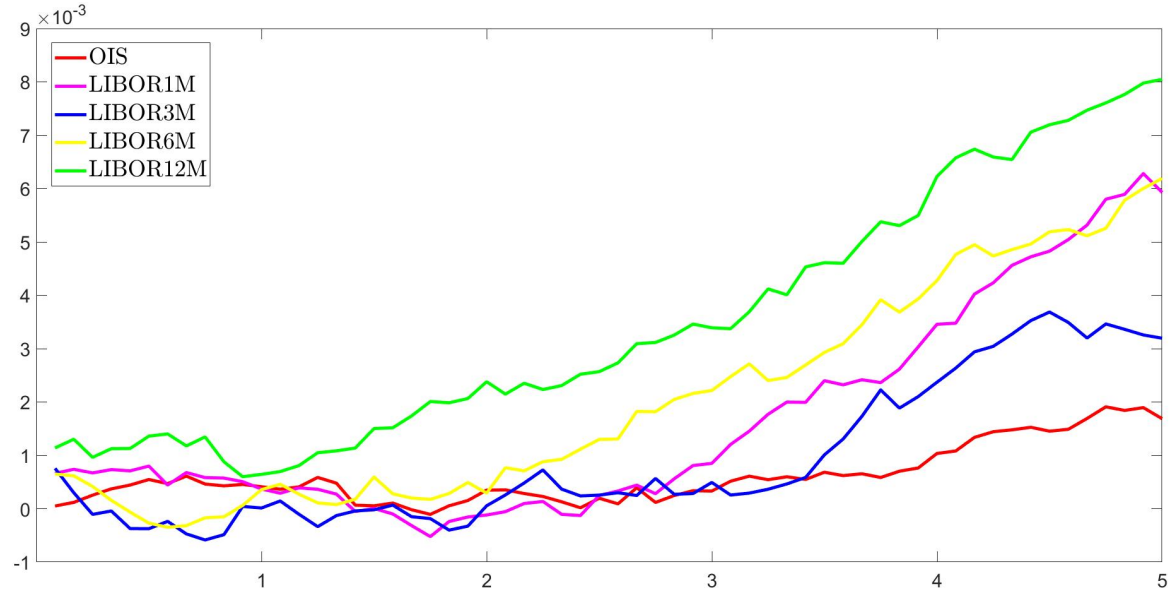

Figure 2.4: Simulated interest rates in the interval from 3 months to 5 years after 19 June 2020. The stochastic factors have lower reversion speed than the factors determining the risk-free rate and the spreads in Figure 2.2.

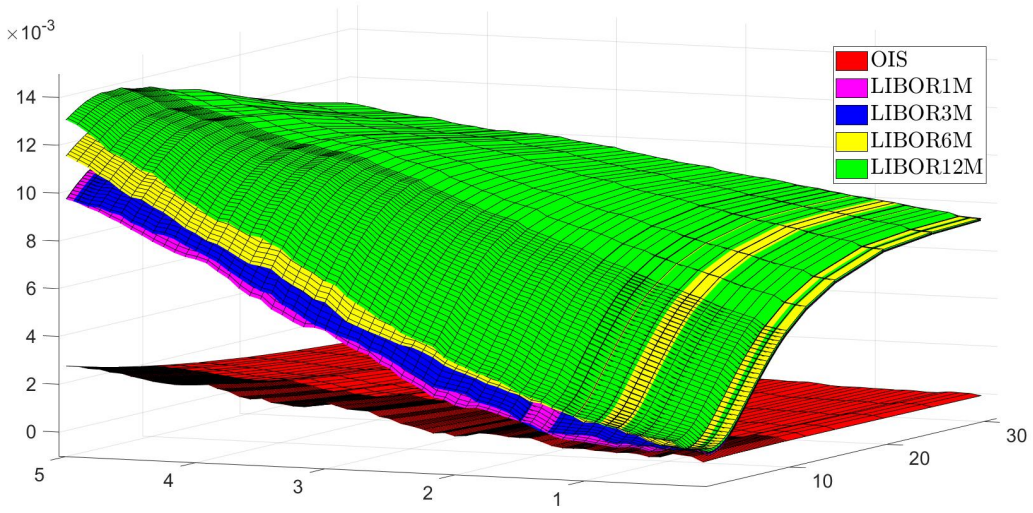

Figure 2.5: Interest rate surfaces for OIS, LIBOR1M, LIBOR3M, LIBOR6M, LIBOR12M. The interest rates are the average of 100 interest rate surfaces retrieved by different simulated price paths.

of the time schedule of the market curves results in the surface displayed in Figure 2.5 and Figure 2.6. The axis on the bottom right of Figure 2.5 indicates the starting dates (e.g. 6 months after 19 June 2020) of each single simulated interest rate curve. The axis on the bottom left indicates the time interval of 5 years we consider for the simulation. The vertical axis represents the interest rate value.

We observe that the surfaces aggregating the simulated curves point the different levels of riskiness up: the LIBOR12M surface is the riskiest one and, on the opposite, the OIS surface is the least risky one; the other surfaces lay between the OIS and the LIBOR12M.

Finally, we consider a zero coupon bond with a notional value of 100 and 5 years of maturity. The bond is issued at time 0 (i.e. 19 June 2020). Eventually, the price of the bond after 3 months is determined using the simulated interest rates and the price expression (2.38). Thus the simulation algorithm can be used to obtain the price of a bond with a notional value of 100, 5 years of maturity and an issuing date belonging to the time schedule of the market interest rate curves we retrieved from Thomson Reuters' Eikon - from 3M to 30Y after 19 June 2020. Therefore, we obtain the path of the price of the bond up to its maturity. The procedure is used to obtain multiple price paths, where the number of price paths is equal to the number of trials of the simulation algorithm. The price paths of a bond on the OIS rate are displayed in Figure 2.7 and the price paths of a bond on the LIBOR3M rate are displayed in Figure 2.8.

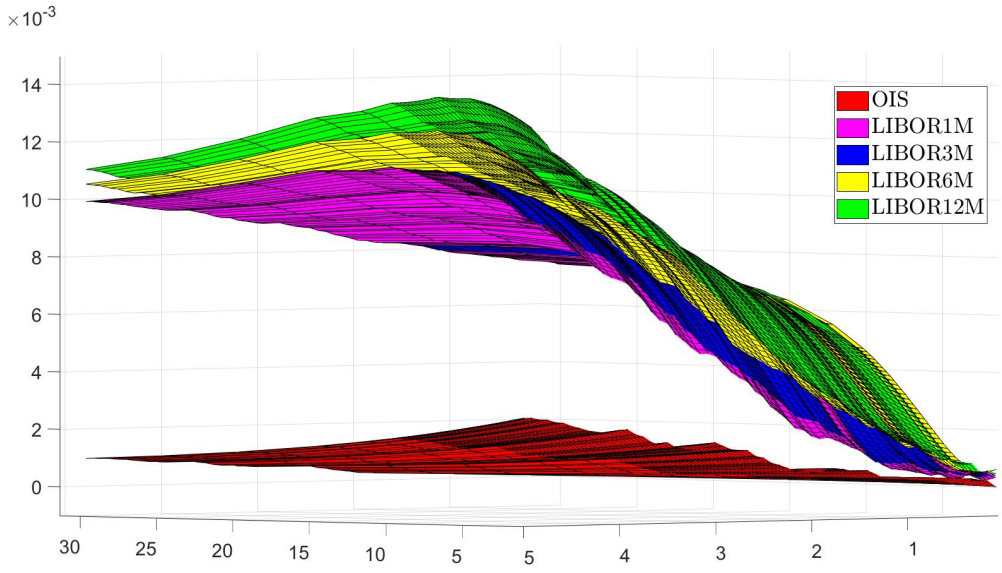

Figure 2.6: Interest rate surfaces for OIS, LIBOR1M, LIBOR3M, LIBOR6M, LIBOR12M.

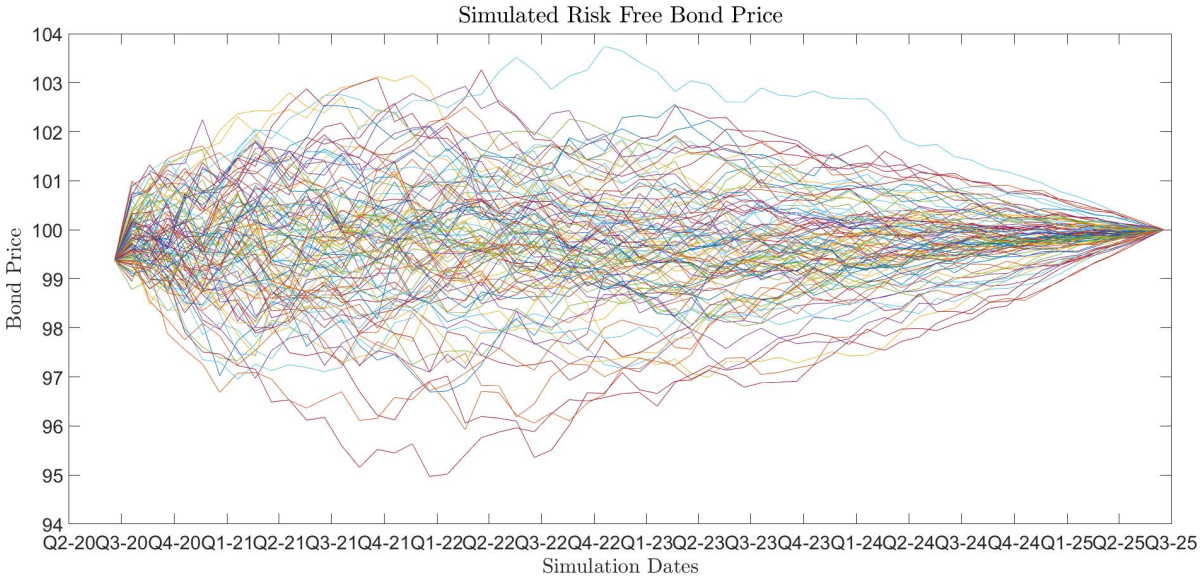

Figure 2.7: Simulation of the price of a risk-free zero coupon bond with 5 years of maturity and a notional value equal to 100.

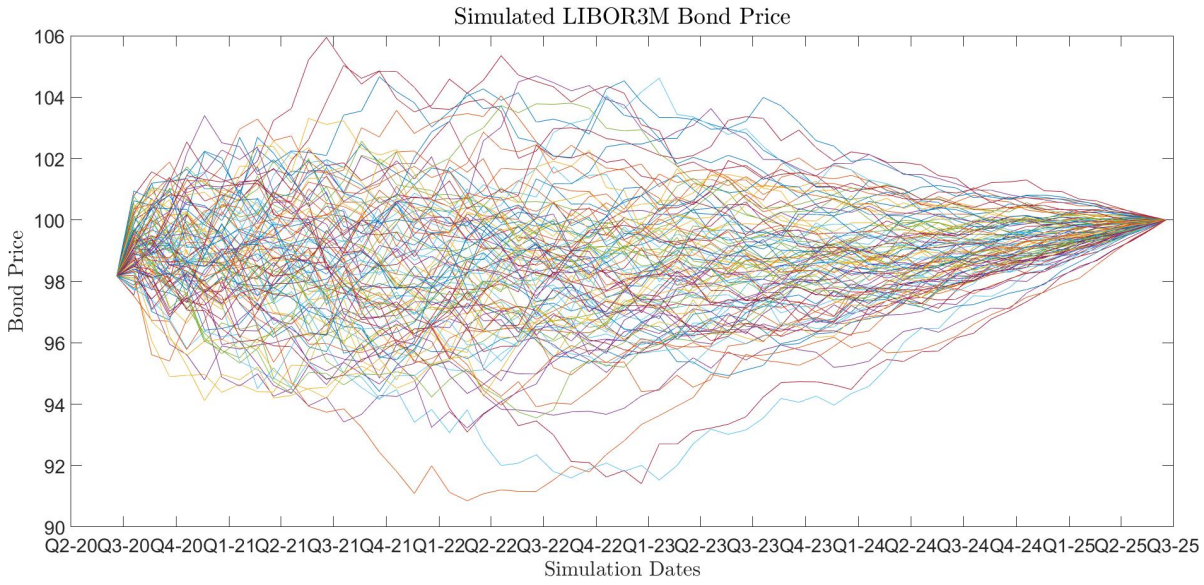

Figure 2.8: Simulation of the price of a risk-free zero coupon bond with 5 years of maturity and a notional value equal to 100.

Part II

An empirical analysis: calibration of the Hull-White model using cap volatilities

A necessary premise

When dealing with the pricing of interest rate derivatives in the multiple curve framework, we need to consider the $\psi_i(t)$ multiple factors specification as in (2.31) under the T-forward measure $\mathbb{Q}^T$. The modelling of the processes of the factors is quite simple when pricing forward rate agreements; however, the complexity increases when approaching more complicated instruments like cap and floor options. The complexity is due to the necessity of considering one different forward measure for each single tenor structure. Notwithstanding the results and the evidence regarding the necessity of adopting a pricing framework which considers the existence of multiple T-forward measure, we have decided to use a strong assumption when building the Hull-White calibration algorithm. Indeed, our calibration algorithm uses only a single curve to evaluate and discount each single caplets. The main reason behind this strong assumption lies in the simplicity and in the clearness of the caps calibration algorithm developed in Chapter 3 of Brigo and Mercurio (2006): indeed, the calibration algorithm is built on the Hull-White model for short rates, an extension of the Vasicek model, and it represents one of the most comprehensible framework for early practitioners. Therefore, the reader can consider the MATLAB written calibration algorithm provided in Chapter 4 as an introductory tool to understand the basics of interest rate derivatives pricing theory. The calibration algorithm uses USD IBOR3M cap volatilities which have been published by Reuters in June 2020. Notwithstanding the assumption that the term structure is described by the Hull-White model, we need to handle market quotes which are presented as Black implied cap volatilities. Therefore, we also present - together with other models which represent nowadays the market practice for cap pricing - the Black model: the Black model is used as part of the calibration algorithm to obtain the Black cap prices from cap volatilities. The Hull-White model is then calibrated by the minimization of the difference between Black cap prices and the fictitious Hull-White cap prices. The calibration algorithm is built on the assumption that the LIBOR rate is lognormal: this property enables the caps to be priced as portfolios of put options, whose future payoffs are described by the two considered models, i.e. Black and Hull-White.

Finally, the Hull-White model is not anymore considered by practitioners when pricing complex interest rate derivatives. Nowadays, pricing frameworks are based on Libor Market Models adjusted with Heston-type or SABR-type volatility stochastic processes, which better fit the volatility smiles of more complex interest rate derivatives.

Chapter 3

The Hull-White model

3.1 A starting point: the Vasicek model

In this section we briefly introduce the Vasicek model, the basic short rate model upon which Hull and White built the short rate model which bears their name. Using the analysis developed in Section 3.2 of Brigo and Mercurio (2006), we describe the short rate process $r(t)$ under the risk-neutral probability $\mathbb{Q}$ as

$$dr(t) = k[\theta - r(t)]dt + \sigma dW^{\mathbb{Q}}(t) \tag{3.1}$$

where k,θ and σ are positive constants and the initial point $r(0) = r_0$ is positive.
Multiplying (3.1) by e^{kt} and integrating the resulting equation in the time interval from s to t, we obtain

$$\begin{aligned}
&dr(t) = k\theta dt - kr(t)dt + \sigma dW^{\mathbb{Q}}(t) \\
&e^{kt}dr(t) + ke^{kt}r(t)dt = e^{kt}k\theta dt + e^{kt}\sigma dW^{\mathbb{Q}}(t) \\
&d\Big(e^{kt}r(t)\Big) = e^{kt}k\theta dt + e^{kt}\sigma dW^{\mathbb{Q}}(t) \\
&\int_s^t d\Big(e^{ku}r(u)\Big) = k\theta\int_s^t e^{ku}du + \sigma\int_s^t e^{ku}dW^{\mathbb{Q}}(u) \\
&e^{kt}r(t) - e^{ks}r(s) = k\theta\frac{e^{kt} - e^{ks}}{k} + \sigma\int_s^t e^{ku}dW^{\mathbb{Q}}(u) \\
&r(t) = r(s)e^{-k(t-s)} + \theta\Big(1 - e^{-k(t-s)}\Big) + \sigma\int_s^t e^{-k(t-u)}dW^{\mathbb{Q}}(u).
\end{aligned} \tag{3.2}$$

We observe that the short rate $r(t)$ has a Normal distribution with a conditional expected value and a conditional variance given by

$$E\big[r(t)\big|\mathcal{F}(s)\big] = r(s)e^{-k(t-s)} + \theta\Big(1 - e^{-k(t-s)}\Big) \tag{3.3}$$

$$
\begin{aligned}
Var\big[r(t)\big|\mathcal{F}(s)\big] &= Var\bigg[\sigma\int_s^t e^{-k(t-u)}dW^{\mathbb{Q}}(u)\bigg] \\
&= \sigma^2\int_s^t \exp\big(-2k(t-u)\big)du \\
&= \frac{\sigma^2}{2k}\bigg(1-\exp\big(-2k(t-s)\big)\bigg).
\end{aligned} \tag{3.4}
$$

The rate $r(t)$ is mean reverting, since it goes close to θ when t goes to infinity; moreover, there is a positive probability that $r(t)$ is smaller than zero.
Now, we study the behaviour of zero coupon bond price. We first integrate the short rate in the time interval from s to T

$$
\begin{aligned}
\int_s^T r(t)dt &= r(s)\int_s^T \exp(-k(t-s))dt + \theta\int_s^T\bigg(1-\exp(-k(t-s))\bigg)dt \\
&\quad + \sigma\int_s^T\int_s^t \exp(-k(t-u))dW^{\mathbb{Q}}(u)dt \\
&= r(s)\bigg(\frac{1-\exp(-k(T-s))}{k}\bigg) + \theta\bigg[\int_s^T dt - \int_s^T \exp(-k(t-s))dt\bigg] \\
&\quad + \sigma\int_s^T\int_u^T \exp(-k(t-u))dtdW^{\mathbb{Q}}(u) \\
&= r(s)\bigg(\frac{1-\exp(-k(T-s))}{k}\bigg) + \theta\bigg[T-s-\frac{1-\exp(-k(T-s))}{k}\bigg] \\
&\quad + \frac{\sigma}{k}\int_s^T\bigg(1-\exp(-k(T-u))\bigg)dW^{\mathbb{Q}}(u)
\end{aligned}
$$

We observe that the distribution of $\int_s^T r(t)dt$ is Normal with mean and variance given respectively by

$$
\begin{aligned}
E\bigg[\int_s^T r(t)dt\bigg] &= r(s)\bigg(\frac{1-\exp(-k(T-s))}{k}\bigg) + \theta\bigg[T-s-\frac{1-\exp(-k(T-s))}{k}\bigg] \\
Var\bigg[\int_s^T r(t)dt\bigg] &= Var\bigg[\frac{\sigma}{k}\int_s^T\bigg(1-\exp(-k(T-u))\bigg)dW^{\mathbb{Q}}(u)\bigg] \\
&= \frac{\sigma^2}{k^2}\int_s^T\bigg(1-\exp(-k(T-u))\bigg)^2du \\
&= \frac{\sigma^2}{k^2}\int_s^T\bigg(1+\exp(-2k(T-u))-2\exp(-k(T-u))\bigg)du \\
&= \frac{\sigma^2}{k^2}\bigg[T-s+\frac{1-\exp(-2k(T-s))}{2k}-\frac{2}{k}\bigg(1-\exp(-k(T-s))\bigg)\bigg] \\
&= \frac{\sigma^2}{2k^3}\bigg[2k(T-s)-\exp(-2k(T-s))+4\exp(-k(T-s))-3\bigg]
\end{aligned} \tag{3.5}
$$

where we used the Itô isometry in the third equation.
Finally, we use the results in (3.5) to find the price of a zero coupon bond

$$\begin{aligned}
P(t,T) &= E\Big[\exp\Big(-\int_t^T r(u)du\Big)\Big|\mathcal{F}(t)\Big] = \exp\Big\{-E\Big[\int_t^T r(u)du\Big] + \frac{1}{2}Var\Big[\int_t^T r(u)du\Big]\Big\} \\
&= \exp\Big\{-r(t)\Big(\frac{1-\exp(-k(T-t))}{k}\Big) - \theta\Big[T-t-\frac{1-\exp(-k(T-t))}{k}\Big] \\
&+ \frac{\sigma^2}{2k^3}\Big[2k(T-t) - \exp(-2k(T-t)) + 4\exp(-k(T-t)) - 3\Big]\Big\} \\
&= \exp\Big\{-r(t)\Big(\frac{1-\exp(-k(T-t))}{k}\Big) + \Big(\theta - \frac{\sigma^2}{2k^2}\Big)\Big[\frac{1-\exp(-k(T-t))}{k} - T + t\Big] \\
&- \frac{\sigma^2}{4k}\Big[\frac{1-\exp(-k(T-t))}{k}\Big]^2\Big\}
\end{aligned} \tag{3.6}$$

where the first equation is valid because it is the Laplace transformation of the exponential of a variable, $\int_s^T r(t)dt$, with Normal distribution.
From Brigo and Mercurio (2006), we know that the price (3.6) can be also represented as

$$P(t,T) = A(t,T)\exp\Big(-B(t,T)r(t)\Big) \tag{3.7}$$

where the functions $A(t,T)$ and $B(t,T)$ are given by

$$\begin{aligned}
A(t,T) &= \exp\Big[\Big(\theta - \frac{\sigma^2}{2k^2}\Big)\Big(B(t,T) - T + t\Big) - \frac{\sigma^2}{4k}B(t,T)^2\Big] \\
B(t,T) &= \frac{1-\exp(-k(T-t))}{k}
\end{aligned} \tag{3.8}$$

Now, we change the probability measure from the risk neutral measure $\mathbb{Q}$, implied by the bank account numeraire $B(t,T)$, to the forward measure $\mathbb{Q}^T$, implied by the zero coupon bond numeraire $P(t,T)$. The conversion from the risk neutral probability is operated through the toolkit developed by Brigo and Mercurio (2006), which is briefly described in Appendix C. We substitute the numeraire $U(t)$ and $S(t)$ in the Appendix with, respectively, $P(t,T)$ and $B(t,T)$; furthermore, the volatility $\sigma^T(t)$ is obtained applying the Itô formula to equation (3.7) and it is hence equal to $-\sigma B(t,T)P(t,T)$; lastly, the equations in Appendix C further simplify because the correlation coefficient is $\rho = 1$. The dynamics of their processes under the forward measure $\mathbb{Q}^T$ are

$$\begin{aligned}
dB(t,T) &= (\cdot)dt \\
dP(t,T) &= (\cdot)dt + \sigma^T(t)dW^{\mathbb{Q}^T}(t).
\end{aligned}$$

The drift of the process $r(t)$ under $\mathbb{Q}^T$ is then equal to

$$\begin{aligned}\mu^T(t,r(t)) &= \left[k\theta - kr(t) - \sigma(t,x(t))(0 - \frac{\sigma^T(t)}{P(t,T)})\right] \\ &= \left[k\theta - kr(t) - \sigma^2(t,x(t))B(t,T)\right]\end{aligned} \tag{3.9}$$

and the diffusion term is characterised by

$$dW^{\mathbb{Q}^T}(t) = dW(t) + \sigma B(t,T)dt. \tag{3.10}$$

Finally, using the equations (3.9) and (3.10), we observe that the $r(t)$ process under the forward measure $\mathbb{Q}^T$ becomes

$$dr(t) = \left[k\Big(\theta - r(t)\Big) - \sigma^2 B(t,T)\right]dt + \sigma dW^{\mathbb{Q}^T}(t). \tag{3.11}$$

Integrating the process (3.11) in the time interval from 0 to s we obtain that $r(t)$ is

$$\begin{aligned}r(t) = r(s)\exp(-k(t-s)) &+ \left(\theta - \frac{\sigma^2}{k^2}\right)\Big(1 - \exp(-k(t-s))\Big) \\ &+ \frac{\sigma^2}{2k^2}\Big[\exp(-k(T-t)) - \exp(-k(T+t-2s))\Big] + \sigma\int_s^t \exp(-k(t-u))dW^{\mathbb{Q}^T}(u)\end{aligned} \tag{3.12}$$

where $r(t)$ follows a Normal distribution with expected value and variance under $\mathbb{Q}^T$ are respectively given by

$$\begin{aligned}E^{\mathbb{Q}^T}\big[r(t)\big|\mathcal{F}(s)\big] &= r(s)\exp(-k(t-s)) + \left(\theta - \frac{\sigma^2}{k^2}\right)\Big(1 - \exp(-k(t-s))\Big) \\ &\quad + \frac{\sigma^2}{2k^2}\Big[\exp(-k(T-t)) - \exp(-k(T+t-2s))\Big], \\ Var^{\mathbb{Q}^T}\big[r(t)\big|\mathcal{F}(s)\big] &= \frac{\sigma^2}{2k}\Big[1 - \exp(-2k(t-s))\Big].\end{aligned} \tag{3.13}$$

The Vasicek model can be calibrated using the quoted prices and the volatilities of interest rate options. The present value of the expected payoff at time T of a European option with a zero coupon bond as underlying asset, strike K and maturity T under the T-forward probability measure is equal to

$$ZBOption(t,T,S,K) = E^{\mathbb{Q}^T}\left[\exp\Big(-\int_t^T r(s)ds\Big)\Big(\omega(P(T,S)-K)\Big)^+\Big|\mathcal{F}(t)\right] \tag{3.14}$$

where the future value of the option's payoff $\Big(\omega(P(T,S)-K)\Big)^+$ is given - according to

the D Appendix of Brigo and Mercurio (2006) - by

$$\omega \exp\left(\mu_p + \frac{1}{2}\sigma_p^2\right)\Phi\left[\omega\frac{\mu_p - \ln(K) + \sigma_p^2}{\sigma_p}\right] - \omega K\Phi\left[\omega\frac{\mu_p - \ln(K)}{\sigma_p}\right]. \tag{3.15}$$

The parameters μ_p and σ_p refer respectively to the mean and the volatility of the natural logarithm of $P(T,S)$; the parameter $\omega \in \{-1,1\}$ is a generalization to consider both for call and put options; $\Phi(\cdot)$ indicates the cumulative standard Normal distribution function. Therefore, using equations (3.14) and (3.15) we obtain that the price of a European option is

$$ZBOption(t,T,S,K) = \omega\Big[P(t,S)\Phi(\omega h) - KP(t,T)\Phi(\omega(h-\sigma_p))\Big] \tag{3.16}$$

where σ_p and h are respectively given by

$$\begin{aligned}\sigma_p &= \sigma\sqrt{\frac{1-\exp(-2k(T-t))}{2k}}B(T,S)\\ h &= \frac{\sigma_p}{2} + \frac{1}{\sigma_p}\ln\left(\frac{P(t,S)}{P(t,T)K}\right).\end{aligned} \tag{3.17}$$

Finally, the calibration of the Vasicek model can be executed applying the equations (3.16) and (3.17): these formulas are used in the calibration algorithm we developed in Chapter 4, where we consider cap options as a portfolio of put options.

3.1.1 Connections between the risk-neutral and the objective world

In this subsection we explore the relationship between the dynamics of the interest rate in the risk-neutral world and in the objective world, which is associated to an objective probability measure $\mathbb{P}$. Indeed, we are going to illustrate the concepts we have previously introduced in Chapter 1, analysing how the process $\lambda(t)$ in equation (1.6) adapts to the Vasicek case.

We are usually interested to study stochastic processes under the risk-neutral probability measure $\mathbb{Q}$, so that we are able to compute prices as expectations under this measure. However, in the real world we observe historical data, not the process $r(t)$ under the risk-neutral measure. As we have explained in Section 1.1, we use the distribution of $r(t)$ in the objective world to compute the diffusion coefficient σ, which is equal to the diffusion parameter under the risk-neutral measure.

The Vasicek model under the objective probability measure takes the form

$$dr(t) = \Big[k\theta - kr(t) - \lambda\sigma r(t)\Big]dt + \sigma dW^{\mathbb{P}} \tag{3.18}$$

where $r(0) = r_0$ and λ is the constant market risk parameter. We observe that the short rate process under the measure $\mathbb{P}$ is equal to the short rate process under $\mathbb{Q}$ in equation

(3.1). Furthermore, we know from Brigo and Mercurio (2006) that the change of measure making equal the process under the risk-neutral and the objective measures is

$$\frac{d\mathbb{Q}}{d\mathbb{P}} = \exp\left(-\frac{1}{2}\int_0^t \lambda^2 r(s)^2 ds + \int_0^t \lambda r(s) dW^{\mathbb{P}}(s) \right) \tag{3.19}$$

where the change of measure is calculated applying the Girsanov's theorem we have introduced in Chapter 1. According to Brigo and Mercurio (2006), the necessary assumption satisfying equation (3.19) is that $\lambda(t)$ in equation (1.6) - the market price of risk - is equal to $\lambda r(t)$.
Therefore, we are able to estimate firstly the diffusion parameter σ under the objective measure $\mathbb{P}$ - e.g. employing an ML estimator (Björk (2009)) - and, afterwards, to calibrate the other parameters to market data.
These assumptions are also valid for an important extension of the Vasicek model, the Hull-White model: indeed, using an approach similar to the one we have outlined in this section, we calibrate the Hull-White model in Chapter 4, using market data of cap volatilities.

3.2 The theoretical model

In this section we describe the Hull-White model of short rate dynamics. The formal description of the model is mainly taken by Brigo and Mercurio (2006). The Hull-White 1990 model is an extension of the Vasicek model and it belongs to the family of the affine-term structure models we described in the previous part of this disseration.
The short rate process under the risk neutral probability measure $\mathbb{Q}$ is assumed to be

$$dr(t) = [\theta(t) - a(t)r(t)]dt + \sigma(t)dW^{\mathbb{Q}}(t) \tag{3.20}$$

where the functions θ, a and σ are deterministic.
The 1990 formalization was modified imposing a and σ as positive constants, in order to exactly fit the term structure of interest rates[1]. The 1994 version of the Hull-White model, the only one we consider from now on, is

$$dr(t) = [\theta(t) - ar(t)]dt + \sigma dW^{\mathbb{Q}}(t). \tag{3.21}$$

In this chapter, we use only the risk neutral probability $\mathbb{Q}$. Hence, we omit the notation in the following equations.
We now derive the Hull-White short rate dynamics. First, we simplify assuming that the short rate is composed by two components $r(t) = x(t) + \alpha(t)$, where $\alpha(t)$ is a deterministic

[1]The Hull-White 1990 was built to be calibrated to the term structure of the interest rates and the term structure of spot-rate volatilities and forward rate volatilities.

function and $x(t)$ is a stochastic process satisfying

$$\begin{cases} dx(t) = -ax(t)dt + \sigma dW(t) \\ x(0) = 0 \end{cases} \tag{3.22}$$

The derivation of the deterministic function $\alpha(t)$ is slightly complicated. In order to achieve this result, we first represent the price of the zero coupon bond with maturity T

$$\begin{aligned} P(0,T) &= E\bigg[\exp\bigg(-\int_0^T r(t)dt\bigg)\bigg] = E\bigg[\exp\bigg(-\int_0^T x(t)+\alpha(t)dt\bigg)\bigg] \\ &= \exp\bigg(-\int_0^T \alpha(t)dt\bigg) E\bigg[\exp\bigg(-\int_0^T x(t)dt\bigg)\bigg] \\ &= \exp\bigg(-\int_0^T \alpha(t)dt\bigg) \exp\bigg\{-E\bigg[\int_0^T x(t)dt\bigg] + \frac{1}{2}Var\bigg[\int_0^T x(t)dt\bigg]\bigg\} \end{aligned} \tag{3.23}$$

where the last equation is valid because it is the Laplace transformation of the exponential of a variable, $\int_0^T r(t)dt$, with Normal distribution.
Solving the problem (3.22), we get

$$\begin{aligned} & dx(t) = -ax(t)dt + \sigma dW(t) \\ & \exp(at)dx(t) + a\exp(at)x(t)dt = \exp(at)\sigma dW(t) \\ & d\bigg(\exp(at)x(t)\bigg) = \exp(at)\sigma dW(t) \\ & \int_s^t d\bigg(\exp(au)x(u)\bigg) = \sigma\int_s^t \exp(au)dW(u) \\ & \exp(at)x(t) - \exp(as)x(s) = \sigma\int_s^t \exp(au)dW(u). \end{aligned}$$

Therefore, we obtain that, for $s < t$, the solution is

$$x(t) = x(s)\exp(-a(t-s)) + \sigma\int_s^t \exp(-a(t-u))dW(u), \tag{3.24}$$

which, for $s = 0$, is equal to

$$\begin{aligned} & x(t) = x(0)\exp(-at) + \sigma\int_0^t \exp(-a(t-u))dW(u) \\ & x(t) = \sigma\int_0^t \exp(-a(t-u))dW(u) \end{aligned} \tag{3.25}$$

Integrating $x(t)$ in the time interval from 0 to T, we obtain

$$\begin{aligned}\int_0^T x(t)dt &= \int_0^T \sigma \int_0^t \exp(-a(t-u))dW(u)dt \\ &= \sigma \int_0^T \int_u^T \exp(-a(t-u))dtdW(u) \\ &= \frac{\sigma}{a}\int_0^T \Big(1-\exp(-a(T-u))\Big)dW(u)\end{aligned} \tag{3.26}$$

where we changed the integration interval and the order of integration in the second equation.

Finally, we can determine the expected value and the variance of $\int_0^T x(t)dt$. Indeed, we have proven in equation (3.26) that the stochastic integral $\int_0^T x(t)dt$ is deterministic and, consequently, it follows a Normal distribution with

$$\begin{aligned}E\Big[\int_0^T x(t)dt\Big] &= E\Big[\frac{\sigma}{a}\int_0^T \Big(1-\exp(-a(T-u))\Big)dW(u)\Big] = 0 \\ Var\Big[\int_0^T x(t)dt\Big] &= Var\Big[\frac{\sigma}{a}\int_0^T \Big(1-\exp(-a(T-u))\Big)dW(u)\Big] \\ &= \frac{\sigma^2}{a^2}\int_0^T \Big[1-\exp(-a(T-u))\Big]^2 du \\ &= \frac{\sigma^2}{a^2}\int_0^T \Big[1+\exp(-2a(T-u))-2\exp(-a(t-u))\Big]du \\ &= \frac{\sigma^2}{a^2}\Big\{\int_0^T du + \int_0^T \exp(-2a(T-u))du - 2\int_0^T \exp(-a(T-u))du\Big\} \\ &= \frac{\sigma^2}{a^2}\Big\{T+\frac{1-\exp(-2aT)}{2a}-2\frac{1-\exp(-aT)}{a}\Big\} \\ &= \frac{\sigma^2}{2a^3}\Big\{2aT-\exp(-2aT)-3-4\exp(-aT)\Big\}.\end{aligned} \tag{3.27}$$

where we used the Itô isometry in the third equation.

Therefore, we can use the expected value and the variance of $\int_0^T x(t)dt$ to get the price of the zero coupon bond with maturity T in equation (3.23)

$$\begin{aligned}P(0,T) &= \exp\Big(-\int_0^T \alpha(t)dt\Big)\exp\Big\{-E\Big[\int_0^T x(t)dt\Big]+\frac{1}{2}Var\Big[\int_0^T x(t)dt\Big]\Big\} \\ &= \exp\Big\{-\int_0^T \alpha(t)dt+\frac{\sigma^2}{4a^3}\Big(2aT-\exp(-2aT)-3+4\exp(-aT)\Big)\Big\}.\end{aligned} \tag{3.28}$$

We get the equation for $\int_0^T \alpha(t)dt$ taking the natural logarithm of equation (3.28)

$$\int_0^T \alpha(t)dt = -lnP(0,T)+\frac{\sigma^2}{4a^3}\Big(2aT-\exp(-2aT)-3+4\exp(-aT)\Big)$$

Therefore, we obtain the values of $\alpha(T)$ and $\frac{\partial \alpha(T)}{\partial T}$

$$\begin{aligned}
\alpha(T) &= \frac{\partial}{\partial T}\int_0^T \alpha(t)dt = \frac{\partial}{\partial T}\Big[- lnP(0,T) \\
&+ \frac{\sigma^2}{4a^3}\Big(2aT - \exp(-2aT) - 3 + 4\exp(-aT)\Big)\Big] \\
&= \frac{\partial}{\partial T}\Big(\int_0^T f(0,u)du\Big) + \frac{\sigma^2}{4a^3}\Big(2a + 2a\exp(-2aT) - 4a\exp(-aT)\Big) \qquad (3.29)\\
&= f(0,T) + \frac{\sigma^2}{2a^2}\Big(1 + \exp(-2aT) - 2\exp(-aT)\Big) \\
&= f(0,T) + \frac{\sigma^2}{2a^2}\Big(1 - \exp(-aT)\Big)^2
\end{aligned}$$

$$\begin{aligned}
\frac{\partial \alpha(T)}{\partial T} &= \frac{\partial}{\partial T}f(0,T) + \frac{\sigma^2}{4a^3}\Big(- 4a^2\exp(-2aT) + 4a^2\exp(-aT)\Big) \\
&= \frac{\partial}{\partial T}f(0,T) + \frac{\sigma^2}{a}\Big(\exp(-aT) - \exp(-2aT)\Big)
\end{aligned} \qquad (3.30)$$

We can use equations (3.29) and (3.30) to determine the value of the deterministic function θ. We define $\theta(t) = a\alpha(t) + \frac{\partial \alpha(T)}{\partial T}$ using the assumption that $r(t) = x(t) + \alpha(t)$ and equations (3.22)

$$\begin{aligned}
dr(t) &= dx(t) + d\alpha(t) \\
&= -ax(t)dt + \sigma dW(t) + d\alpha(t) \\
&= -a(r(t) - \alpha(t))dt + \sigma dW(t)) + d\alpha(t) \\
&= \Big(a\alpha(t) + \frac{\partial \alpha(t)}{\partial t} - ar(t)\Big)dt + \sigma dW(t).
\end{aligned}$$

Substituting equations (3.29) and (3.30) in $\theta(t) = a\alpha(t) + \frac{\partial \alpha(t)}{\partial t}$ we obtain

$$\begin{aligned}
\theta(t) &= a\alpha(t) + \frac{\partial \alpha(t)}{\partial t} \\
&= af(0,t) + \frac{\sigma^2}{2a}\Big(1 + \exp(-2at) - 2\exp(-at)\Big) \\
&+ \frac{\partial}{\partial t}f(0,t) + \frac{\sigma^2}{a}\Big(\exp(-at) - \exp(-2at)\Big) \\
&= af(0,t) + \frac{\sigma^2}{2a}\Big(1 + \exp(-2at) - 2\exp(-at)\Big) \\
&+ \frac{\partial}{\partial t}f(0,t) + \frac{\sigma^2}{a}\Big(\exp(-at) - \exp(-2at)\Big) \\
&= af(0,t) + \frac{\sigma^2}{2a}\Big(1 - \exp(-2at)\Big) + \frac{\partial}{\partial t}f(0,T).
\end{aligned}$$

Finally, we can represent the short rate process of the Hull-White model as

$$\begin{aligned} dr(t) &= (\theta(t) - ar(t))dt + \sigma dW(t) \\ &= \left[af(0,t) + \frac{\sigma^2}{2a}\Big(1 - \exp(-2at)\Big) + \frac{\partial}{\partial t}f(0,t) - ar(t)\right]dt + \sigma dW(t). \end{aligned} \tag{3.31}$$

Now we discuss the Normal distribution of the short rate and the dynamics of the zero coupon bond price in the Hull-White model. We first multiply equation (3.31) for e^{at}; then, we integrate the resulting equation in the time interval from s to t in order to obtain the short rate behaviour

$$\begin{aligned} e^{at}dr(t) + ar(t)e^{at}dt &= \left[ae^{at}f(0,t) + e^{at}\frac{\partial}{\partial t}f(0,t) + \frac{\sigma^2}{2a}\Big(e^{at} - e^{-at}\Big)\right]dt + \sigma dW(t) \\ \int_s^t d\Big(e^{au}r(u)\Big) &= \int_s^t d\Big(e^{au}f(0,u)\Big) + \frac{\sigma^2}{2a}\int_s^t \Big(e^{au} - e^{-au}\Big)du + \sigma\int_s^t e^{au}dW(u) \\ e^{at}r(t) - e^{as}r(s) &= e^{at}f(0,t) - e^{as}f(0,s) + \frac{\sigma^2}{2a^2}\Big(e^{at} - e^{as} + e^{-at} - e^{-as}\Big) + \sigma\int_s^t e^{au}dW(u). \end{aligned}$$

Therefore, the short rate $r(t)$ can be represented as

$$\begin{aligned} r(t) &= \exp(-a(t-s))\Big(r(s) - f(0,s)\Big) + f(0,t) + \frac{\sigma^2}{2a^2}\Big[1 - \exp(-a(t-s)) \\ &\quad + \exp(-2at) - \exp(-a(t+s))\Big] + \sigma\int_s^t \exp(-a(t-u))dW(u) \\ &= \exp(-a(t-s))\Big(r(s) - f(0,s)\Big) + f(0,t) \\ &\quad + \frac{\sigma^2}{2a^2}\Big(1 - \exp(-a(t-s))\Big)\Big(1 - \exp(-a(t+s))\Big) \\ &\quad + \sigma\int_s^t \exp(-a(t-u))dW(u) \\ &= r(s)\exp(-a(t-s)) + \alpha(t) - \alpha(s)\exp(-a(t-s)) \\ &\quad + \sigma\int_s^t \exp(-a(t-u))dW(u). \end{aligned} \tag{3.32}$$

We observe that $r(t)$ has a Normal distribution with a conditional expected value and a conditional variance given by

$$\begin{aligned} E[r(t)|\mathcal{F}(s)] &= r(s)\exp(-a(t-s))\Big(r(s) - f(0,s)\Big) + f(0,t) \\ &\quad + \frac{\sigma^2}{2a^2}\Big(1 - \exp(-a(t-s))\Big)\Big(1 - \exp(-a(t+s))\Big) \\ &= r(s)\exp(-a(t-s)) + \alpha(t) - \alpha(s)\exp(-a(t-s)) \end{aligned} \tag{3.33}$$

$$
\begin{aligned}
Var[r(t)|\mathcal{F}(s)] &= Var\left[\sigma \int_s^t \exp(-a(t-u))dW(u)\right] \\
&= \sigma^2 \int_s^t \exp(-2a(t-u))du \qquad (3.34) \\
&= \frac{\sigma^2}{2a}\Big(1-\exp(-2a(t-s))\Big)
\end{aligned}
$$

Now, we study the behaviour of zero coupon bond price. We first integrate the short rate in the time interval from s to T

$$
\begin{aligned}
\int_s^T r(t)dt &= (r(s)-f(0,s))\int_s^T \exp(-a(t-s))dt + \int_s^T f(0,t)dt \\
&+ \frac{\sigma^2}{2a^2}\int_s^T \Big(1-\exp(-a(t-s))\Big)\Big(1-\exp(-a(t+s))\Big)dt \\
&+ \sigma \int_s^T \int_s^t \exp(-a(t-u))dW(u)dt \\
&= (r(s)-f(0,s))\left(\frac{\exp(-a(t-s))-1}{-a}\right) + \int_s^T f(0,t)dt \\
&+ \frac{\sigma^2}{2a^2}\left[\int_s^T dt - \int_s^T \exp(-a(t-s))dt + \int_s^T \exp(-2at)dt - \int_s^T \exp(-a(t+s))dt\right] \\
&+ \sigma \int_s^T \int_u^T \exp(-a(t-u))dtdW(u) \\
&= (r(s)-f(0,s))\left(\frac{\exp(-a(t-s))-1}{-a}\right) + \int_s^T f(0,t)dt \\
&+ \frac{\sigma^2}{2a^2}\left[\int_s^T dt - \int_s^T \exp(-a(t-s))dt + \int_s^T \exp(-2at)dt - \int_s^T \exp(-a(t+s))dt\right] \\
&+ \sigma \int_s^T \int_u^T \exp(-a(t-u))dtdW(u) \\
&= (r(s)-f(0,s))\left(\frac{\exp(-a(t-s))-1}{-a}\right) + \int_s^T f(0,t)dt \\
&+ \frac{\sigma^2}{2a^2}\left[(T-s) + \frac{1}{a}\Big(\exp(-a(T-s))-1\Big) - \frac{1}{2a}\Big(\exp(-2aT)-\exp(-2as)\Big)\right. \\
&\left. + \frac{1}{a}\Big(\exp(-a(T+s))-\exp(-2as)\Big)\right] + \frac{\sigma}{a}\int_s^T \Big(1-\exp(-a(T-u))\Big)dW(u) \\
&= (r(s)-f(0,s))\left(\frac{\exp(-a(t-s))-1}{-a}\right) + \int_s^T f(0,t)dt \\
&+ \frac{\sigma^2}{2a^2}\left[(T-s) + \frac{\exp(-a(T-s))}{a} - \frac{1}{a} - \frac{\exp(-2aT)+\exp(-2as)-2\exp(-a(T-s))}{2a}\right] \\
&+ \frac{\sigma}{a}\int_s^T \Big(1-\exp(-a(T-u))\Big)dW(u)
\end{aligned}
$$

$$
\begin{aligned}
&= (r(s) - f(0,s))\bigg(\frac{1-\exp(-a(t-s))}{a}\bigg) + \int_s^T f(0,t)dt \\
&+ \frac{\sigma^2}{2a^3}\bigg[a(T-s) + \exp(-a(T-s)) - 1 - \frac{1}{2}\bigg(\exp(-aT) - \exp(-as)\bigg)^2\bigg] \\
&+ \frac{\sigma}{a}\int_s^T \bigg(1 - \exp(-a(T-u))\bigg)dW(u).
\end{aligned}
$$

Therefore, we observe that $\int_s^T r(t)dt$ has a Normal distribution with expected value and variance given respectively by

$$
\begin{aligned}
E\bigg[\int_s^T r(t)dt\bigg|\mathcal{F}(s)\bigg] &= (r(s) - f(0,s))\bigg(\frac{1-\exp(-a(T-s))}{a}\bigg) - ln\frac{P(0,T)}{P(0,s)} \\
&+ \frac{\sigma^2}{2a^3}\bigg[a(T-s) + \exp(-a(T-s)) - 1 \\
&- \frac{1}{2}\bigg(\exp(-aT) - \exp(-as)\bigg)^2\bigg] \\
Var\bigg[\int_s^T r(t)dt\bigg|\mathcal{F}(s)\bigg] &= Var\bigg[\frac{\sigma}{a}\int_s^T \bigg(1 - \exp(-a(T-u))\bigg)dW(u)\bigg] \\
&= \frac{\sigma^2}{a^2}\int^T s\bigg(1 + \exp(-2a(T-u)) - 2\exp(-a(T-u))\bigg)du \\
&= \frac{\sigma^2}{a^2}\bigg[(T-s) - \frac{3}{2a} - \frac{\exp(-2a(T-s))}{2a} + \frac{2\exp(-a(T-s))}{a}\bigg]
\end{aligned}
\tag{3.35}
$$

Hence, using (3.35) we obtain the zero coupon bond price at time t

$$
\begin{aligned}
P(t,T) &= E\bigg[\exp\bigg(-\int_t^T r(u)du\bigg)\bigg] \\
&= \exp\bigg\{-E\bigg[\int_t^T r(u)du\bigg] + \frac{1}{2}Var\bigg[\int_t^T r(u)du\bigg]\bigg\} \\
&= \exp\bigg\{(f(0,t) - r(t))\bigg(\frac{1-\exp(-a(T-t))}{a}\bigg) + ln\frac{P(0,T)}{P(0,t)} \\
&- \frac{\sigma^2}{4a^3}\bigg[-2\exp(-a(T-t)) + \exp(-2a(T-t)) - \bigg(\exp(-aT) - \exp(-as)\bigg)^2 + 1\bigg]\bigg\} \\
&= \exp\bigg\{(f(0,t) - r(t))\bigg(\frac{1-\exp(-a(T-t))}{a}\bigg) + ln\frac{P(0,T)}{P(0,t)} \\
&- \frac{\sigma^2}{4a^3}\bigg[\bigg(1 - \exp(-a(T-t))\bigg)^2 - \bigg(\exp(-aT) - \exp(-as)\bigg)^2\bigg]\bigg\} \\
&= \frac{P(0,T)}{P(0,t)}\exp\bigg\{(f(0,t) - r(t))\bigg(\frac{1-\exp(-a(T-t))}{a}\bigg) \\
&- \frac{\sigma^2}{4a^3}\bigg[\bigg(\exp(-aT) - \exp(-as)\bigg)^2\bigg(\exp(2as) - 1\bigg)\bigg]\bigg\}.
\end{aligned}
\tag{3.36}
$$

Using the analysis of Brigo and Mercurio (2006), we observe that the price of the

zero coupon bond can be also represented as

$$P(t,T) = A(t,T)e^{-B(t,T)r(t)}, \tag{3.37}$$

where the terms $A(t,T)$ and $B(t,T)$ are the solutions of the affine term structure we have generally described in (1.16) and (1.29)

$$\begin{cases} B_t(t,T) - aB(t,T) = -1 \\ B(T,T) = 1 \end{cases} \tag{3.38}$$

and

$$\begin{cases} A_t(t,T) = \theta(t)B(t,T) - \frac{1}{2}\sigma^2 B^2(t,T) \\ A(T,T) = 0. \end{cases} \tag{3.39}$$

Finally, the solutions of the systems can be represented as

$$B(t,T) = \frac{1}{a}[1 - \exp(-a(T-t))] \tag{3.40}$$

$$A(t,T) = \frac{P(0,T)}{P(0,t)} \exp\left\{B(t,T)f(0,t) - \frac{\sigma^2}{4a}\left[1 - \exp(-2at)\right]B(t,T)^2\right\}. \tag{3.41}$$

3.3 Caps/Floors: pre-crisis pricing framework

In this section we analyse one of the most popular families of interest rate derivatives, the caps and floors. The aim of this section is to provide the pricing framework we use to calibrate the Hull-White model. The results exposed in this section are mostly taken by Brigo and Mercurio (2006) and Kienitz (2014).

The discounted payoff of a cap and the discounted payoff of a floor can be generally represented as

$$\sum_{i=1}^{n} P(t,T_i)N\tau(L(T_{i-1},T_i) - K)^+$$

$$\sum_{i=1}^{n} P(t,T_i)N\tau(K - L(T_{i-1},T_i))^+$$

where $P(t,T_i)$ is the single yield curve curve[2], N is the notional amount, τ is the time interval separating each caplet/floorlet payment, K is the strike price and $L(T_{i-1},T_i)$ is the IBOR rate.

The pricing approach that was commonly adopted before the financial crisis considers a cap as a portfolio of European puts written on zero coupon bond and, conversely, a floor option as a portfolio of European calls. In this section we analyze the price of a cap by

[2]Note that there is no need to distinguish between the curve used to discount and the one used for derive the forward rates; indeed, we are discussing option pricing in the single curve framework. Therefore, we don't use the subscript notation d to distinguish between the two curves.

considering it as a portfolio of puts. Therefore, the first step is to remark that the price of a put option written on a zero coupon bond under the risk-neutral probability $\mathbb{Q}$ is

$$Put(t,T,S,K) = E\bigg[\exp\bigg(-\int_t^T r(s)ds\bigg)\bigg(K - P(T,S)\bigg)^+\bigg|\mathcal{F}(t)\bigg] \tag{3.42}$$

and, changing the bank account numeraire $B(t)$ with the zero coupon bond numeraire $P(t,T)$, we are able to move to the forward measure $\mathbb{Q}^T$ through the Radon-Nikodym derivative

$$\frac{d\mathbb{Q}^T}{\mathbb{Q}} = \frac{P(T,T)B(0)}{P(0,T)B(T)} = \frac{\exp\bigg(-\int_0^T r(s)ds\bigg)}{P(0,T)}. \tag{3.43}$$

Finally, the price of the put option under the forward measure $\mathbb{Q}^T$ can be expressed as

$$Put(t,T,S,K) = P(t,T)E^{\mathbb{Q}^T}\bigg[\bigg(K - P(T,S)\bigg)^+\bigg|\mathcal{F}(t)\bigg]. \tag{3.44}$$

Equation (3.44) is very useful when the distribution of $P(T,S)$ is lognormal with zero drift conditional on the sigma-algebra $\mathcal{F}(t)$: indeed, it reduces to the Black price formula we introduce later.

Given that the price of a cap is equal to the sum of the present values of each single caplet, we first consider the present value of a general i-caplet

$$\begin{aligned}
Caplet(\cdot) &= E\bigg[\exp\bigg(-\int_t^{T_i} r(s)ds\bigg)\tau N\bigg(L(T_{i-1},T_i) - K\bigg)^+\bigg|\mathcal{F}(t)\bigg] \\
&= NE\bigg[\exp\bigg(-\int_t^{T_{i-1}} r(s)ds\bigg)P(T_{i-1},T_i)\tau\bigg(L(T_{i-1},T_i) - K\bigg)^+\bigg|\mathcal{F}(t)\bigg] \\
&= NE\bigg[\exp\bigg(-\int_t^{T_{i-1}} r(s)ds\bigg)P(T_{i-1},T_i)\bigg(\frac{1}{P(T_{i-1},T_i)} - 1 - \tau K\bigg)^+\bigg|\mathcal{F}(t)\bigg] \\
&= NE\bigg[\exp\bigg(-\int_t^{T_{i-1}} r(s)ds\bigg)\bigg(1 - P(T_{i-1},T_i) - \tau P(T_{i-1},T_i)K\bigg)^+\bigg|\mathcal{F}(t)\bigg] \\
&= N(1+K\tau)Put(t,T_{i-1},T_i,K_{adj})
\end{aligned} \tag{3.45}$$

where, in the fourth equation, we simplified by considering a put option with a strike value $K_{adj} = \frac{1}{1+K\tau}$.
Eventually, summing up the present value of each caplet we obtain that the price of a cap is

$$Cap(t,\tau,N,K) = \sum_{i=1}^{n} N(1+K\tau)Put(t,T_{i-1},T_i,K_{adj}). \tag{3.46}$$

The price of a floor option can be obtained using the same method and, conversely, the

final price is the sum of the present values of call options with strike $K_{adj} = \frac{1}{1+K\tau}$

$$Floor(t, \tau, N, K) = \sum_{i=1}^{n} N(1 + K\tau)Call(t, T_{i-1}, T_i, K_{adj}). \tag{3.47}$$

A cap/floor is defined to be at-the-money (ATM) iff the strike value K is equal to

$$K_{ATM} = \frac{P(0,t) - P(0,T_n)}{\sum_{i=1}^{n} \tau P(0,T_i)} \tag{3.48}$$

The cap is defined to be in-the-money (ITM) if $K < K_{ATM}$ and it is called out-of-the-money (OTM) if $K > K_{ATM}$.

The general framework we have just depicted can be used to get explicit methods to derive the prices of caps and floors. In the following sections, we provide two principal pricing frameworks. In the first one, we present the price of a cap as a portfolio of put options, whose underlying asset $P(t, T_i)$ depend on an Hull-White rate. In the second framework the price of a cap is determined assuming that the future payoffs are described by a Black formula. These two pricing frameworks are then used in the calibration algorithm presented in Chapter 4. The necessary assumption for the validity of the two frameworks is that the IBOR rate $L(T_{i-1}, T_i)$ has a lognormal distribution.

3.3.1 Pricing under the Hull-White model

In the previous sections we have analysed option pricing when the short rate dynamics follows the Vasicek model. In this section we finally bring together the findings we have previously acquired: we show how to price cap option written on a zero coupon bond whose short rate is determined by the Hull-White model.

We remember that the price of a European put written on a zero coupon bond $P(t, T)$ with strike K and maturity T is obtained from (3.44), where the expectation is taken under the forward measure $\mathbb{Q}^T$.
From Brigo and Mercurio (2006), we know that the stochastic process $x(t)$ in (3.22) is equal to the $r(t)$ Vasicek-process (3.11) with the parameter $\theta = 0$. Therefore, the $x(t)$ process is

$$dx(t) = \Big[- ax(t) - B(t,T)\sigma^2 \Big] dt + \sigma dW^T(t) \tag{3.49}$$

where $dW^T(t)$ is equal to (3.10), the Brownian motion under the forward measure $\mathbb{Q}^T$.

Integrating the process $x(t)$ we obtain an equation equal to (3.12) with $\theta = 0$

$$\begin{aligned} x(t) = x(s)\exp(-a(t-s)) - \frac{\sigma^2}{a^2}\Big(1 - \exp(-a(t-s))\Big) + \frac{\sigma^2}{2a^2}\Big[\exp(-a(T-t)) \\ - \exp(-a(T+t-2s))\Big] + \sigma\int_s^t \exp(-a(t-u))dW^{\mathbb{Q}^T}(u) \end{aligned} \tag{3.50}$$

Therefore, using the same technique we developed in section 3.2, we observe that $r(t)$ has a Normal distribution also under the forward measure $\mathbb{Q}^T$, with a conditional expected value and a conditional variance equal to

$$\begin{aligned} E^{\mathbb{Q}^T}\big[r(t)\big|\mathcal{F}_s\big] &= x(s)\exp(-a(t-s)) - \frac{\sigma^2}{a^2}\Big[1 - \exp(-a(t-s))\Big] \\ &\quad + \frac{\sigma^2}{2a^2}\Big[\exp(-a(T-t)) - \exp(-a(T+t-2s))\Big] + \alpha(t) \\ Var^{\mathbb{Q}^T}\big[r(t)\big|\mathcal{F}_s\big] &= \frac{\sigma^2}{2a}\Big[1 - \exp(-2a(t-s))\Big]. \end{aligned} \tag{3.51}$$

Finally, the price of a put option written on a zero coupon bond $P(t,S)$ with strike K and maturity T is equal to the general formulation we provided in (3.16) with $\omega = -1$

$$Put(t,T,S,K) = KP(t,T)\Phi(-h+\sigma_p) - P(t,S)\Phi(-h) \tag{3.52}$$

where σ_p and h coincide with (3.17)

$$\begin{aligned} \sigma_p &= \sigma\sqrt{\frac{1-\exp(-2a(T-t))}{2a}}B(T,S) \\ h &= \frac{\sigma_p}{2} + \frac{1}{\sigma_p}\ln\left(\frac{P(t,S)}{P(t,T)K}\right). \end{aligned} \tag{3.53}$$

We know from Section 3.3 and - particularly - from equation (3.46), that a cap option can be treated as a portfolio of different put options. Therefore, we are able to obtain the price of a cap with strike K, nominal value N and a payment schedule divided into n time intervals with an equal length τ

$$\begin{aligned} Cap(t,\tau,N,K) &= N\sum_{i=1}^{n}\Big(1+\tau K\Big)Put(t,T_{i-1},T_i,K_{adj}) \\ &= N\sum_{i=1}^{n}\Big[P(t,T_{i-1})\Phi(-h_i+\sigma_p^i) - (1+\tau K)P(t,T_i)\Phi(-h_i)\Big] \end{aligned} \tag{3.54}$$

where

$$K_{adj} = \frac{1}{1+\tau K}$$
$$\sigma_p^i = \sigma\sqrt{\frac{1-\exp(-2a(T_{i-1}-t))}{2a}}B(T_{i-1},T_i)$$
$$h_i = \frac{\sigma_p^i}{2} + \frac{1}{\sigma_p^i}\ln\left(\frac{(1+\tau K)P(t,T_i)}{P(t,T_{i-1})}\right).$$

In a similar way, the price of a floor option with corresponding parameters is

$$Floor(t,\tau,N,K) = N\sum_{i=1}^{n}\Big[(1+\tau K)P(t,T_i)\Phi(h_i) - P(t,T_{i-1})\Phi(h_i-\sigma_p^i)\Big]. \tag{3.55}$$

3.3.2 Other pricing models

In the next subsections we show how to derive the price of cap and floor with the Black model - the one we use in the calibration in Chapter 4 to transform the quoted volatilities into cap prices - and we briefly introduce option pricing under the Bachelier model and the Shifted Black model, which represent the new market practice for pricing interest rate derivatives.

Black model

In this section, we price a cap as the sum of the expected values of each i-caplet under the T_i-forward measure associated with the zero coupon bond numeraire $P(0,T_i)$.
As observed by Kienitz (2014), we note that applying the change of numeraire (3.43) to equation (3.45) we obtain the following formulation of the i-caplet's present value under the T_i-forward probability measure

$$\begin{aligned} Caplet(\cdot) &= P(0,T_i)E^{\mathbb{Q}^{T_i}}\left[\frac{1}{P(T_i,T_i)}\tau N\Big(L(T_{i-1},T_i)-K\Big)^+\Big|\mathcal{F}(t)\right] \\ &= P(0,T_i)N\tau E^{\mathbb{Q}^{T_i}}\left[\Big(L(T_{i-1},T_i)-K\Big)^+\Big|\mathcal{F}(t)\right] \end{aligned} \tag{3.56}$$

The calibration algorithm in Chapter 4 is built on the assumption that the forward rate $L(t,T_{i-1},T_i)$ has a lognormal distribution under the T_i-forward measure with the zero coupon bond numeraire $P(0,T_i)$, therefore its process can be described using a Black model[3]. If lognormality is satisfied, the value of a cap can be represented as the discounted

[3]This assumption was not necessary before the financial crisis: indeed, the forward rate was described by a martingale process under the T_i-forward measure, with the lognormality of its distribution as a consequence.

sum of each single i-caplet

$$Cap^{Black}(\cdot) = N\sum_{i=1}^{n} P(0,T_i)\tau Black(K, F(0,T_{i-1},T_i), \nu_i, 1) \tag{3.57}$$

where the Black formula[4] is

$$Black(K,F,\nu,\omega) = F\omega\Phi(\omega d_1(K,F,\nu)) - K\omega\Phi(\omega d_2(K,F,\nu)) \tag{3.58}$$

with

$$\begin{aligned} d_1(K,F,\nu,\omega) &= \frac{\ln(\frac{F}{K}) + \frac{\nu^2}{2}}{\nu} \\ d_2(K,F,\nu,\omega) &= \frac{\ln(\frac{F}{K}) - \frac{\nu^2}{2}}{\nu} \\ \nu_i &= \sigma_{cap}\sqrt{T_{i-1}} \end{aligned}$$

where σ_{cap} is the volatility quoted in the market for a given cap.
The same pricing formula applies to the floor option

$$Floor^{Black} = N\sum_{i=1}^{n} P(0,T_i)\tau Black(K, F(0,T_{i-1},T_i), \nu_i, -1) \tag{3.59}$$

The reader should note that the cap price under the forward measure is calculated as the sum of the present values of a portfolio of call options, while, in the general formulation we have provided in (3.45), we have treated caps as portfolios of put options.

Finally, we show how to derive Greeks formulas for a single caplet in the price equation (3.57). The Greeks are the sensitivities which are calculated for risk management purposes and they correspond to the derivatives of the caplet's formula with respect to the parameters of the model.
Before illustrating the main Greeks, we mention again two important concepts. The first is that the price of a single caplet at time $t = 0$ can be represented as

$$Caplet(\cdot) = NP(0,T_i)\tau\Big[F\Phi(d_1) - K\Phi(d_2)\Big], \tag{3.60}$$

where Φ is the cumulative standard Normal distribution function. For simplicity we call σ_{cap} as σ until the end of the Black model's subsection. The second concept is that the

[4]The derivation of the Black formula is provided in the Appendix B.

probability density function $f(d_2)$ can be written as

$$\begin{aligned} f(d_2) = f(d_1 - \sigma\sqrt{T_{i-1}}) &= \frac{\exp\left(-\frac{1}{2}(d_1 - \sigma\sqrt{T_{i-1}})^2 \right)}{\sqrt{2\pi}} \\ &= \frac{\exp\left(-\frac{d_1^2}{2} - \frac{\sigma^2 t}{2} + d_1\sigma\sqrt{T_{i-1}} \right)}{\sqrt{2\pi}} \\ &= f(d_1)\exp\left(-\frac{\sigma^2 t}{2} + d_1\sigma\sqrt{T_{i-1}} \right) \\ &= f(d_1)\frac{F}{K} \end{aligned}$$

Finally, we can list the following Greeks

$$\begin{aligned} \Delta &= \frac{\partial Caplet(\cdot)}{\partial F} = NP(t,T_i)\tau\left[\Phi(d_1) + f(d_1)F\frac{\partial d_1}{\partial F} - f(d_1 - \sigma\sqrt{T_{i-1}})K\frac{\partial d_1}{\partial F}\right] \\ &= NP(t,T_i)\tau\left[\Phi(d_1) + f(d_1)F\frac{\partial d_1}{\partial F} - f(d_1)F\frac{\partial d_1}{\partial F}\right] \\ &= NP(t,T_i)\tau\Phi(d_1) \\ \Gamma &= \frac{\partial^2 Caplet(\cdot)}{\partial F^2} = NP(t,T_i)\tau\left[f(d_1)\frac{\partial d_1}{\partial F}\right] \\ &= NP(t,T_i)\tau\left[\frac{f(d_1)}{F\sigma\sqrt{T_{i-1}}}\right] \\ \mathcal{V} &= \frac{\partial Caplet(\cdot)}{\partial \sigma} = NP(t,T_i)\tau\left[f(d_1)F\frac{\partial d_1}{\partial \sigma} - Kf(d_1)\frac{F}{K}\frac{\partial d_1 - \sigma\sqrt{T_{i-1}}}{\partial \sigma}\right] \\ &= NP(t,T_i)\tau\left[F\sqrt{T_{i-1}}f(d_1)\right] \\ \Theta &= \frac{\partial Caplet(\cdot)}{\partial t} = NP(t,T_i)\tau\frac{\partial}{\partial t}\left[F\Phi(d_1) - K\Phi(d_2)\right] + N\frac{\partial P(t,T_i)}{\partial t}\tau\left[F\Phi(d_1) - K\Phi(d_2)\right] \\ &= NP(t,T_i)\tau\left[f(d_1)F\frac{\partial d_1}{\partial t} - f\big(d_1 - \sigma\sqrt{T_{i-1}}\big)K\right] + N\frac{\partial P(t,T_i)}{\partial t}\tau\left[F\Phi(d_1) - K\Phi(d_2)\right] \\ &= NP(t,T_i)\tau\left[f(d_1)F\frac{\partial d_1}{\partial t} - f(d_1)F\big(\frac{\partial d_1}{\partial t} + \frac{\sigma}{2\sqrt{T_{i-1}}}\big)\right] + \frac{Caplet(\cdot)}{P(t,T_i)}\frac{\partial P(t,T_i)}{\partial t} \\ &= NP(t,T_i)\tau\left[f(d_1)\frac{F\sigma}{2\sqrt{T_{i-1}}}\right] + \frac{Caplet(\cdot)}{P(t,T_i)}\frac{\partial P(t,T_i)}{\partial t} \end{aligned} \tag{3.61}$$

Normal model

In the first part of this thesis, we have discussed the evolution interest rate modelling has faced after the financial crisis of 2008. The shift to OIS discounting and the negative rates implied by the yield curves of several currencies forced financial operators to consider models other than the Black model, which represented the common practice before interest

rates related to several primary currencies turned to be negative.

The Normal model, which is also referred as Bachelier model, provides a different formulation of the dynamic of the asset $S(t)$[5] with respect to the one given by the Black model

$$\begin{cases} dS(t) = \sigma_N dW(t) \\ S(0) = s \end{cases} \tag{3.62}$$

The prices of European Call and European Put options written on the asset $S(t)$ with strike K and maturity T are, according to Kienitz (2014), respectively given by

$$\begin{aligned} Call_N &= \Big(S(0) - k\exp(-rT)\Big)\Phi\bigg(\frac{S(0)-K}{\sigma_N\sqrt{T}}\bigg) + \sigma\sqrt{T}\Phi\bigg(\frac{S(0)-K}{\sigma_N\sqrt{T}}\bigg) \\ Put_N &= \Big(K - S(0)\Big)\Phi\bigg(-\frac{S(0)-K}{\sigma_N\sqrt{T}}\bigg) + \sigma\sqrt{T}\Phi\bigg(\frac{S(0)-K}{\sigma_N\sqrt{T}}\bigg) \end{aligned} \tag{3.63}$$

where Φ is the cumulative standard Normal distribution function and σ is the volatility of the option. The volatility σ can be substituted by the implied volatilities quoted on the market to retrieve the market price of the option.

Shifted Black model

The Shifted Black model, which is also called Displaced diffusion model, assume that the dynamics of the asset $S(t)$ follows

$$\begin{cases} dS(t) = (S+a)\sigma dW(t) \\ S(0) = s \end{cases} \tag{3.64}$$

where a is the shift parameter. The prices of European Call and European Put options written on the asset $S(t)$ with strike K and maturity T are respectively given by

$$\begin{aligned} Call_{SB} &= (S(0)+a)\Phi(d_1) - (K+a)\Phi(d_2) \\ Put_{SB} &= (K+a)\Phi(-d_2) - (S(0)+a)\Phi(-d_1) \end{aligned} \tag{3.65}$$

where d_1 and d_2 are respectively given by

$$\begin{aligned} d_1 &= \frac{\ln\left(\frac{S+a}{K+a}\right) + \frac{\sigma^2 T}{2}}{\sigma\sqrt{T}} \\ d_2 &= d_1 - \sigma\sqrt{T}. \end{aligned}$$

[5]We refer to a general asset $S(t)$ and not to the forward rate we indicate in the formulation of the Black model.

Shifted models are used by practitioners because they are useful to model term structures with skewed volatilities. Indeed, the introduction of the displacement parameter a allows for a more representative volatility surface. For a complete discussion of displaced diffusion models we refer to Chapter 7 of Andersen and Piterbarg (2010).

Chapter 4

Calibration of the Hull-White model

In this chapter we analyze the calibration algorithm for the Hull-White short rate model. We use market quotes for the volatilities of USD LIBOR3M caps. The calibration algorithm reproduces the formulas we provided in Chapter 3. As already explained in the introduction to the second part of this dissertation, the calibration of the Hull-White model is done using a single yield curve both for discounting and for retrieving forward rates. We stress again that the assumption validating this bootstrapping technique is that the USD LIBOR3M curve has a lognormal distribution. Furthermore, the choice of using a single yield curve - even if conceptually wrong in a multiple curve world - shouldn't lead to considerable errors when comparing the market prices of derivatives with the prices computed using the single curve approach: indeed, the interbank credit and liquidity risks are weakened in a market environment where the Federal Reserve Bank (FED) is still committed on monetary easing policies[1] and where the FED promptly and effectively reacts in order to prevent financial distress, as it did during the Covid-19 pandemic crisis[2]. We test this hypothesis in Section 4.1, where we find a reasonable mean squared error between the market prices and the prices of cap options computed using the single curve approach.

In the first Section, we present the market data related to caps' volatilities and premia and how we built the discount curve. In the second Section, we describe the algorithm used to calibrate the Hull-White model, whose theoretical basis is rooted in the results we present throughout Chapter 3 and particularly in Section 3.3.1. In the final Section, we report the results of our study.

[1] See the Statement on Longer-Run Goals and Monetary Policy Strategy adopted by the FED on 24 January 2012 and amended as effective on 27 August 2020.

[2] See the transcript of the Chair Powell's press conference after the Federal Open Market Committee (FOMC) meeting on 29 July 2020.

4.1 Market data selection

The market data we use to calibrate the Hull-White model are the quotes of USD LIBOR3M caps' volatilities and premium; the single curve is instead bootstrapped by a set of financial instruments and it was directly calculated using the Thomson Reuters' Eikon bootstrapping tool for Microsoft Excel.

Quotes for cap options

In this thesis we often referred to caps' volatilities and premia as *market* data. However, since interest rate derivatives are OTC traded, caps' volatilities and premia shouldn't be interpreted as quotes resulting of public market transactions. On the opposite, their prices are not directly executed on public exchanges and they are quoted for informational purposes only.
Caps' volatilities and premium data were retrieved by the tables published by ICAP PLC on the financial data streaming platform Thomson Reuters' Eikon. ICAP PLC is an inter-dealer broker providing execution and information services. It is a global supplier of financial data for OTC fixed income and derivative pricing. When providing these quotes, ICAP PLC also publishes the statement "These prices are not executable. They are for informational purposes only".
ICAP PLC publishes volatilities and premia implied both by the Black and the Normal model for USD caps whose caplets occur every three months. The notional amount is equal to USD 10000. We took the data for Black-implied volatilities and premia as of 19 June 2020, their tables are respectively depicted in 4.1 and in 4.2. We also provided the premium surface in Figure 4.1 and the volatility surface in Figure 4.2. We can appreciate that the cap's premium is increasing on the maturity of the cap and it increases as long as its strike gets closer to the ATM-strike. On the other hand, volatility is greater for caps with shorter maturities and it is greater for caps whose strike is closer to the value quoted as ATM-strike. We observe in Table 4.1 that, obviously, the data provider doesn't quote premia for in-the-money (ITM) caps, but only for out-of-the-money (OTM) and at-the-money (ATM) caps. Unfortunately, the data doesn't clearly disclose any other information other than the ones we already provided: indeed, the data provider doesn't reveal if it imposes any additional constraint or if it formulates additional assumption on the Black model we have presented in section 3.3.2; moreover, we don't know which instruments were used to build the discount curve and the forward yield curve to assess caps' prices and volatilities.

USD Caps - Premium Indications														
	STK	ATM	0.25	0.50	0.75	1.00	1.50	2.00	2.50	3.00	4.00	5.00	6.00	7.00
1Y	0.28	4.6		1.3	0.8	0.6	0.4	0.3	0.3	0.3	0.2	0.2	0.2	0.2
2Y	0.24	18.6	18.1	6.6	4.3	3.4	2.6	2.3	2.0	1.9	1.8	1.7	1.6	1.6
3Y	0.26	43.7		21.9	13.7	9.9	6.7	5.3	4.6	4.2	3.6	3.3	3.1	3.0
4Y	0.30	80.5		54.8	36.3	25.2	13.8	9.0	6.8	5.5	4.3	3.7	3.4	3.2
5Y	0.37	130.0		106	75.6	54.6	30.2	18.6	12.8	9.6	6.5	5.1	4.3	3.9
6Y	0.44	191.0		176	132	99.2	57.6	35.7	24.0	17.4	10.9	8.0	6.4	5.4
7Y	0.51	259.0			202	157	95.1	60.1	40.3	28.9	17.4	12.2	9.4	7.7
8Y	0.57	335.0			284	225	142	91.8	62.2	44.5	26.4	18.1	13.6	10.9
9Y	0.63	413.0			374	301	196	129	88.4	63.4	37.4	25.3	18.7	14.8
10Y	0.68	494.0			468	382	255	171	119	85.9	50.6	34.0	24.9	19.5
12Y	0.76	666.0				561	388	270	192	141	84.2	56.5	41.2	32.0
15Y	0.84	934.0				842	604	435	318	238	147	101	75.2	59.3
20Y	0.93	1391				1332	990	735	551	421	265	183	136	107

Table 4.1: Indications of Cap premia for USD as of 19.06.2020. Source: Thomson Reuters' Eikon - Inter-dealer broker (IDB), ICAP PLC.

USD Caps - Black Implied Volatilities														
	STK	ATM	0.25	0.50	0.75	1.00	1.50	2.00	2.50	3.00	4.00	5.00	6.00	7.00
1Y	0.28	77.41	84.6	81.6	96.4	106	120	129	136	142	151	158	164	169
2Y	0.24	119.8	117	96.3	101	106	114	120	125	129	135	140	144	148
3Y	0.26	150.2	154	107	99.2	96.5	96.4	98.2	100	102	106	109	112	114
4Y	0.30	155.1	185	116	97.7	87.6	77.7	74.3	73.5	73.9	75.7	77.8	79.9	81.8
5Y	0.37	149.4	223	121	97.5	84.3	70.5	64.5	61.8	60.8	60.8	61.8	63.1	64.4
6Y	0.44	136.8	290	124	96.2	81.4	65.9	58.7	55.1	53.4	52.3	52.6	53.2	54.1
7Y	0.51	123.1	499	124	94.3	78.7	62.5	54.7	50.7	48.6	47.0	46.8	47.1	47.6
8Y	0.57	112.3	485	125	92.9	76.9	60.4	52.3	48.0	45.7	43.7	43.2	43.3	43.6
9Y	0.63	104.1	486	126	91.9	75.6	58.9	50.7	46.2	43.7	41.4	40.7	40.7	40.9
10Y	0.68	98.97	414	129	91.9	75.2	58.3	50.0	45.4	42.7	40.2	39.3	39.1	39.1
12Y	0.76	91.33	498	136	92.4	74.7	57.4	48.9	44.1	41.2	38.3	37.2	36.7	36.6
15Y	0.84	85.70	706	161	94.8	74.9	56.8	48.0	43.0	40.0	36.9	35.7	35.1	35.0
20Y	0.93	81.31	729	487	100	76.0	56.2	47.0	41.7	38.5	35.0	33.4	32.6	32.2

Table 4.2: USD Caps/Floors/ATM straddles Black volatilities for USD as of 19.06.2020. Source: Thomson Reuters' Eikon - Inter-dealer Broker (IDB), ICAP PLC.

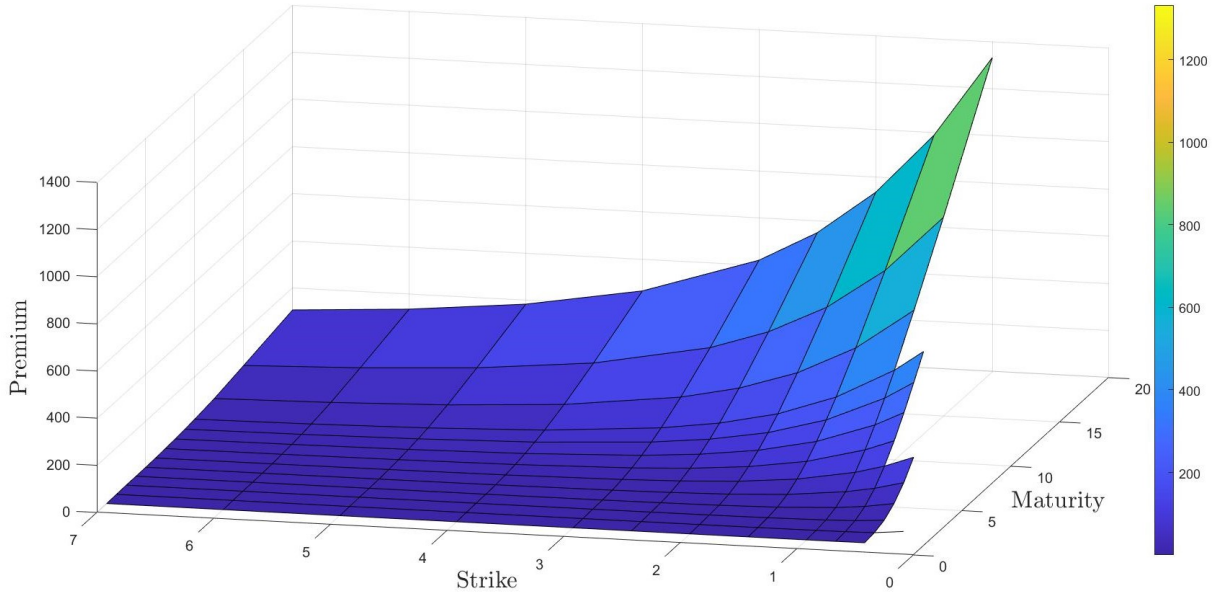

Figure 4.1: Caps' premia surface. Source: Thomson Reuters' Eikon - Inter-dealer Broker (IDB), ICAP PLC.

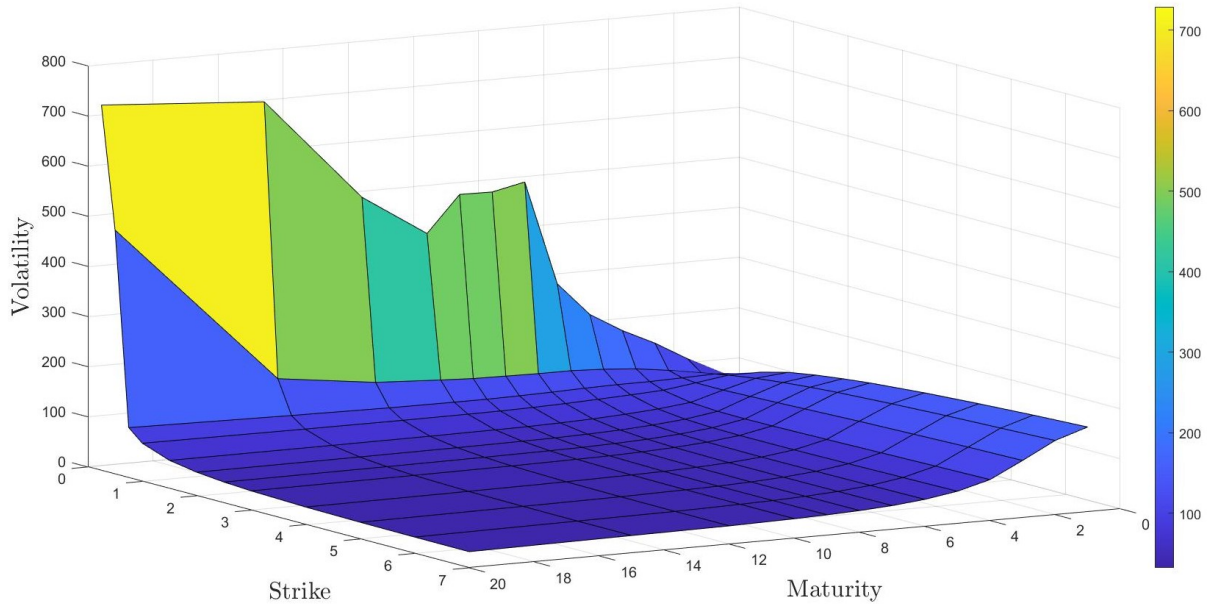

Figure 4.2: Black implied volatility surface of Caps/Floors/ATM straddles for USD as of 19.06.2020. Source: Thomson Reuters' Eikon - Inter-dealer Broker (IDB), ICAP PLC.

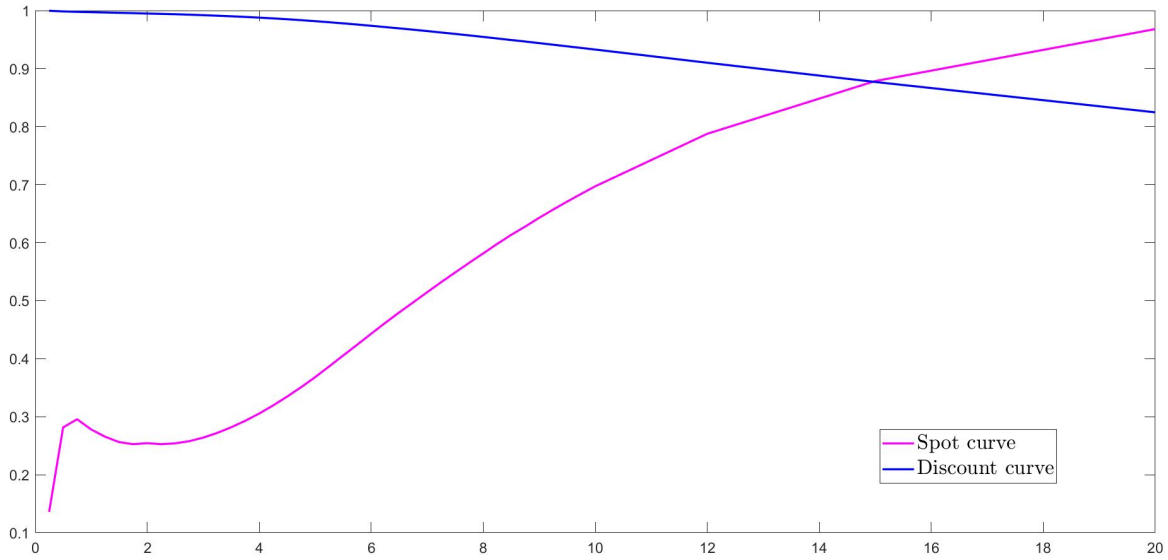

Figure 4.3: The discount curve we used in the calibration algorithm and the corresponding spot rate curve. The two curves are bootstrapped using USD Deposit, USD LIBOR3M futures and USD LIBOR3M IRS as of 19 June 2020. Source: Thomson Reuters' Eikon.

Single yield curve bootstrapping

The single interest rate yield curve was directly bootstrapped using the Thomson Reuters' Eikon bootstrapping tool for Microsoft Excel. The yield curve is bootstrapped from the prices of linear interest rate instruments with different maturities as of 19 June 2020: we select short-term USD deposit to bootstrap the pillar at the third month, i.e. 3M-pillar, USD LIBOR3M futures for the pillars in the interval from 6M and 1Y9M and, for the long term period, USD LIBOR3M IRS covering the interval from 2Y to 20Y. The selection of linear interest rate instruments is done according to the indications provided by Bianchetti and Morini (2013) when discussing the single curve framework. The bootstrapping formulas adopted by Thomson Reuters' Eikon are equal to the bootstrapping equations (2.3), (2.7) and (2.12) we provided in Section 2.1.1. According to the methodology disclosure of Thomson Reuters' Eikon as of June 2020, the curves "are calculated using Adfin Analytics and source the best-in-class real-time quotes from major trading platforms such as Tradeweb as well as major broking firms". Furthermore, the curves are bootstrapped interpolating the missing pillars with the Anderson version of the basis spline approach.
The spot curve and the discount curve are displayed in Figure 4.3.

The goodness of the single curve is tested by computing the mean squared error between the prices provided by ICAP PLC in Table 4.1 and the prices retrieved by applying the Black formula to the Black implied volatilities provided by ICAP PLC in Table 4.2. The resulting mean squared error is equal to 0.0126, a value we consider acceptable for our modelling purposes.

4.2 Calibration algorithm

In this section we present the MATLAB implementation of the calibration technique. We present the MATLAB code, explaining the meaning and the reasoning behind each different function.

Data entry

The data are entered into the calibration algorithm by converting prices and volatilities into usable arrays. We present below lines from 1 to 26 of the *main.m* function.

```
1  cap_dataset = readtable('cap.xlsx');
2  zcurve_dataset = readtable('zcurve.xlsx');
3  cap_dataset = table2array(cap_dataset);
4
5  n_cap = length(cap_dataset);
6
7  sigma_data = cap_dataset(:,2);
8  sigma_data = sigma_data./100;
9
10 strike_data = cap_dataset(:,3);
11 strike_data = strike_data./100;
12
13 premium_data = cap_dataset(:,4);
14
15 zc_maturity = table2array(zcurve_dataset(:,5));
16 zc_maturity = [0,transpose(zc_maturity)];
17 zc_maturity = transpose(zc_maturity);
18
19 discount = table2array(zcurve_dataset(:,3));
20 discount = transpose([1,transpose(discount)]);
21
22 tau = 0.25;
23
24 P_m2 = interp1(zc_maturity,discount,0.001,'linear');
25 P_m1 = interp1(zc_maturity,discount,0,'linear');
26 f_0 = -(log(P_m2)-log(P_m1))/(0.001);
```

The lines from 24 to 26 are used to determine the instantaneous forward rate. Since the interpolated discount curve is not differentiable, we use a numerical method to

compute the derivative: we take the logarithm of the discount curve at time 0 and at time 0.001, then we divide the difference between the two logarithms for the time delta. The instantaneous forward rate is equal to 0.0014.

Determine the prices using implied volatilities

We present below the lines from 27 to 59 of the *main.m* function. The lines describe how to compute the mean squared error we use to test the goodness of the discount curve.
We first price each single cap using the Black implied volatilities in Table 4.2 and the Black formula for cap options. Then, we compute the mean square error between the quoted prices and the prices obtained by applying the Black formula.
Unfortunately, we are not able to test the quality of the Black prices whose strikes are smaller than the quoted strike for a given maturity. Indeed, ICAP doesn't publish this type of premium data. Therefore, we don't consider the observations whose quoted prices are missing.

```
1  cap_builder = cell(1,n_cap);
2
3  for i = 1:n_cap
4      n = 1+round(cap_dataset(i,5)/tau);
5      i_cap = zeros(n,4);
6      i_cap(:,1) = transpose(0:tau:cap_dataset(i,5));
7
8      for j = 1:n
9          i_cap(j,2) = interp1(zc_maturity,discount,i_cap(j,1),'
               spline');
10     end
11
12     i_cap(:,3) = sigma_data(i,1);
13     i_cap(:,4) = strike_data(i,1);
14
15     cap_builder{i} = i_cap;
16
17 end
18
19 caps_black = zeros(n_cap,1);
20
21 for i = 1:n_cap
22
23     i_cap = cap_builder{i};
24     i_cap_black_price = cap_black_formula(i_cap);
```

```
25      caps_black(i) = i_cap_black_price;
26
27  end
28
29  undefined_premium = sum(isnan(premium_data));
30  premium_data(isnan(premium_data),1) = caps_black(isnan(
        premium_data),1);
31  premium_diff = ((caps_black./premium_data)-1).^2;
32  mse_premium = (sum(premium_diff))/(size(premium_diff,1)-
        undefined_premium);
```

The function *cap_black_formula.m* refers to the Black pricing formula for cap options in equation (3.57) and it is equal to

```
1   function y = cap_black_formula(i_cap)
2       h = size(i_cap,1);
3       cap = 0;
4       N = 10000;
5       tau = 0.25;
6
7       for j = 2:h
8           P = i_cap(j,2);
9           F = ((i_cap(j-1,2)/i_cap(j,2))-1)/tau;
10          STK = i_cap(j,4);
11          sigma = i_cap(j,3);
12          v = sigma*sqrt(i_cap(j-1,1));
13          d_1 = (log(F/STK)+(v^2)/2)/v;
14          d_2 = (log(F/STK)-(v^2)/2)/v;
15          Nd_1 = normcdf(d_1);
16          Nd_2 = normcdf(d_2);
17          black = F*Nd_1-STK*Nd_2;
18          caplet = N*P*tau*black;
19          cap = cap+caplet;
20      end
21
22      y = cap;
23
24  end
```

Minimization function

For $t = 0$ we observe that equation (3.41) reduces to

$$A(0,T) = P(0,T)\exp\big(B(0,T)r(0)\big),$$

where we substitute the instantaneous forward rate with the short rate at time $t = 0$, since $f(0,0) = r(0)$. Hence, we don't need to calibrate the value $r(0)$.
Furthermore, we observe that for $t = 0$ we are not able to calibrate the parameters of the Hull-White model, a and σ, using equations (3.40) and (3.41). However, we know that the bond price $P(0,T)$ is equal to the bond price $P^{mkt}(0,T)$ implied by the zero rates observed in the market at time $t = 0$, thus leading to equation (3.37). Therefore, we are able to calibrate the Hull-White model directly by using equation (3.37) in equation (3.52): indeed, we observe that the parameters of the model, a and σ, finally enter into the newly obtained equation for $t = 0$.

We use a minimization function to calibrate the Hull-White model's parameters a and σ in equation (3.21). The reverse calibration procedure can be summarized as:

1. define an interest rate dynamics using the Hull-White model;
2. price a zero coupon bond using the Hull-White interest rate dynamics;
3. price a put option using the zero coupon bond;
4. price the caplets using the zero coupon put;
5. price the cap as a sum of caplets (HW cap);
6. find the Black implied volatilities minimizing the absolute difference between the Black prices and the HW prices;
7. minimize the mean squared error between the quoted Black implied volatilities and the volatilities we found in the previous step.

The minimization function is indicated in lines from 61 to 68 of the *main.m* function.

```
1 target = @(x)mse(x(1),x(2),cap_builder,sigma_data);
2 setup_x = [0.1,1];
3 lb = [0,0.01];
4 ub = [+Inf,+Inf];
5 [x,mse_sigma] = fmincon(target,setup_x,[],[],[],[],lb,ub);
6
```

```
a_star = x(1);
sigma_star = x(2);
```

The function *mse.m* computes the mean squared error between the quoted Black implied volatilities and the *fictitious* Black implied volatilities minimizing the MSE between Black and the HW prices.

```
function y = mse(a,sigma,cap_builder,sigma_data)

    n = size(cap_builder,2);

    diff_value = sigma_data-sigma_black_finder(a,sigma,
        cap_builder);
    y = (sum(diff_value.^2))/n;

end
```

The function *sigma_black_finder.m* finds the *fictitious* Black implied volatilities by the minimization of the absolute difference between Black and HW prices.

```
function y = sigma_black_finder(a,sigma,cap_builder)

    n = size(cap_builder,2);
    caps_hw = zeros(n,1);
    sigma_black = zeros(n,1);

    for i = 1:n

        i_cap = cap_builder{i};
        caps_hw(i) = cap_hw_put_formula(a,sigma,i_cap);

        target = @(x)(abs(cap_black_formula_vol(i_cap,x(1)) -
            caps_hw(i)));
        setup_x = 0;
        lb = 0;
        ub = Inf;

        sigma_black(i) = fmincon(target,setup_x,[],[],[],[],lb,ub
            );

```

```
    end

    y = sigma_black;

end
```

The function *cap_black_formula_vol.m* is used to find the value for Black implied volatilities.

```
capfunction y = cap_black_formula_vol(i_cap,sigma)
    h = size(i_cap,1);
    cap = 0;
    N = 10000;
    tau = 0.25;

    for j = 2:h
        P = i_cap(j,2);
        F = ((i_cap(j-1,2)/i_cap(j,2))-1)/tau;
        STK = i_cap(j,4);
        v = sigma*sqrt(i_cap(j-1,1));
        d_1 = (log(F/STK)+(v^2)/2)/v;
        d_2 = (log(F/STK)-(v^2)/2)/v;
        Nd_1 = normcdf(d_1);
        Nd_2 = normcdf(d_2);
        black = F*Nd_1-STK*Nd_2;
        caplet = N*P*tau*black;
        cap = cap+caplet;
    end

    y = cap;
end
```

The function *cap_hw_put_formula.m* computes the price of a cap by considering a cap as a portfolios of put options, summing up the present values of the future payments.

```
function y = cap_hw_put_formula(a,sigma,i_cap)

    n = size(i_cap,1);
    price = 0;

```

```
6       for i = 2:n
7
8           price = price+caplets_hw_put_formula(a,sigma,i_cap(i
                -1,1),i_cap(i,1),i_cap(i-1,2),i_cap(i,2),i_cap(i,4));
9
10      end
11
12      y = price;
13
14  end
```

The function *caplets_hw_put_formula.m* computes the price of a single caplets applying equation (3.54).

```
1   function y = caplets_hw_put_formula(a,sigma,T,S,P_1,P,STK)
2
3       N = 10000;
4       tau = 0.25;
5       STK_model = 1+STK*tau;
6       y = N*(1+STK*tau)*zbp_hw(a,sigma,T,S,P_1,P,STK_model);
7
8   end
```

The function *zbp_hw.m* finds the price of a put option whose underlying asset is a zero coupon bond depending on a interest rate process described by the Hull-White model.

```
1   function y = zbp_hw(a,sigma,T,S,P_1,P,STK)
2
3       t = 0;
4
5       B_T_S = (1/a)*(1-exp(-a*(S-T)));
6
7       sigma_p = sigma*sqrt((1-exp(-2*a*(T-t)))/(2*a))*B_T_S;
8       h = (1/sigma_p)*log((P*STK)/(P_1))+sigma_p/2;
9
10      PHI_STK = normcdf(-h+sigma_p);
11      PHI_1 = normcdf(-h);
12
13      y = STK*P_1*PHI_STK-P*PHI_1;
14
```

```
15 end
```

We test the goodness of the calibration algorithm by rearranging the structure of the *main.m* function in the following way: after having selected some a priori values for the parameters a and σ, we calculate the zero rate curve and the Black implied volatilities; then, we calibrate the model using the implied volatilities. We observe that the values of the calibrated parameters are equal to the values we selected at the beginning of the testing procedure. Therefore, we conclude that the algorithm is correct and that it can be used to calibrate the Hull-White model from cap volatilities.
Finally, executing the MATLAB code returns us the following values of the calibrated parameters:

- $a = 0.0771$
- $\sigma = 0.0102$.

Using this parameters, we build a vector of Black implied volatilities using the function *sigma_black_finder.m* and we compare this vector with the one containing quoted Black implied volatilities. We observe that the average absolute deviation is equal to 1.3710. Therefore, we conclude that there some disturbance elements in the calibration algorithm. We already know that we have not lost any relevant information using the bootstrapped LIBOR3M curve, notwithstanding we adopt a single curve approach instead of the multiple curve one. Furthermore, we know that the MATLAB code shouldn't lose relevant informations while calibrating the algorithm: as already mentioned, we test the algorithm inputting fictitious values for a and σ parameters and we observe that the procedure is able to reproduce the original values. The reason we obtain a huge value for the average absolute deviation lies, according to Kienitz (2014), on the fact that the volatility is increasing for in-the-money (ITM) and out-of-the-money (OTM) options[3]. Indeed, we observe that cap volatilities in Figure 4.2 have extreme values for ITM and OTM strikes. This problem could be solved by restricting the size of the matrix in Table 4.2, selecting an area which presents more homogeneous volatilities. However, we also know that applying this selection will reduce consistently the size of the data, thus imposing an additional loss of information.

According to Caspers and Kienitz (2017), we could solve the volatility problem by shifting to models which incorporates non constant volatilities. Caspers and Kienitz (2017) divide volatility models in two main classes. In the first class they account for local volatility models, which consider a deterministic function $\sigma(r(t), t)$ depending both on the

[3]The graph displaying volatilities as a function of strike values is called volatility smile and it is a bidimensional version of the volatility surface we have depicted in Figure 4.2. The volatility is normally higher when the strike tends to be more ITM or more OTM.

rate $r(t)$ and on the time t. The second class represents stochastic volatility models, which are characterised by a stochastic representation of the volatility term

$$d\sigma(t) = \mu_\sigma(t)dt + \nu(t)dW(t)$$

where μ_σ is the drift parameter, ν is the diffusion parameter and W is a Brownian motion.

The calibrated parameters can then be used to model the term structure equation, determining the future evolution of the single yield curve. Indeed, we could apply the term structure model for pricing purposes, following the steps we have outlined at the beginning of Chapter 2. According to Caspers and Kienitz (2017), the requirements that a calibrated model should satisfy in order to be used for pricing are robustness, flexibility and efficiency; the model should enable the analyst to turn the model parameters into market prices.

Appendix A

SDE and PDE

Given three functions $\mu(t,x)$, $\sigma(t,x)$ and $\Phi(x)$, we have the following problem

$$\begin{aligned} \frac{\partial F}{\partial t}(t,x) + \mu(t,x)\frac{\partial F}{\partial x}(t,x) + \frac{1}{2}\sigma^2(t,x)\frac{\partial^2 F}{\partial x^2}(t,x) = 0, \\ F(T,x) = \Phi(x). \end{aligned} \tag{A.1}$$

We assume that there exists a solution F to the problem A.1 on $[0,T] \times R$.
Firstly, we define a stochastic process X as a solution of the following SDE in the interval $[t,T]$ under the probability measure $\mathbb{Q}$

$$\begin{aligned} dX_s = \mu(s,X_s)ds + \sigma(s,X_s)dW_s^{\mathbb{Q}}, \\ X_t = x. \end{aligned} \tag{A.2}$$

Therefore, we apply the Itô formula to $F(s,X(s))$ and we obtain

$$\begin{aligned} F(T,X_T) = F(t,X_t) + \int_t^T \left\{ \frac{\partial F}{\partial t}(s,X_s) + \mu(t,x)\frac{\partial F(s,X_s)}{\partial x} \right. \\ \left. + \frac{1}{2}\sigma^2(t,x)\frac{\partial^2 F(s,X_s)}{\partial x^2} \right\} ds + \int_t^T \sigma(s,X_s)\frac{\partial F}{\partial x}(s,X_s)dW_s. \end{aligned} \tag{A.3}$$

We can avoid to consider the time integral and the stochastic integral because of the assumption that F is a solution of the problem A.1 and because $\sigma(s,X_s)\frac{\partial F}{\partial x}(s,X_s)$ is integrable. Finally, given a value $X_t = x$ at the start point t, we provide the Feynman-Kac representation

$$F(t,x) = E_{t,x}[\Phi(X_T)]. \tag{A.4}$$

We now have the following parabolic problem with the functions $\mu(t,x)$, $\sigma(t,x)$, $\Phi(t,x)$

and $r(t,x)$

$$\begin{aligned}\frac{\partial F}{\partial t}(t,x)+\mu(t,x)\frac{\partial F}{\partial x}(t,x)+\frac{1}{2}\sigma^2(t,x)\frac{\partial^2 F}{\partial x^2}(t,x)-r(t,x)F(t,x)=0,\\ F(T,x)=\Phi(x).\end{aligned} \tag{A.5}$$

We define a stochastic process equal to (A.2) under the probability measure $\mathbb{Q}$ and the process

$$Z(s)=exp\Big\{-\int_t^s r(u,X_u)du\Big\}F(s,X_s). \tag{A.6}$$

We apply the product decomposition to the Itô process (A.6)

$$\begin{aligned}dZ=d\Big[exp\Big\{-\int_t^s r(u,X_u)du\Big\}\Big]F(s,X_s)+exp\Big\{-\int_t^s r(u,X_u)du\Big\}dF(s,X_s)\\ +d\Big[exp\Big\{-\int_t^s r(u,X_u)du\Big\}\Big]dF(s,X_s)\end{aligned} \tag{A.7}$$

where the third term is equal to zero because

$$d\Big[exp\Big\{-\int_t^s r(u,X_u)du\Big\}\Big]=-r(s,X_s)exp\Big\{-\int_t^s r(u,X_u)du\Big\}ds. \tag{A.8}$$

Therefore, we apply the Itô formula to $dF(s,X_s)$ and we get

$$\begin{aligned}dZ=exp\Big\{-\int_t^s r(u,X_u)du\Big\}\Big(-r(s,X_s)F(s,X_s)+\mu(s,X_s)\frac{\partial F}{\partial x}+\frac{\partial F}{\partial t}\\ +\frac{1}{2}\sigma^2(s,X_s)\frac{\partial^2 F}{\partial x^2}\Big)ds+exp\Big\{-\int_t^s r(u,X_u)du\Big\}\sigma(s,X_s)\frac{\partial F}{\partial x}dW^{\mathbb{Q}}.\end{aligned} \tag{A.9}$$

The time integral vanishes and, integrating equation (A.9), we obtain

$$Z(T)=Z(t)+\int_t^T exp\Big\{-\int_t^s r(u,X_u)du\Big\}\sigma(s,X_s)\frac{\partial F}{\partial x}dW^{\mathbb{Q}}. \tag{A.10}$$

Taking the conditional expectation, we observe that the Itô integral has zero expected value. Therefore, it follows that

$$E[Z(T)|X_t=x]=E[Z(t)|X_t=x]=F(t,x) \tag{A.11}$$

and, finally, we obtain the solution of the parabolic problem under the probability measure $\mathbb{Q}$

$$F(t,x)=E^{\mathbb{Q}}\Big[exp\Big\{-\int_t^T r(u,X_u)du\Big\}\times\Phi(X_T)\Big|X_t=x\Big]. \tag{A.12}$$

Appendix B

Derivation of option prices under the Black model

We derive the price of an option whose underlying asset's dynamics is described by the Black model

$$dS(t) = \sigma S(t) dW(t). \tag{B.1}$$

Applying Itô's lemma to the natural logarithm of the underlying asset, we have

$$\begin{aligned} &f(t, S(t)) = \ln S(t) \\ &df(t, S(t)) = -\frac{1}{2S^2(t)} S^2(t)\sigma^2 dt + \frac{1}{S(t)} S(t)\sigma dW(t) = \sigma dW(t) - \frac{\sigma^2 t}{2} \end{aligned}$$

Integrating the last equation in the time interval from 0 to t, we obtain

$$\begin{aligned} &\int_0^t d\ln S(u) = \sigma \int_0^t dW(u) - \frac{\sigma^2}{2} \int_0^t du \\ &\ln \frac{S(t)}{S(0)} = \sigma W(t) - \frac{\sigma^2 t}{2} \\ &S(t) = S(0) \exp\left(\sigma W(t) - \frac{\sigma^2 t}{2}\right) \end{aligned}$$

Therefore, $f(t, S(t)) = \ln S(t)$ has a Normal distribution and its mean and variance are given respectively by

$$\begin{aligned} E[f(t, S(t))] &= E\left[\ln S(0) + \sigma W(t) - \frac{\sigma^2 t}{2}\right] = \ln S(0) - \frac{\sigma^2 t}{2} \\ Var[f(t, S(t))] &= Var\left[\ln S(0) + \sigma W(t) - \frac{\sigma^2 t}{2}\right] = \sigma^2 (t - 0) = \sigma^2 t \end{aligned}$$

The payoff at time t of a call option under the risk-neutral probability measure is expressed as

$$Call = E^{\mathbb{Q}}\Big[(S(t)-K)^{+}\Big] = E^{\mathbb{Q}}\Big[S(t)\times 1_{\{S(t)>K\}}\Big] - E^{\mathbb{Q}}\Big[K\times 1_{\{S(t)>K\}}\Big].$$

Before we analyse separately the two terms, we introduce the density function f of $y(t) = f(t, S(t))$

$$f_{y(t)}(y) = \frac{1}{\sigma\sqrt{2\pi t}}\exp\left[-\frac{\left(y-\ln S(0)+\frac{\sigma^2 t}{2}\right)^2}{2\sigma^2 t}\right] \tag{B.2}$$

and, consequently, the density function $f_{S(t)}(S)$ of the underlying asset

$$f_{S(t)}(S) = \frac{dy}{dS}f_{y(t)}(y) = \frac{1}{S\sigma\sqrt{2\pi t}}\exp\left[-\frac{\left(y-\ln S(0)+\frac{\sigma^2 t}{2}\right)^2}{2\sigma^2 t}\right].$$

Therefore, we can calculate the first expectation

$$E^{\mathbb{Q}}\Big[S(t)\times 1_{\{S(t)>K\}}\Big] = \int_K^{\infty} S\frac{dy}{dS}f_{y(t)}(y) = \frac{1}{S\sigma\sqrt{2\pi t}}\exp\left[-\frac{\left(y-\ln S(0)+\frac{\sigma^2 t}{2}\right)^2}{2\sigma^2 t}\right]dS$$

We introduce a variable x

$$x = \frac{\ln S - \ln S(0) + \frac{\sigma^2 t}{2}}{\sigma\sqrt{t}}$$

where

$$dS = S\sigma\sqrt{t}dx = \exp\left(x\sigma\sqrt{t} + \ln S(0) - \frac{\sigma^2 t}{2}\right)\sigma\sqrt{t}dx.$$

When the call is at-the-money, i.e. the asset value S is equal to the strike K, we have

$$x = \frac{\ln\frac{K}{S(0)} + \frac{\sigma^2 t}{2}}{\sigma\sqrt{t}}.$$

Therefore, changing the integration variable S with x we obtain

$$\begin{aligned} E^{\mathbb{Q}}\Big[S(t)\times 1_{\{S(t)>K\}}\Big] &= \int_{\frac{\ln\frac{K}{S(0)}+\frac{\sigma^2 t}{2}}{\sigma\sqrt{t}}}^{\infty} \frac{1}{\sigma\sqrt{2\pi t}}\exp\left(-\frac{x^2}{2} + x\sigma\sqrt{t} + \ln S(0) - \frac{\sigma^2 t}{2}\right)\sigma\sqrt{t}dx \\ &= S(0)\int_{\frac{\ln\frac{K}{S(0)}+\frac{\sigma^2 t}{2}}{\sigma\sqrt{t}}}^{\infty} \frac{1}{\sqrt{2\pi}}\exp\left(-\frac{(x-\sigma\sqrt{t})^2}{2}\right)dx \end{aligned}$$

Notice that the term $x - \sigma\sqrt{t}$ has a standard Normal distribution function which allows us to represent the expectation as

$$E^{\mathbb{Q}}\Big[S(t)\times 1_{\{S(t)>K\}}\Big] = S(0)\Phi\left(\frac{\ln\frac{S(0)}{K} + \frac{\sigma^2 t}{2}}{\sigma\sqrt{t}}\right)$$

The second expectation reduces to

$$E^{\mathbb{Q}}\left[K \times 1_{S(t)>K}\right] = KE^{\mathbb{Q}}[1_{S(t)>K}] = KP[S(t) > K] = KP\left[S(0)\exp\left(\sigma W(t) - \frac{\sigma^2 t}{2}\right) > K\right]$$
$$= KP\left[\frac{W(t)}{\sqrt{t}} > \frac{\ln\frac{K}{S(0)} + \frac{\sigma^2 t}{2}}{\sigma\sqrt{t}}\right] = K\Phi\left(\frac{\ln\frac{S(0)}{K} - \frac{\sigma^2 t}{2}}{\sigma\sqrt{t}}\right)$$

where the last equivalence is true because the term $\frac{W(t)}{\sqrt{t}}$ has a standard Normal distribution. Finally, we can express the payoff of the Call option as

$$Call^{Black} = S(0)\Phi\left(\frac{\ln\frac{S(0)}{K} + \frac{\sigma^2 t}{2}}{\sigma\sqrt{t}}\right) - K\Phi\left(\frac{\ln\frac{S(0)}{K} - \frac{\sigma^2 t}{2}}{\sigma\sqrt{t}}\right) = S(0)\Phi(d_1) - K\Phi(d_2)$$

We can apply a further generalization introducing the parameter ω, which is equal to 1 if the option is a call and to -1 if the option is a put. Hence, we have

$$Black = \omega S(0)\Phi(\omega d_1) - \omega K\Phi(\omega d_2).$$

Appendix C

Change of numeraire: the Brigo-Mercurio toolkit

We first consider the dynamics of a process $x(t)$ under the measure $\mathbb{Q}^S$

$$dx(t) = \mu^S(t, x(t))dt + \sigma(t, x(t))CdW^S(t).$$

Brigo and Mercurio (2006) developed a toolkit to express the process $x(t)$ under a different measure $\mathbb{Q}^U$

$$dx(t) = \mu^U(t, x(t))dt + \sigma(t, x(t))CdW^U(t).$$

The toolkit requires that the processes of the two numeraires S and U are - under the measure $\mathbb{Q}^U$- equal to

$$dS(t) = (\cdot)dt + \sigma^S(t)CdW^{\mathbb{Q}^U}(t)dU(t) = (\cdot)dt + \sigma^U(t)CdW^{\mathbb{Q}^U}(t) \tag{C.1}$$

The authors use the following formulas to determine, respectively, the drift and the diffusion terms

$$\mu^U(t, x(t)) = \mu^S(t, x(t)) - \sigma(t, x(t))\rho\left(\frac{\sigma^S(t)}{S(t)} - \frac{\sigma^U(t)}{U(t)}\right)$$

$$CdW^S(t) = CdW^U(t) - \rho\left(\frac{\sigma^S(t)}{S(t)} - \frac{\sigma^U(t)}{U(t)}\right)dt.$$

Appendix D

Simulation algorithm

D.1 Main function

```
OIS_curve = readtable('OIS_USD.xlsx');
OIS_dates = table2array(OIS_curve(1:45,7));
OIS_rates = table2array(OIS_curve(1:45,3));
OIS_rates = OIS_rates./100;

LIBOR1M_curve = readtable('swap_1m.xlsx');
LIBOR1M_dates = table2array(LIBOR1M_curve(1:45,7));
LIBOR1M_rates = table2array(LIBOR1M_curve(1:45,3));
LIBOR1M_rates = LIBOR1M_rates./100;

LIBOR3M_curve = readtable('swap_3m.xlsx');
LIBOR3M_dates = table2array(LIBOR3M_curve(1:45,7));
LIBOR3M_rates = table2array(LIBOR3M_curve(1:45,3));
LIBOR3M_rates = LIBOR3M_rates./100;

LIBOR6M_curve = readtable('swap_6m.xlsx');
LIBOR6M_dates = table2array(LIBOR6M_curve(1:45,7));
LIBOR6M_rates = table2array(LIBOR6M_curve(1:45,3));
LIBOR6M_rates = LIBOR6M_rates./100;

LIBOR12M_curve = readtable('swap_12m.xlsx');
LIBOR12M_dates = table2array(LIBOR12M_curve(1:45,7));
LIBOR12M_rates = table2array(LIBOR12M_curve(1:45,3));
LIBOR12M_rates = LIBOR12M_rates./100;

```

```
26 trial = 100;
27 n = 12*5; %12months * 5years
28
29 %Dates are equal for each type of interest rate. Therefore we
       only use OIS_dates
30
31 settlement_date = datenum('19-Jun-2020');
32 dates = datemnth(settlement_date,12*OIS_dates);
33
34 OIS_properties = intenvset('Rates',OIS_rates,'EndDates',dates,'
       StartDate',settlement_date);
35 LIBOR1M_properties = intenvset('Rates',LIBOR1M_rates,'EndDates',
       dates,'StartDate',settlement_date);
36 LIBOR3M_properties = intenvset('Rates',LIBOR3M_rates,'EndDates',
       dates,'StartDate',settlement_date);
37 LIBOR6M_properties = intenvset('Rates',LIBOR6M_rates,'EndDates',
       dates,'StartDate',settlement_date);
38 LIBOR12M_properties = intenvset('Rates',LIBOR12M_rates,'EndDates
       ',dates,'StartDate',settlement_date);
39
40 alpha1 = 0.1;
41 sigma1 = 0.004;
42 theta1 = 0.002;
43 alpha2 = 0.1;
44 sigma2 = 0.003;
45 theta2 = 0.004;
46 alpha3 = 0.08;
47 sigma3 = 0.006;
48
49 interest_rate1 = hwfactor(OIS_properties,LIBOR1M_properties,
       alpha1,sigma1,theta1,...
50     alpha2,sigma2,theta2,alpha3,sigma3,0.004);
51 interest_rate3 = hwfactor(OIS_properties,LIBOR3M_properties,
       alpha1,sigma1,theta1,...
52     alpha2,sigma2,theta2,alpha3,sigma3,0.008);
53 interest_rate6 = hwfactor(OIS_properties,LIBOR6M_properties,
       alpha1,sigma1,theta1,...
54     alpha2,sigma2,theta2,alpha3,sigma3,0.011);
55 interest_rate12 = hwfactor(OIS_properties,LIBOR12M_properties,
       alpha1,sigma1,theta1,...
```

```
56      alpha2,sigma2,theta2,alpha3,sigma3,0.014);
57
58 % rf_rate1, rf_rate3, rf_rate6 and rf_rate12 are all equal.
59
60 [rf_rate1,market1M_rate] = rate_simulator(interest_rate1,n,'
      nTrials',trial,'DeltaTimes',1/12);
61 [rf_rate3,market3M_rate] = rate_simulator(interest_rate3,n,'
      nTrials',trial,'DeltaTimes',1/12);
62 [rf_rate6,market6M_rate] = rate_simulator(interest_rate6,n,'
      nTrials',trial,'DeltaTimes',1/12);
63 [rf_rate12,market12M_rate] = rate_simulator(interest_rate12,n,'
      nTrials',trial,'DeltaTimes',1/12);
64
65 maturity = datemnth(settlement_date,n);
66 coupon = 0;
67
68 sim_date = datemnth(settlement_date,1:n);
69
70 sim_OIS_price = zeros(n+1,trial);
71 sim_OIS_price(1,:,:) = bondbyzero(OIS_properties,coupon,
      settlement_date,maturity);
72 sim_OIS_price(end,:,:) = 100;
73
74 sim_market1M_price = zeros(n+1,trial);
75 sim_market1M_price(1,:,:) = bondbyzero(LIBOR1M_properties,coupon
      ,settlement_date,maturity);
76 sim_market1M_price(end,:,:) = 100;
77
78 sim_market3M_price = zeros(n+1,trial);
79 sim_market3M_price(1,:,:) = bondbyzero(LIBOR3M_properties,coupon
      ,settlement_date,maturity);
80 sim_market3M_price(end,:,:) = 100;
81
82 sim_market6M_price = zeros(n+1,trial);
83 sim_market6M_price(1,:,:) = bondbyzero(LIBOR6M_properties,coupon
      ,settlement_date,maturity);
84 sim_market6M_price(end,:,:) = 100;
85
86 sim_market12M_price = zeros(n+1,trial);
```

```
87 sim_market12M_price(1,:,:) = bondbyzero(LIBOR12M_properties,
       coupon,settlement_date,maturity);
88 sim_market12M_price(end,:,:) = 100;
89
90 for i=1:n-1
91
92     struct_rf_rate1 = intenvset('StartDate',sim_date(i),'
           EndDates',...
93         datemnth(sim_date(i),12*OIS_dates),'Rates',squeeze(
               rf_rate1(i+1,:,:)));
94     sim_OIS_price(i+1,:) = bondbyzero(struct_rf_rate1,coupon,
           sim_date(i),maturity);
95
96     struct_market1M_rate = intenvset('StartDate',sim_date(i),'
           EndDates',...
97         datemnth(sim_date(i),12*OIS_dates),'Rates',squeeze(
               market1M_rate(i+1,:,:)));
98     sim_market1M_price(i+1,:) = bondbyzero(struct_market1M_rate,
           coupon,sim_date(i),maturity);
99
100 end
101
102 for i=1:n-1
103
104     struct_rf_rate3 = intenvset('StartDate',sim_date(i),'
           EndDates',...
105         datemnth(sim_date(i),12*OIS_dates),'Rates',squeeze(
               rf_rate3(i+1,:,:)));
106     sim_OIS_price(i+1,:) = bondbyzero(struct_rf_rate3,coupon,
           sim_date(i),maturity);
107
108     struct_market3M_rate = intenvset('StartDate',sim_date(i),'
           EndDates',...
109         datemnth(sim_date(i),12*OIS_dates),'Rates',squeeze(
               market3M_rate(i+1,:,:)));
110     sim_market3M_price(i+1,:) = bondbyzero(struct_market3M_rate,
           coupon,sim_date(i),maturity);
111
112 end
113
```

```
114 for i=1:n-1
115
116     struct_rf_rate6 = intenvset('StartDate',sim_date(i),'
        EndDates',...
117         datemnth(sim_date(i),12*OIS_dates),'Rates',squeeze(
            rf_rate6(i+1,:,:)));
118     sim_OIS_price(i+1,:) = bondbyzero(struct_rf_rate6,coupon,
        sim_date(i),maturity);
119
120     struct_market6M_rate = intenvset('StartDate',sim_date(i),'
        EndDates',...
121         datemnth(sim_date(i),12*OIS_dates),'Rates',squeeze(
            market6M_rate(i+1,:,:)));
122     sim_market6M_price(i+1,:) = bondbyzero(struct_market6M_rate,
        coupon,sim_date(i),maturity);
123
124 end
125
126 for i=1:n-1
127
128     struct_rf_rate12 = intenvset('StartDate',sim_date(i),'
        EndDates',...
129         datemnth(sim_date(i),12*OIS_dates),'Rates',squeeze(
            rf_rate12(i+1,:,:)));
130     sim_OIS_price(i+1,:) = bondbyzero(struct_rf_rate12,coupon,
        sim_date(i),maturity);
131
132     struct_market12M_rate = intenvset('StartDate',sim_date(i),'
        EndDates',...
133         datemnth(sim_date(i),12*OIS_dates),'Rates',squeeze(
            market12M_rate(i+1,:,:)));
134     sim_market12M_price(i+1,:) = bondbyzero(
        struct_market12M_rate,coupon,sim_date(i),maturity);
135
136 end
137
138 estimated_rf_rate = mean(rf_rate1(2:61,:,:),3);
139 estimated_1M_rate = mean(market1M_rate(2:61,:,:),3);
140 estimated_3M_rate = mean(market3M_rate(2:61,:,:),3);
141 estimated_6M_rate = mean(market6M_rate(2:61,:,:),3);
```

```
estimated_12M_rate = mean(market12M_rate(2:61,:,:),3);

figure(1)
plot([settlement_date sim_date],sim_OIS_price)
datetick
ylabel('Bond Price')
xlabel('Simulation Dates')
title('Simulated Risk-free Bond Price')
plot_dates = transpose(OIS_dates);
figure(2)
surf(plot_dates,1:60,estimated_rf_rate,'FaceColor','r')
yticks(12:12:60)
yticklabels({'1','2','3','4','5'})
hold on
surf(plot_dates,1:60,estimated_1M_rate,'FaceColor','m')
hold on
surf(plot_dates,1:60,estimated_3M_rate,'FaceColor','b')
hold on
surf(plot_dates,1:60,estimated_6M_rate,'FaceColor','y')
hold on
surf(plot_dates,1:60,estimated_12M_rate,'FaceColor','g')
hold off
```

D.2 hwfactor object

```
classdef hwfactor

    properties
        OIS_curve
        risky_curve
        alpha1
        sigma1
        theta1
        alpha2
        sigma2
        theta2
        alpha3
        sigma3
        theta3
    end
```

```
16      properties (Access = private)
17          SDE1
18          SDE2
19          SDE3
20          PM
21      end
22
23      methods (Access = public)
24          function obj = hwfactor(inOIS_curve,inrisky_curve,
                inalpha1,insigma1,intheta1,inalpha2,insigma2,intheta2
                ,inalpha3,insigma3,intheta3)
25
26              narginchk(11,11);
27
28              if isafin(inOIS_curve,'RateSpec')
29                  obj.OIS_curve = IRDataCurve('Zero',inOIS_curve.
                        ValuationDate,inOIS_curve.EndDates,...
30                          inOIS_curve.Rates,'Basis',inOIS_curve.Basis,
                                'Compounding',inOIS_curve.Compounding);
31              elseif isa(inOIS_curve,'IRDataCurve')
32                  obj.OIS_curve = inOIS_curve;
33              else
34                  error('error');
35              end
36
37              if isafin(inrisky_curve,'RateSpec')
38                  obj.risky_curve = IRDataCurve('Zero',
                        inrisky_curve.ValuationDate,inrisky_curve.
                        EndDates,...
39                          inrisky_curve.Rates,'Basis',inrisky_curve.
                                Basis,'Compounding',inrisky_curve.
                                Compounding);
40              elseif isa(inrisky_curve,'IRDataCurve')
41                  obj.risky_curve = inrisky_curve;
42              else
43                  error('error');
44              end
45
46              if isa(inalpha1,'function_handle')
47                  obj.alpha1 = @(t,V) inalpha1(t);
```

```
48              elseif isscalar(inalpha1)
49                  if inalpha1 == 0
50                      obj.alpha1 = @(t,V) eps;
51                  else
52                      obj.alpha1 = @(t,V) inalpha1;
53                  end
54              else
55                  error('error');
56              end
57
58              if isa(inalpha2,'function_handle')
59                  obj.alpha2 = @(t,V) inalpha2(t);
60              elseif isscalar(inalpha2)
61                  if inalpha2 == 0
62                      obj.alpha2 = @(t,V) eps;
63                  else
64                      obj.alpha2 = @(t,V) inalpha2;
65                  end
66              else
67                  error('error');
68              end
69
70              if isa(inalpha3,'function_handle')
71                  obj.alpha3 = @(t,V) inalpha3(t);
72              elseif isscalar(inalpha3)
73                  if inalpha3 == 0
74                      obj.alpha3 = @(t,V) eps;
75                  else
76                      obj.alpha3 = @(t,V) inalpha3;
77                  end
78              else
79                  error('error');
80              end
81
82              if isa(insigma1,'function_handle')
83                  obj.sigma1 = @(t,V) insigma1(t);
84              elseif isscalar(insigma1)
85                  obj.sigma1 = @(t,V) insigma1;
86              else
87                  error('error');
```

```
88              end
89
90              if isa(insigma2,'function_handle')
91                  obj.sigma2 = @(t,V) insigma2(t);
92              elseif isscalar(insigma2)
93                  obj.sigma2 = @(t,V) insigma2;
94              else
95                  error('error');
96              end
97
98              if isa(insigma3,'function_handle')
99                  obj.sigma3 = @(t,V) insigma3(t);
100             elseif isscalar(insigma3)
101                 obj.sigma3 = @(t,V) insigma3;
102             else
103                 error('error');
104             end
105
106             if isa(intheta1,'function_handle')
107                 obj.theta1 = @(t,V) intheta1(t);
108             elseif isscalar(intheta1)
109                 obj.theta1 = @(t,V) intheta1;
110             else
111                 error('error');
112             end
113
114             if isa(intheta2,'function_handle')
115                 obj.theta2 = @(t,V) intheta2(t);
116             elseif isscalar(intheta1)
117                 obj.theta2 = @(t,V) intheta2;
118             else
119                 error('error');
120             end
121
122             if isa(intheta3,'function_handle')
123                 obj.theta3 = @(t,V) intheta3(t);
124             elseif isscalar(intheta3)
125                 obj.theta3 = @(t,V) intheta3;
126             else
127                 error('error');
```

```
128             end
129
130             if any(obj.OIS_curve.Basis == [0 2 3 8 9 10 12])
131                 obj.PM = @(t) obj.OIS_curve.getDiscountFactors(
                        daysadd(obj.OIS_curve.Settle,round(365*t),obj
                        .OIS_curve.Basis))';
132             else
133                 obj.PM = @(t) obj.OIS_curve.getDiscountFactors(
                        daysadd(obj.OIS_curve.Settle,round(360*t),obj
                        .OIS_curve.Basis))';
134             end
135
136             obj.SDE1 = hwv(@(t,X) obj.alpha1(t),@(t,X)obj.theta1
                    (t),@(t,X) obj.sigma1(t),'StartState',0);
137             obj.SDE2 = hwv(@(t,X) obj.alpha2(t),@(t,X)obj.theta2
                    (t),@(t,X) obj.sigma2(t),'StartState',0);
138             obj.SDE3 = hwv(@(t,X) obj.alpha3(t),@(t,X)obj.theta3
                    (t),@(t,X) obj.sigma3(t),'StartState',0);
139
140         end
141         function [rf_rate, market_rate] = rate_simulator(obj,
                n_period,varargin)
142
143             narginchk(2,12);
144
145             p = inputParser;
146
147             p.addParameter('nTrials',1);
148             p.addParameter('DeltaTimes',1);
149             p.addParameter('tenor',[]);
150             p.addParameter('Antithetic',false);
151             p.addParameter('Z',[]);
152
153             try
154                 p.parse(varargin{:});
155             catch ME
156                 newMsg = message('fininst:HullWhite1F:
                        optionalInputError');
157                 newME = MException(newMsg.Identifier, getString(
                        newMsg));
```

```
158                 newME = addCause(newME, ME);
159                 throw(newME)
160             end
161
162             n = p.Results.nTrials;
163             delta = p.Results.DeltaTimes;
164             tenor = p.Results.tenor;
165             Antithetic = p.Results.Antithetic;
166             Z = p.Results.Z;
167
168             if isempty(tenor)
169                 tenor = yearfrac(obj.OIS_curve.Settle,obj.
                        OIS_curve.Dates,obj.OIS_curve.Basis);
170                 initzero_rate = obj.OIS_curve.Data;
171                 initmarket_rate = obj.risky_curve.Data;
172             else
173                 t_dates = daysadd(obj.OIS_curve.Settle,360*tenor
                        ,1);
174                 initzero_rate = obj.OIS_curve.getzero_rate(
                        t_dates);
175                 initmarket_rate = obj.risky_curve.getzero_rate(
                        t_dates);
176             end
177
178             tenor = reshape(tenor,1,length(tenor));
179
180             % Generate factors and short rates
181             [factor1,SimTimes1] = obj.SDE1.simBySolution(
                    n_period,'nTrials',n,'DeltaTime',delta,'
                    Antithetic',Antithetic,'Z',Z);
182
183             [factor2,SimTimes2] = obj.SDE2.simBySolution(
                    n_period,'nTrials',n,...
184                  'DeltaTime',delta,'Antithetic',Antithetic,'Z',Z)
                        ;
185
186             [factor3,SimTimes3] = obj.SDE3.simBySolution(
                    n_period,'nTrials',n,'DeltaTime',delta,'
                    Antithetic',Antithetic,'Z',Z);
187
```

```
188 n_tenor = length(tenor);
189
190 rf_rate = zeros(n_period+1,n_tenor,n);
191 market_rate = zeros(n_period+1,n_tenor,n);
192
193 rf_rate(1,:,:) = repmat(initzero_rate',[1 1 n]);
194 market_rate(1,:,:) = repmat(initmarket_rate',[1 1 n
    ]);
195
196 k = 0.4;
197
198 B_1 = @(t,T) -1/obj.alpha1(t)*(exp(-obj.alpha1(t)*(T
    -t))-1);
199 B_2 = @(t,T) -1/obj.alpha2(t)*(exp(-obj.alpha2(t)*(T
    -t))-1);
200 B_3 = @(t,T) -1/obj.alpha1(t)*(exp(-obj.alpha1(t)*(T
    -t))-1);
201
202 B_1_squared = @(t,T) (-1/obj.alpha1(t)*(exp(-obj.
    alpha1(t)*(T-t))-1)).^2;
203 B_2_squared = @(t,T) (-1/obj.alpha2(t)*(exp(-obj.
    alpha2(t)*(T-t))-1)).^2;
204 B_3_squared = @(t,T) (-1/obj.alpha3(t)*(exp(-obj.
    alpha3(t)*(T-t))-1)).^2;
205
206 A_1 = @(t,T) (B_1(t,T)-T+t)*(obj.theta1(t)*obj.
    alpha1(t)*((obj.sigma1(t))^2))/(obj.alpha1(t)^2)
    ...
207   -((obj.sigma1(t))^2).*B_1_squared(t,T)./(4*obj.
        alpha1(t));
208 A_2 = @(t,T) (B_2(t,T)-T+t)*(obj.theta2(t)*obj.
    alpha2(t)*((obj.sigma2(t))^2))/(obj.alpha2(t)^2)
    ...
209   -((obj.sigma2(t))^2).*B_2_squared(t,T)./(4*obj.
        alpha2(t));
210 A_3 = @(t,T) (B_3(t,T)-T+t)*(obj.theta3(t)*obj.
    alpha3(t)*((obj.sigma3(t))^2))/(obj.alpha3(t)^2)
    ...
211   -((obj.sigma3(t))^2).*B_3_squared(t,T)./(4*obj.
        alpha3(t));
```

```
212                 disc = @(t,T) obj.PM(T)./obj.PM(t);
213
214                 A_m = @(t,T) (1+k)*A_1(t,T)+A_2(t,T)+A_3(t,T);
215
216                 for i=2:n_period+1
217                     t = SimTimes1(i);
218                     discount_zero = exp(bsxfun(@plus,A_1(t,t+tenor),
                            A_2(t,t+tenor))) ...
219                         .*exp(-bsxfun(@times,B_1(t,t+tenor),factor1(
                                i,:,:))) ...
220                         .*exp(-bsxfun(@times,B_2(t,t+tenor),factor2(
                                i,:,:)));
221                     rf_rate(i,:,:) = bsxfun(@rdivide,-log(
                            discount_zero),tenor);
222
223                     discount_market = disc(t,t+tenor).*exp(A_m(t,t+
                            tenor)).*...
224                         exp(-bsxfun(@times,B_1(t,t+tenor),factor1(i
                                ,:,:))).* ...
225                         exp(-bsxfun(@times,B_2(t,t+tenor),factor2(i
                                ,:,:))).* ...
226                         exp(-bsxfun(@times,B_3(t,t+tenor),factor3(i
                                ,:,:))).* ...
227                         exp(-bsxfun(@times,k*B_1(t,t+tenor),factor1(
                                i,:,:)));
228                     market_rate(i,:,:) = bsxfun(@rdivide,-log(
                            discount_market),tenor);
229                 end
230             end
231         end
232     end
```

Bibliography

Ametrano, F. M. and M. Bianchetti (2013). *Everything You Always Wanted to Know About Multiple Interest Rate Curve Bootstrapping but Were Afraid to Ask*. Available at SSRN: https://ssrn.com/abstract=2219548.

Andersen, L. B. (2007). "Discount curve construction with tension splines". In: *Review of Derivatives Research* 10.3, pp. 227–267.

Andersen, L. B. and V. V. Piterbarg (2010). *Interest Rate Modeling. Volume 1: Foundations and Vanilla Models*. Atlantic Financial Press.

Bianchetti, M. (2011). *The Zeeman Effect in Finance: Libor Spectroscopy and Basis Risk Management*. Available at SSRN: https://ssrn.com/abstract=1951578.

Bianchetti, M. and M. Carlicchi (2013). "Evolution of the Markets after the Credit Crunch". In: *Interest Rate Modelling after the Financial Crisis*. Ed. by M. Bianchetti and M. Morini. Risk Books, pp. 5–59.

Bianchetti, M. and M. Morini (2013). *Interest Rate Modelling after the Financial Crisis*.

Björk, T. (2009). *Arbitrage Theory in Continuous Time*. Third edn. Oxford Finance.

Brigo, D. and F. Mercurio (2006). *Interest Rate Models - Theory and Practice. With Smile, Inflation and Credit*. Second edn. Springer-Verlag Berlin Heidelberg.

Caspers, P. and J. Kienitz (2017). *Interest Rate Derivatives Explained. Volume 2: Term Structure and Volatility Modelling*. Palgrave Macmillan UK.

European Central Bank (2020). *Financial Stability Review - May 2020*. Available at: https://www.ecb.europa.eu/pub/pdf/fsr/ecb.fsr201911 facad0251f.en.pdf.

Filipovic, D. and A. B. Trolle (2013). "The term structure of interbank risk". In: *Journal of Financial Economics* 109.4, pp. 707–733.

Grasselli, M. and G. Miglietta (2016). "A flexible spot multiple-curve model". In: *Quantitative Finance* 16.10, pp. 1465–1477.

Grbac, Z. and W. J. Runggaldier (2015). *Interest Rate Modeling: Post-Crisis Challenges and Approaches*. Springer International Publishing.

Hagan, P. and G. West (2006). "Interpolation Methods for Curve Construction". In: *Applied Mathematical Finance* 13.2, pp. 89–129.

Henrard, M. (2014). *Interest Rate Modelling in the Multi-Curve Framework. Foundations, Evolution and Implementation*. Palgrave Macmillan UK.

Hull, J. C. and A. White (2013). "LIBOR vs. OIS: The Derivatives Discounting Dilemma". In: *The Journal of Investment Management, Forthcoming*. Available at SSRN: https://ssrn.com/abstract=2211800.

Kienitz, J. (2014). *Interest Rate Derivatives Explained. Volume 1: Products and Markets*. Palgrave Macmillan UK.

Kienitz, J. and D. Wetterau (2012). *Financial Modelling. Theory, Implementation and Practice with MATLAB Source*. John Wiley & Sons.

Tebaldi, C. and P. Veronesi (2016). "Risk-Neutral Pricing: Monte Carlo Simulations". In: *Handbook of Fixed-Income Securities*. Ed. by P. Veronesi. John Wiley & Sons, pp. 437–468.

Veronesi, P. (2016). "Discounting and Derivative Pricing Before and After the Financial Crisis: An Introduction". In: *Handbook of Fixed-Income Securities*. Ed. by P. Veronesi. John Wiley & Sons, pp. 414–434.